

# CATALYSIS: from science to industry



**PROCEEDINGS OF VI INTERNATIONAL SCIENTIFIC  
SCHOOL-CONFERENCE FOR YOUNG SCIENTISTS**

October 6-10, 2020  
Tomsk State University, Tomsk

## **CATALYSIS: FROM SCIENCE TO INDUSTRY**

*Proceedings of  
VI International scientific school-conference for young scientists*

October 6-10, 2020

Tomsk 2020

UDC 544.47/544.72+661.7  
LBC 24.54  
P75

P75 **Catalysis: from science to industry:** Proceedings of VI International scientific school-conference for young scientists "Catalysis: from science to industry" / Tomsk State University. – Tomsk: "Ivan Fedorov" publishing, 2020. – 108 p.

ISBN 978-5-91701-145-5

The collection is devoted to important and perspective directions of modern catalysis: fundamentals of catalyst preparation and catalytic processes, promising catalytic processes and industrial implementation of catalytic processes.

**UDC 544.47/544.72+661.7**  
**LBC 24.54**

*Editorial staff*

O.V. Vodyankina, Doctor of sciences, Professor  
T.S. Kharlamova, PhD., Associate professor  
V.S. Malkov, PhD., Senior researcher

© Tomsk state university, 2020

© Cover. "Ivan Fedorov" publishing, 2020

# VI INTERNATIONAL SCIENTIFIC SCHOOL-CONFERENCE FOR YOUNG SCIENTISTS

## “CATALYSIS: FROM SCIENCE TO INDUSTRY”

### ORGANIZERS

National Research Tomsk State University



National Research  
**Tomsk  
State  
University**



The Scientific School for Young Scientists “New catalysts and catalytic processes to solve the challenges of environmental responsible and resource-saving energy production” organized within a project supported by the Russian Science Foundation was held during the 6<sup>th</sup> International School-Conference for Young Scientists “Catalysis: from Science to Industry”



**Russian  
Science  
Foundation**

### INFORMATION SUPPORT

Journal “Kinetics and Catalysis”



## **SCIENTIFIC COMMITTEE**

### **CHAIRPERSON:**

VODYANKINA O.V., TSU, TOMSK, RUSSIA

### **MEMBERS:**

BUKHTIYAROV V.I., BIC SB RAS, NOVOSIBIRSK, RUSSIA  
LAVRENOV A.V., IHP SB RAS, OMSK, RUSSIA  
VOSMERIKOV A.V., IPC SB RAS, TOMSK, RUSSIA  
SADYKOV V.A., BIC SB RAS, NOVOSIBIRSK, RUSSIA  
SLIZHOV YU.G., TSU, TOMSK, RUSSIA  
KHOLDEEVA O.A., BIC SB RAS, NOVOSIBIRSK, RUSSIA  
BORONIN A.I., BIC SB RAS, NOVOSIBIRSK, RUSSIA  
SVETLICHNYI V.A., TSU, TOMSK, RUSSIA  
CADETE SANTOS AIRES F.J., IRCELYON, LYON, FRANCE  
LIOTTA L.F., INM CNR, PALERMO, ITALY  
CORTES CORBERAN V., ICP, CSIC, MADRID, SPAIN  
LOKTEVA E.S., LOMONOSOV MSU, MOSCOW, RUSSIA  
PESTRYAKOV A.N., TPU, TOMSK, RUSSIA  
KOZLOVA E.A., BIC SB RAS, NOVOSIBIRSK, RUSSIA  
MENSHCHIKOVA T.V., TSU, TOMSK, RUSSIA

## **ORGANIZING COMMITTEE**

### **CHAIRPERSON:**

KHARLAMOVA T.S., TSU, TOMSK, RUSSIA

### **SECRETARY:**

TUGULDUROVA V.P., TSU, TOMSK, RUSSIA

### **MEMBERS:**

BUGROVA T.A., TSU, TOMSK, RUSSIA  
GRABCHENKO M.V., TSU, TOMSK, RUSSIA  
SAVEL'EVA A.S., TSU, TOMSK, RUSSIA  
ROMANOVA E.V., TSU, TOMSK, RUSSIA  
DOROFEEVA N.V., TSU, TOMSK, RUSSIA  
ZOLOTUKHINA N.YU., TSU, TOMSK, RUSSIA  
SALAEV M.A., TSU, TOMSK, RUSSIA  
MALKOV V.S., TSU, TOMSK, RUSSIA  
VODOREZOVA O.YU., TSU, TOMSK, RUSSIA  
SAVENKO D.YU., TSU, TOMSK, RUSSIA  
VODYANKIN A.A., TSU, TOMSK, RUSSIA  
EDGULOVA T.V., TSU, TOMSK, RUSSIA  
MAGAEV O.V., TSU, TOMSK, RUSSIA  
URAZOV KH.KH., TSU, TOMSK, RUSSIA  
TEN S.A., TSU, TOMSK, RUSSIA  
BELIK YU. A., TSU, TOMSK, RUSSIA  
VYSHEGORODTSEVA E.V., TSU, TOMSK, RUSSIA  
VERKHOV V.A., TSU, TOMSK, RUSSIA  
KOTOV A.V., TSU, TOMSK, RUSSIA  
TIMOFEEV K.L., TSU, TOMSK, RUSSIA  
ZUBKOV A.V., TSU, TOMSK, RUSSIA  
SMETANOVA YU.V., TSU, TOMSK, RUSSIA

# PLENARY LECTURES



## Environmental (scanning & transmission) electron microscopy contribution to the study of silver-based catalysts during ethylene epoxidation

T. Cavoué<sup>1</sup>, A. Caravaca<sup>1</sup>, L. Burel<sup>1</sup>, M. Aouine<sup>1</sup>, M. Rieu<sup>2</sup>, J.P. Viricelle<sup>2</sup>, P. Vernoux<sup>1</sup>, F.J. Cadete Santos Aires<sup>1,3</sup>

<sup>1</sup>Université de Lyon, IRCELYON, UMR5256 CNRS/UCB Lyon1, Lyon, France

<sup>2</sup>Université de Lyon, LGF, UMR5307 CNRS/Mines Saint-Etienne, Saint-Etienne, France

<sup>3</sup>National Research Tomsk State University, LCR, Tomsk, Russia

philippe.vernoux@ircelyon.univ-lyon1.fr, francisco.aires@ircelyon.univ-lyon1.fr

Ethylene oxide (EO) is a chemical intermediate of paramount importance and it is one of the most produced petrochemicals. It is used as a precursor for the further production of added value molecules, including plastics, polyester and ethylene glycol [1]. The most widely used catalytic process for the production of EO is the partial oxidation (epoxidation) of ethylene with air (or oxygen) on Ag/ $\alpha$ -Al<sub>2</sub>O<sub>3</sub> catalysts at low reaction temperatures (220 – 280 °C) but at high pressures (10-30 Bar) [2]. In the absence of any chemical promoters, the selectivity towards EO is in the range of 50%; to enhance the efficiency of the epoxidation process, the addition of chlorinated hydrocarbons (e.g. dichloroethene or vinyl chloride) is known to improve the selectivity to values ~90 %. However, chlorinated promoters are not environmentally friendly, and their eventual accumulation leads to a significant poisoning of the catalyst.

Following an alternative approach, Stoukides and Vayenas reported the promotional effect of O<sup>2-</sup> ions on an Ag catalyst film on Ag//YSZ (catalyst-electrode//solid electrolyte) electrochemical catalysts for ethylene epoxidation [3]. It was found that pumping O<sup>2-</sup> ions towards the Ag electrode via electrical polarization allowed to dramatically enhance the selectivity and yield of EO production at 400 °C and atmospheric pressure.

The idea of this study is to take advantage of the main features of both the electrochemical catalysts (i.e., the possibility to *in situ* supply O<sup>2-</sup> promoters) and the conventional industrial catalysts (i.e., higher metallic dispersion and accessibility to active sites). We studied the ethylene epoxidation reaction on Ag/YSZ composites supported on dense yttria-stabilized zirconia (YSZ) solid electrolytes at atmospheric pressure and in the absence of chlorinated promoters. The experiments performed showed a dynamic performance, where the activity evolved with time in an unprecedented manner. Before reaching a “steady-state” (with EO selectivity lower than 10 %) the system passed through an “optimized state”, where the EO selectivity was ~ 40-50 %. The pretreatment of the catalyst under oxidizing and reducing atmospheres, the influence of the oxide support (Gd-doped CeO<sub>2</sub> and  $\alpha$ -Al<sub>2</sub>O<sub>3</sub>) and the impact of the catalyst loading were studied. In addition, *in situ* electron scanning and transmission microscopy observations were performed on the Ag/YSZ composite. All these experiments suggest that the “optimized-state” takes place due to the production of small silver clusters formed after the evaporation, decomposition and further condensation of Ag<sub>x</sub>O species from the bulk of the composite to the YSZ powder. The activity of these Ag clusters species would be dramatically enhanced due to the promotional effect of the O<sup>2-</sup> ions supplied by the YSZ support, due to metal-support interactions. However, once the YSZ support is saturated with Ag clusters, they start to agglomerate, leading to bigger nanoparticles with lower selectivity towards the desired EO product. This study clearly demonstrates therefore the possibility to use active catalytic supports (e.g. YSZ) to drastically enhance, in a significant manner, the performance of Ag catalysts for the ethylene epoxidation reaction without the addition of non-environmentally-friendly chlorinated promoters (commonly used for industrial applications). Also, to the best of our knowledge, the use of Ag/YSZ catalysts (without electrical polarization) has never been reported for ethylene epoxidation.

*This work is part of the “EPOX” project funded by the French National Research Agency, ANR-2015-CE07-0026.*

### References

1. Özbek, M.O.; van Santen, R.A. *Catal. Lett.* **2013**, *143*, 131–141.
2. Chongterdtoonskul, A.; Schwank, J.W.; Chavadej, S. *J. Mol. Catal. A-Chem.*, **2012**, *358*, 58–66.
3. Stoukides, M.; Vayenas, C.G. *J. Catal.* **1981**, *70*, 137–146.



## Selective liquid phase oxidation of alcohols: effect of supports and active metals

V. Cortés Corberán

*Institute of Catalysis and Petroleumchemistry (ICP), CSIC, 28049 Madrid, Spain.*

vcortes@icp.csic.es

Sustainability of processes for selective oxidation of alcohols, a key transformation in industrial organic chemistry which conventional processes have a high environmental impact, requires the research and development of catalysts able to operate using clean oxidants (air, oxygen) at moderate temperatures. This latter involves liquid phase processes for most of the C<sub>6+</sub> alcohols, and makes notably challenging the oxidation of the less reactive, non-activated primary C<sub>6+</sub> linear alkanols (higher alcohols) [1].

Due to their exceptional catalytic properties in redox reactions, supported Au nanoparticles (NPs) catalysts were firstly investigated for these latter reactions, using n-octanol as model molecule and oxygen at atmospheric pressure as oxidant. It was found the support nature strongly influences their catalytic performance and the support itself can play a role in the product distribution [2]. This opened a way to improve catalytic performance by modifying the support surface. Furthermore, the nature of the support determines the influence of metal load on the catalytic performance [3,4], revealing the role of the role of the metal-support interactions.

Combination of gold with a second metal has been often explored as a way to improve its performance and decrease catalyst costs. Thus, we applied the support-modifying strategy to bimetallic Au-Ag NPs catalysts as alternative to gold catalysts. The results showed similar trends and clear activity increases by modifying the support [5] and revealed the influence of catalyst redox pretreatment in such effects. The effect of catalyst components (both active metal and support) has also been studied with nano gold and silver catalysts, using model oxide supports to identify the influence of the acid-base properties [6]. Selectivity in n-octanol oxidation was determined by redox properties of the gold species, the acid-base properties of the supports and the catalyst pretreatment. Silver addition modified the acid base properties of the catalytic system, thus influencing the selectivity in n-octanol oxidation.

All these effects will be analyzed and discussed in terms of the nature and size of the active species and the electronic state of the active metal.

*This work was supported by MINECO project CTQ2017-86170-R. Collaboration with the research teams of ICMS, CSIC (Spain), TPU (Russia), CNN, UNAM (Mexico), IST (Portugal) and AMU (Poland) is gratefully acknowledged.*

### References

1. Cortés Corberán, V.; González-Pérez, M.E.; Martínez-González, S.; Gómez-Avilés, A. *Appl. Catal. A: Gen.* **2014**, *474C*, 211–223.
2. Martínez-González, S.; Ivanova, S.; Dominguez, M.I.; Cortés Corberán, V. *Catal. Today* **2016**, *278*, 113–119.
3. Kotolevich, Y.; Kolobova, E.; Mamontov, G.; Khramov, E.; Cabrera Ortega, J.E.; Tiznado, H.; Farias, M.H.; Bogdanchikova, N.; Zubachivus, Y.; Mota-Morales, J.D.; Cortés Corberán, V.; Zanella, R.; Pestryakov, A. *Catal. Today* **2016**, *278*, 104–112.
4. Kolobova, E.; Pakrieva, E.; Pascual, L.; Cortés Corberán, V.; Bogdanchikova, N.; Farias, M.; Pestryakov, A.; *Catal. Today* **2019**, *333*, 127–132.
5. Kotolevich, Y.; Kolobova, E.; Pestryakov, A.; Cabrera Ortega, J.E.; Bogdanchikova, N.; Cortés Corberán, V.; Khramov, E.; Zubavichus, Ya.; Zanella, R.; Pakrieva, E. *Current Org. Synth.*, **2017**, *14*, 323–331.
6. Kaskow, I.; Sobczak, I.; Ziolk, M.; Cortés Corberán, V. *Molecular Catal.*, **2020**, *482*, 11067.

## **Methane conversion to syngas**

Valeria La Parola

*Institute for Nanostructured Materials- National Research Council*

valeria.laparola@cnr.it

Methane conversion to syngas may be achieved by different reaction which yield to different syngas formulation. Methane steam reforming ( $\text{CH}_4 + \text{H}_2\text{O} \rightarrow \text{CO} + 3 \text{H}_2$ ) is the most industrial developed process for syngas production by methane. Others processes like dry reforming ( $\text{CH}_4 + \text{CO}_2 \rightarrow 2\text{CO} + 2 \text{H}_2$ ), partial oxidation ( $\text{CH}_4 + 0.5\text{O}_2 \rightarrow \text{CO} + 2 \text{H}_2$ ) or autothermal reforming ( $4\text{CH}_4 + 2 \text{H}_2\text{O} + \text{O}_2 \rightarrow 4\text{CO} + 10 \text{H}_2$ ) are at a lower degree of industrial development, but widely studied for their energetic characteristic. For all these reactions the rate determining step is the C-H bond activation in methane.

All these reactions are well promoted by Ni-based catalysts. Metallic Nickel present a high activity toward C-H activation, but for all the considered reactions, it suffers of deactivation by carbon formation, sintering of active phase and impurities in the methane feed.

Here the activity of different Ni based catalysts toward some of the above mentioned methane reforming reaction will be presented and their activity and coke resistance will be correlated to the nature of nickel particles. The effect of metal support interaction, of catalyst formulation and of catalyst synthetic procedure will be exposed.

*This work was supported by CNR-HAS and CNR-BAS bilateral program*

## Ni/CeO<sub>2</sub>-based catalysts for CO<sub>2</sub> methanation reaction: Insights into promotion effects

L.F. Liotta

*Istituto per lo Studio dei Materiali Nanostrutturati (ISMN)-CNR,  
Via Ugo La Malfa, 153, 90146, Palermo, Italy*

leonardafrancesca.liotta@cnr.it

The concentration of CO<sub>2</sub> in the atmosphere has been growing since the industrial revolution and is causing many environmental issues. Nowadays the recycle of CO<sub>2</sub> is mandatory in order to reduce the globe warming due to such greenhouse gas. Many studies are focusing on the CO<sub>2</sub> chemical recycling and CO<sub>2</sub> methanation, also called Sabatier's reaction ( $\text{CO}_2 + 4\text{H}_2 = \text{CH}_4 + 2\text{H}_2\text{O}$ ), is regarded as one of the most useful ways for CO<sub>2</sub> utilization [1].

Noble metals, like Ru and Rh based catalysts, have been reported as effective in CO<sub>2</sub> conversion and selective towards CH<sub>4</sub> formation [2,3]. However, noble metals were not appropriate for industrial scale application, because of their high cost and sintering at high temperature.

Among non-noble metals, Ni supported catalysts represent good alternatives for methanation reaction as their benefits of relatively high catalytic activity, low cost and great availability.

The nature of the supports and the preparation methods play an important role in enhancing CO<sub>2</sub> conversion and selectivity towards CH<sub>4</sub> of Ni catalysts.

CeO<sub>2</sub> has attracted plenty of interest because of its unique redox property. It can create oxygen vacancies during the redox process Ce (III)/Ce (IV), promoting the activation of CO<sub>2</sub> [4].

The present contribution will focus on an overview of Ni/CeO<sub>2</sub> based catalysts for CO<sub>2</sub> methanation reaction with recent results on the effect of CeO<sub>2</sub> promotion.

*Leonarda F. Liotta carried the research in the field of the COST Action 18224 "Green Chemical Engineering Network towards upscaling sustainable processes" and acknowledges the CNR Program Short Term Mobility (2018) for supporting her research mobility in the group of Professor Patrick Da Costa in Sorbonne University, Institut Jean Le Rond d'Alembert, F-78210, Saint-Cyr-l'École, Paris, France.*

### References

1. Yan, Y.; Dai, Y.; Yang, Y.; Lapkin, A.A. *Appl. Catal. B Environ.* **2018**, 237, 504–512.
2. Solymosi, F.; Erdöhelyi, A. *Stud. Surf. Sci. Catal.* **1981**, 7, 1448–1449
3. Upham, D.C.; Derk, A.R.; Sharma, S.; Metiu, H.; McFarland, E.W. *Catal. Sci. Technol.* **2015**, 5, 1783–1791
4. Wang, F.; Wei, M.; Evans, D.G.; Duan, X.; *J. Mater. Chem. A.* **2016**, 4, 5773–5783.

## **NO<sub>x</sub> SCR by ammonia in naval sector. An Italian industrial research project**

G. Pantaleo

*Istituto per lo studio dei materiali nanostrutturati (ISMN-CNR)*

Via Ugo La Malfa 153, 90146 Palermo, Italy

giuseppe-pantaleo@cnr.it

The IMO (international maritime organization) is the agency of the United Nations has been formed to promote maritime safety and which is in charge to promote ship pollution rules. The rules are contained in the international convention for the prevention of pollution from ships MARPOL (**MAR**itime **POL**lution) which inside the Annex VI introduce regulations for NO<sub>x</sub> and SO<sub>x</sub> emissions. It was recently announced that the regulations for generating energy in maritime applications will become significantly more restrictive in terms of emissions. In particular, in 2021 the (IMO) will adopt strict limits in its Tier III standards concerning the NO<sub>x</sub> abatement. For emission control areas (ECA), these requirements will be mandatory and difficult to comply with traditional diesel engines and heavy fuels [1]. The SCR (Selective Catalytic Reduction) technology has been chosen by several truck manufacturers to meet Euro V (2008) standards. Its introduction is more recent in the case of light duty engines: starting from 2012 many Euro 6 vehicles are equipped with SCR. Keeping in mind the experience done in automotive sector it is necessary to adjust NO<sub>x</sub> SCR technology to the maritime sector adopting all the strategies in order to comply with its environment peculiarity, engines and fuels.

In the framework of this industrial project are studied some new materials, in collaboration with an industrial partner (Isotta Fraschini Motori S.p.A), starting from the conventional WO<sub>3</sub>-V<sub>2</sub>O<sub>5</sub> oxides, normally proposed as active and selective for the NO<sub>x</sub> abatement from engines gas exhausts [2].

The more interesting materials thanks to a preliminary study in laboratory scale are investigated as well in more realistic conditions, taking into account a lifelike gas exhaust.

*This work was supported by the Project TecBia: “Tecnologie a basso impatto ambientale per la produzione di energia sui mezzi navali”.*

### **References**

1. Brynolf, S.; Magnusson, M.; Fridell, E.; Andersson, K.; *Transp. Res. Part D Transp. Environ.* **2014**, 28, 6.
2. Zhang, W.; Qi, S.; Pantaleo, G.; Liotta, L. F. *Catalysts* **2019**, 9, 527.



# KEYNOTE LECTURES



## Pt/CeO<sub>2</sub> catalysts: active sites and reaction mechanisms in CO oxidation

A.I. Boronin

*Boreskov Institute of Catalysis, Novosibirsk, Russia*

boronin@catalysis.ru

The combination of platinum group metals (PGM) and ceria creates very efficient catalysts with capability to oxidize CO at room temperature and above. In general, this catalytic effect is due to strong metal support interaction leading to the formation of new interacted surface phases and active sites. Until recently, one could assume that PGM/CeO<sub>2</sub> catalysts are not capable to effectively oxidize CO at temperatures below room temperature, in contrast to gold-based catalysts. However experimental investigations of Pt/CeO<sub>2</sub> samples with variation of Pt concentration in catalysts revealed that this system has comparable features as in golden catalysts. In this work it is demonstrated the capability of Pt/CeO<sub>2</sub> catalysts with increased Pt loading to oxidize CO starting -50°C. The discovered phenomenon was designated as abnormally low-temperature CO oxidation (ALTO CO) on the Pt/CeO<sub>2</sub> catalysts.

In this work the application of structural (XRD, HRTEM), spectral (XPS, Raman) and kinetic (TPR-CO, TPR-CO+O<sub>2</sub>) methods allowed us to obtain information about full set of Pt-species formed on ceria surface. According to XRD, HRTEM, and XPS data, the low loading catalysts contained only ionic Pt in the 2+ state as single atom species. Pt/CeO<sub>2</sub> samples with high Pt loading contained Pt<sup>2+</sup> and Pt<sup>4+</sup> ions combined to PtOx clusters like Pt<sub>3</sub>O<sub>4</sub> surface structures [1]. XRD and HRTEM did not detect any metal Pt particles in these samples.

Variation of platinum loading in the catalysts substantially affected their CO oxidation performance. The catalysts with low Pt loading were capable of catalyzing the CO oxidation reaction only at T > 100°C, while the catalysts with higher Pt loadings showed ALTO activity below 0°C. The incorporation of Pt<sup>4+</sup> ions into ceria lattice resulted in generation of highly mobile and reactive ceria lattice oxygen in the samples with increased Pt loading. This observation evidences the Mars-van Krevelen mechanism of CO oxidation through the lattice oxygen participation at room temperature. However the detailed catalytic experiments allowed answering the question of whether the mobile lattice oxygen is capable of providing stationary catalysis at very low temperatures. According to thorough comparison of the TPR-CO+O<sub>2</sub> and TPR-CO data the reaction rate of CO oxidation by gas-phase O<sub>2</sub> at room temperature is two orders of magnitude higher than that of CO oxidation solely by mobile oxygen from the catalyst that is direct indication on new mechanism of ALTO.

The observed abnormally high low-temperature CO oxidation is discussed in terms of a reaction mechanism that involves weak adsorption of nearby O<sub>2</sub> and CO molecules. From a general point of view such mechanisms of the products formation from molecular states of reactants are effective at low temperature due to redistribution of chemical bonds without involving strongly bound intermediate dissociative states requiring high activation energies.

*This work was conducted within the framework of the budget Project No. AAAA-A17-117041710084-2 for the Boreskov Institute of Catalysis.*

### References

1. Derevyannikova E.A., Kardash T.Y., Stadnichenko A.I., Stonkus O.A., Slavinskaya E.M., Svetlichnyi V.A., Boronin A.I. *J. Phys. Chem. C* **2019**, 123,1320–1334.



## Particles size determination in supported catalysts: new technique of light scattering

Yu.V. Larichev

*Boreskov Institute of Catalysis, Novosibirsk, Russia  
Novosibirsk State University, Novosibirsk, Russia*

ylarichev@gmail.com

Particle size is one of important parameters for supported metal catalysts. Activity and selectivity of supported catalysts can depend on this parameter. Typically, for particle size determination TEM and XRD methods are used. Nevertheless, such methods need expensive equipments and services. Moreover treatment of data obtained by these methods is time consuming also. In some cases, it is important to get information about particle sizes quickly and at low price. For example, brute force methods for searching and preparing optimal catalyst are often limited by budget for samples analysis. It is expensive to make TEM or XRD analysis for several dozens or even hundreds samples especially for routine tasks. Probably, using more cheap and express methods of particle size determination could get new information about catalysts preparation through the deep analysis of big datasets [1]. Moreover conventional methods have not enough sensitivity for particle sizes determination of low percentage industrial catalysts. More simple and cheap chemisorption methods it is not always suitable for all types of supported metal catalysts. Therefore, development or adaptation of cheaper, sensitive and simple methods for particle size determination in supported catalysts is an actual task.

One of perspective methods from this point of view is Dynamic Light Scattering (DLS) [2]. It is a cheap, sensitive and fast method for particle size determination. According to basic principles DLS is not applicable to analysis of heterogeneous catalysts or any solid materials since it works only in liquid media. In our work has been shown how to overcome of this limitation. A new technique (STS) for study of supported metal catalysts by DLS has been proposed in this work. This technique has been tested on a set of supported metal catalysts with different types of noble metals (Pt, Pd, Ru and etc.). A good agreement between TEM data and DLS for studied catalysts set it is found. Thereby, possibility of determination particle sizes in supported catalysts using more simple, sensitive and quick method was demonstrated in this work.

*The author is grateful to A.V. Ischenko, D.A. Zyuzin, N.N. Sankova and E.V. Parkhomchuk for assistance in the investigation samples. This work was supported by Ministry of Science and Higher Education of the Russian Federation (project AAAA-A17-117041710079-8).*

### References

1. Rajan, K. *Annu. Rev. Mater. Res.* **2015**, *45*, 153–69.
2. Hassan, P. A.; Rana, S.; Verma, G. *Langmuir* **2015**, *31*(1), 3–12.

## Microscopy study of the catalytic etching of platinum alloy catalyst gauzes during ammonia oxidation

A.N. Salanov, N.M. Chesnokova

*Boreskov Institute of Catalysis, Novosibirsk, Russia*

salanov@catalysis.ru

Ammonia oxidation with air on platinum catalyst gauzes is widely used in chemical industry for synthesis of nitric acid [1]. Catalytic etching during the oxidation of  $\text{NH}_3$  results in a loss of platinum metals, mechanical degradation of gauzes, and reduction of the period of efficient catalyst operation. To overcome these problems, investigation of the catalytic etching of platinum alloy gauzes should be performed.

In this work, to reveal the mechanism of the initial step of catalytic etching, images of the etch pits emerging during the catalytic oxidation of  $\text{NH}_3$  with air oxygen were obtained, and distribution of such pits over the surface and in subsurface layers of platinum alloy gauzes was analyzed. The oxidation of  $\text{NH}_3$  with air was performed on a pack of four gauzes with the total weight of 0.61 g in a laboratory flow-type quartz reactor at the linear feed rate of the mixture ( $\sim 10\%$   $\text{NH}_3$  in air) 2.57 m/s, catalyst temperature  $1133 \pm 5$  K, and total pressure  $\sim 3.6$  bar for 50 h. The surface morphology and microstructure were studied on the first gauze along the gas stream using a JSM-6460 LV (Jeol) scanning electron microscope (SEM) at the energy of beam electrons ( $E_0$ ) from 1 to 25 keV in the secondary electron (SE) mode.

After  $\text{NH}_3$  oxidation, the frontal side of the gauze has mostly a solid rough layer consisting of the “cauliflower”-like agglomerates and regions with a smooth surface. Etch pits with the size of  $\sim 60$  nm were detected on this surface with the concentration  $6.0 \times 10^8 \text{ cm}^{-2}$ . At the boundary with the rough layer, their size increased to 130 nm and concentration decreased to  $1.0 \times 10^8 \text{ cm}^{-2}$ , testifying to the growth and merging of etch pits. In the central part of grains, the concentration of etch pits was approximately threefold higher than in the region near grain boundaries. On the back side of the gauze, close values of the etch pits size and concentration were reported [2]. The observed etch pits residing on dislocations and other defects can serve as the “hotspot”-like sites, which create a temperature gradient in the region of defects on the catalyst surface; this provides a transfer of metal from “hot” regions to “cold” ones, thus leading to etching of the catalyst surface. In the region of defects, there may proceed an intense highly exothermic oxidation of  $\text{NH}_3$  with the oxygen incorporated into subsurface layers. The occurrence of this reaction on defects leads to a local increase in temperature due to strong exothermicity of  $\text{NH}_3$  oxidation. The increase in temperature accelerates the transfer of metal atoms from defects and their migration to the surface. This process results in the emergence and growth of etch pits on the surface in the region of dislocations and grain boundaries, which are seen in images on the back and frontal sides of platinoid gauze. The increased concentration of etch pits in the subsurface layer as compared to the deeper layers and also in the central part of grains as compared to the regions near grain boundaries may be caused by the migration of dislocations during  $\text{NH}_3$  oxidation.

The observed rearrangement of the wire surface layer is caused to a great extent by the formation of “hotspot”-like etch pits, which create a temperature gradient in the region of defects. Thus, metal atoms migrating from defects to the surface during surface diffusion can form crystalline terraces with a low concentration of defects, which cover the entire surface of grains. The growing terraces close etch pits, so a considerable part of the pits appears in subsurface layers.

*This work was supported by Ministry of Science and Higher Education of the Russian Federation (project AAAA-A17117041710079-8).*

### References

1. Hatscher, S. et al. Handbook of Heterogeneous Catalysis, WILEY-VCH Verlag GmbH & Co. KGaA: Weinheim, 2008.
2. Salanov, A. et al. *Kinet. Catal.* **2018**, 59, 792–809

**Diesel oxidation catalyst PtPd/MnO<sub>x</sub>-Al<sub>2</sub>O<sub>3</sub>: prospects for diesel soot emission control**

S.A. Yashnik

*Boreskov Institute of Catalysis, Novosibirsk, Russia*

yashnik@catalysis.ru

Together with the diesel exhaust, soot and toxic nitrogen oxides are emitted into the environment. To clean the diesel exhaust from CO and CH, we proposed a honeycomb monolithic catalyst with Pt – Pd/MnO<sub>x</sub>-Al<sub>2</sub>O<sub>3</sub> as a catalytic washcoating [1]. The catalyst has a low content of noble metals (10–15 g/ft<sup>3</sup> or 0.17–0.35 g/l), but it provides high oxidation efficiency for hydrocarbons and CO due to the thermal activation effect of the Mn–Al–O system [2] as well as the synergism effect between Pt/Pd and defective Mn<sub>3</sub>O<sub>4</sub> particles in catalytic activity [3,4].

In this work, we consider the possibility of diesel soot combustion on the surface of the Pt–Pd/MnO<sub>x</sub>-Al<sub>2</sub>O<sub>3</sub> oxidation catalyst, which differs in the content, particle size, and Pt–Pd state, and attempt to reveal the structure – RedOx – activity correlations.

A comparative study of oxidation mono- and bimetallic catalysts showed the higher activity of Pt–Pd/MnO<sub>x</sub>-Al<sub>2</sub>O<sub>3</sub> in the oxidation of diesel soot with oxygen and nitrogen oxides at temperatures of 400–450 and 375–425 °C, respectively. For this catalyst, the strongest promotion of soot oxidation with nitric oxide (300–500 ppm) was manifested, accompanied by a decrease in the activation energy of the process,  $E_a = 45 \pm 2$  vs.  $225 \pm 20$  kJ/mol.

Raman and DRIFT revealed predominant burnout of amorphous carbon (1500 cm<sup>-1</sup>) with soot conversion of 25-30%, the formation of O-containing groups on the surface of graphite-like soot (G-line), an increase in its defectiveness (D-line), which helps to increase the rate of further burning of soot.

The studies indicate the prospects of application of Pt–Pd/MnO<sub>x</sub>-Al<sub>2</sub>O<sub>3</sub> oxidation catalyst (as washcoating) in the diesel particulate filter.

*This work was performed as part of the state assignment of the BIC SB RAS (project AAAA-A17-117041710086-6).*

**References**

1. Yashnik, S. A.; Denisov, S. P.; Danchenko, N. M.; Ismagilov, Z.R. *Appl. Catal. B.* **2016**, *185*, 322–336.
2. Tsyrlunikov, P. G.; Salnikov, V. S.; Drozdov, V. A.; Stuken, S. A.; Bubnov, A. V.; Grigorov, E. I.; Kalinkin, A. V.; Zaikovskii, V. I. *Kinet. Catal.* **1991**, *32*, 387–394.
3. Yashnik, S. A.; Porsin, A. V.; Denisov, S. P., Danchenko, N. M.; Ismagilov, Z. R. *Top. Catal.* **2007**, *42–43*, 465–469.
4. Yashnik, S. A.; Ishchenko, A. V.; Dovlitova, L. S.; Ismagilov Z. R. *Top. Catal.* **2017**, *60*, 52–72.

# SECTION 1

## CATALYST PREPARATION



## Effect of preparation conditions on photocatalytic performance of Bi-based composites

Yu.A. Belik, E.D. Fakhrutdinova, V.A. Svetlichyi, O.V. Vodyankina

*Tomsk State University, Tomsk, Russia*

belik99q@gmail.com

In the field of the photocatalysis, the low efficiency of generation of charge carriers, their fast recombination in bulk or on surface of material, wide band gap value of semiconductors are the major challenges that reduce the photocatalytic performance. Bi-containing photocatalysts have attracted increased attention due to their peculiar electronic structure that provides absorbance of visible light. Heterojunction or Z-scheme is the most attractive technique as solution for stated issue. Considering the above, the report is focused on the influence of preparation method of composite Bi-based materials on their photocatalytic activity as well as phase composition and physical-chemical properties.

Solvo/hydro-thermal treatment (STT/HTT) of solution/suspension was employed respectively for the synthesis of BSO and BSN seria of photocatalysts. STT/HTT was carried out in Teflon-lined stainless-steel autoclave at 180°C for 12/24 hours, respectively. Then the samples were dried at 60°C for 24 h. The materials were characterized with a number of physico-chemical methods: XRF, TG-DSC, XRD, SEM, TEM, IR, Raman, and UV-Vis diffuse reflectance spectroscopies, electrochemical methods of analysis. Photocatalytic activity of products was tested with two contaminants: Rhodamine B (RhB) under irradiation of 250W Xe lamp and LEDs (378 nm) and phenol (PhOH) solution (LEDs).

Upon co-precipitation of aqueous homogeneous solution, containing  $\text{Bi}(\text{NO}_3)_3$  and  $\text{Na}_2\text{O} \cdot 3\text{SiO}_2$ , the suspension of bismuth oxo/hydroxyl phases was formed, which were then subjected to HTT, resulting in BSN\_NaSi\_pH\_12 sample. It is well-crystalline and contains  $\text{Bi}_2\text{SiO}_5$  phase (96 %wt.) and  $\text{Bi}_{12}\text{SiO}_{20}$  as impurity. Obviously, in aqueous media of HTT stage the growth of crystallites occurred, mainly, eventually leading to the formation of large particles of the photocatalyst.

When  $\text{Bi}(\text{NO}_3)_3 \cdot 5\text{H}_2\text{O}$  being dissolved in EG, the stable complex  $\text{Bi}_2(\text{C}_2\text{H}_4\text{O}_2)_3$  is formed [1]. After STT of solution consisting of  $\text{Bi}_2(\text{C}_2\text{H}_4\text{O}_2)_3$  and TEOS, the obtained BSO sample was synthesized. According to XRD data, the BSO material contains metallic  $\text{Bi}^0$ ,  $\alpha\text{-Bi}_2\text{O}_3$ ,  $\text{Bi}_2(\text{C}_2\text{H}_4\text{O}_2)_3 \cdot 6\text{H}_2\text{O}$ . Apparently, during STT partial reduction of bismuth EG-complexes to metallic bismuth by EG took place. Particles of metallic Bi, in turn, partially oxidized into bismuth oxide.

In other case, the homogeneous solution of  $\text{Bi}_2(\text{C}_2\text{H}_4\text{O}_2)_3$  combined with  $\text{Na}_2\text{O} \cdot 3\text{SiO}_2$  was precipitated with NaOH, which led to formation bismuth oxo/hydroxyl particles with adsorbed EG molecules on their surface. Solvothermal treatment of BSO\_NaSi\_OH sample allowed obtaining material with large semi-transparent plates of  $\text{Bi}_{12}\text{SiO}_{20}$  phase and unidentified spherical globules. If  $\text{Na}_2\text{O} \cdot 3\text{SiO}_2$  was replaced by TEOS solution in the above synthesis, the BSO\_OH sample shows feather-like morphology formed by bismuth metasilicate  $\text{Bi}_2\text{SiO}_5$  phase with small pieces of semi-transparent plates.

All samples prepared from EG solution were calcined at 600 °C for 2 h in order to complete the phase formation. Thus, BSO\_OH\_600 and BSO\_NaSi\_OH\_600 photocatalysts consist of two well-crystalline phases of  $\text{Bi}_2\text{SiO}_5$  and  $\text{Bi}_{12}\text{SiO}_{20}$ , whereas BSO\_600 contains 4 phases:  $\text{Bi}_2\text{SiO}_5$ ,  $\text{Bi}_{12}\text{SiO}_{20}$ ,  $\alpha\text{-Bi}_2\text{O}_3$ , and  $\beta\text{-Bi}_2\text{O}_3$ . Optical properties of materials obtained are in a good agreement with phase formation for both dried and calcined products.

A four-phased composite material decomposes RhB and phenol solutions via selective deethylation and mineralization process, respectively, in a higher extent than the reference  $\alpha\text{-Bi}_2\text{O}_3$  sample and other synthesized photocatalysts. Such photoactivity is connected with better separation of charge carriers in the composite product and the presence of  $\beta\text{-Bi}_2\text{O}_3$ . Furthermore, all photocatalysts prepared are promising materials for water splitting reactions.

*This research project is supported by Russian Science Foundation (project 19-73-30026).*

### References

1. Cloutt, B.A.; Sagatys, D.S.; Smith, G.; Bott, R.C. *Aust. J. Chem.* **1997**, *50*, 947.

## The effect of linker composition on the Pd NPs distribution in UiO-66-type matrix

Burachevskaya O.A.<sup>1</sup>, Butova V.V.<sup>1</sup>, Surzhikova Y.I.<sup>2</sup>, Soldatov A.V.<sup>1</sup>

<sup>1</sup>*The Smart Materials Research Institute, Rostov-on-Don, Russia*

<sup>2</sup>*Institute of Physical and Organic Chemistry, Rostov-on-Don, Russia*

oburachevskaya@sfedu.ru

Metal–organic frameworks (MOFs) are porous materials with high surface area attracting attention due to their numerous potential applications. This class of materials has a wide range of potential applications in gas storage<sup>1</sup>, bio-medical studies<sup>2</sup>, and catalysis.<sup>3</sup>

The high flexibility of MOF structure and composition is the main reason for their success in various fields. MOFs are constructed from two components: inorganic metal clusters – secondary building units (SBU) – and organic molecules acting as linkers. The pair – SBU and linker – determines the symmetry of the resulting MOF. The great number of possible SBUs and linkers results in a great variety of MOF types. This broad field of molecular design is one of the reasons why MOFs are so popular nowadays.

In 2008, Cavka and co-authors described a new family of Zr-based MOFs with high chemical, thermal and mechanical stability.<sup>4</sup> The first member of this family is UiO-66 – MOF based on Zr<sup>4+</sup> with 1,4-benzendicarboxylate (BDC) as a linker. UiO-66 is stable up to 500 °C; it is quite resistant to many solvents. These properties are crucial for the catalytic application. Moreover, it was reported that the UiO-66 matrix combined with polypyrrole enhances the catalytic properties of Pd nanoparticles.<sup>5</sup> The incorporation of the linkers with amino-groups leads to high dispersion of Pd nanoparticles in the porous support.<sup>6</sup> Moreover, the UiO-66 exhibits extreme tolerance to a high concentration of defects. It allowed tuning its properties using the “defect engineering” approach.<sup>7,8</sup> The presence of defects affects MOF's properties.<sup>9</sup> Moreover, it was reported that defects could be post-synthetically functionalized.<sup>10</sup>

The aim of the present work is the design of hybrid material with palladium nanoparticles located in defect-pores of UiO-66, while non-defect pores should be free to decline hindrances due to mass transport effect.

In the first part of our work, we have compared two ways of the incorporation of amino-groups into the UiO-66 structure. First, we have synthesized UiO-66 type MOFs with BDC-NH<sub>2</sub> and BDC-NO<sub>2</sub> linkers. In this way, we have obtained UiO-66-NH<sub>2</sub> and UiO-66-NO<sub>2</sub> with NH<sub>2</sub>- and NO<sub>2</sub>-groups, respectively, in all non-defect pores. Then, both materials were functionalized with Pd nanoparticles by impregnation and reduction method. Powder XRD patterns of obtained composites revealed new reflections, which could be attributed to the palladium phase. According to TEM images, a uniform distribution of the smallest Pd particles was observed for the sample UiO-66-NH<sub>2</sub>@Pd.

Secondly, we have synthesized UiO-66 with the addition of modulator – benzoic acid. In this way, we have obtained UiO-66 with defect pores, where Zr<sup>4+</sup> ions are temporarily compensated with benzoate ions. Then we have applied the post-synthetic treatment to replace benzoate ions in defect pore with amino-benzoate and sulfamoylbenzoate ones. Therefore, in this case, we have obtained UiO-66 with amino-groups only in defect pores. After this, both materials were functionalized with Pd nanoparticles by impregnation and reduction method.

In the second part of our work, we have investigated catalytic properties obtained materials for low-temperature CO oxidation by analysis of the IR absorption spectra of the reaction products.<sup>11</sup>

The highest percentage of carbon dioxide conversion was observed for the two samples. At a temperature of 210 °C, the carbon dioxide conversion for the UiO-66-NH<sub>2</sub>@Pd sample was about 50% and for UiO-66-NH<sub>2</sub>-SO<sub>2</sub>@Pd about 26%. For the remaining samples, this parameter at the same temperature was about 10% and 12%.

*This work was supported by RFBR project 18-29-04053.*

### References

1. Suh, M. P.; Park, H. J.; Prasad, T. K.; Lim, D.-W. *Chemical Reviews* **2012**, *112*, 782-835.

2. Horcajada, P.; Gref, R.; Baati, T.; Allan, P. K.; Maurin, G.; Couvreur, P.; Ferey, G.; Morris, R. E.; Serre, C. *Chem. Rev.* **2012**, *112*, 1232-1268.
3. Llabres i Xamena, F. X. G., J. *Metal Organic Frameworks as Heterogeneous Catalysts*; Royal Society of Chemistry: Cambridge, 2013.
4. Cavka, J. H.; Jakobsen, S.; Olsbye, U.; Guillou, N.; Lamberti, C.; Bordiga, S.; Lillerud, K. P. *J. Am. Chem. Soc.* **2008**, *130*, 13850-13851.
5. Zhao, Y.; Li, Y.; Pang, H.; Yang, C.; Ngai, T. *Journal of Colloid and Interface Science* **2019**, *537*, 262-268.
6. Zhang, Y.; Li, Y.-X.; Liu, L.; Han, Z.-B. *Inorganic Chemistry Communications* **2019**, *100*, 51-55.
7. Atzori, C.; Shearer, G. C.; Maschio, L.; Civalieri, B.; Bonino, F.; Lamberti, C.; Svelle, S.; Lillerud, K. P.; Bordiga, S. *J. Phys. Chem. C* **2017**, *121*, 9312-9324.
8. Taddei, M. *Coord. Chem. Rev.* **2017**, *343*, 1-24.
9. Butova, V. V.; Budnyk, A. P.; Guda, A. A.; Lomachenko, K. A.; Bugaev, A. L.; Soldatov, A. V.; Chavan, S. M.; Oien-Odegaard, S.; Olsbye, U.; Lillerud, K. P.; Atzori, C.; Bordiga, S.; Lamberti, C. *Crystal Growth & Design* **2017**, *17*, 5422-5431.
10. Taddei, M.; Wakeham, R. J.; Koutsianos, A.; Andreoli, E.; Barron, A. R. *Angewandte Chemie International Edition* **2018**, *57*, 11706-11710.
11. Kaichev, V. V.; Chesalov, Y. A.; Saraev, A. A.; Tsapina, A. M. *The Journal of Physical Chemistry C* **2019**, *123*, 19668-19680.



## Metalorganic frameworks for catalytic applications

V.V. Butova, A.L. Bugaev, E.A. Erofeeva, V.A. Polyakov, O.A. Burachevskaya, A.V. Soldatov

*The Smart Materials Research Institute, Southern Federal University, Rostov-on-Don, Russia*

vbutova@sfed.ru

Metalorganic frameworks (MOFs) are porous materials with module structure.<sup>1</sup> They could be considered as a combination of two counterparts – secondary building units (SBUs) and linkers. SBUs are inorganic clusters contained one or more metal ions coordinated by oxygen or nitrogen. These clusters are bonded to each other through organic molecules – linkers. Due to the module structure, MOFs could be designed for a particular application. It leads to the success of MOFs in various fields, including catalysis.<sup>2</sup>

MOFs could be applied to a catalytic direction in various ways. A porous MOF matrix could be considered as a nanoreactor for the synthesis of catalytic nanoparticles (NP). In this way, particle growth will be limited by the volume of a single pore, preventing both recrystallization and aggregation of catalysts.

As an example of this approach, we provide results of the functionalization of MOF-199 with gold nanoparticles.<sup>3</sup> For the localization of gold ions inside MOF-199 pores, we used the two-solvents method. At the first step, MOF powder was suspended in hexane. Then the water solution of the gold precursor was added dropwise. It led to the concentration of hydrophilic MOF inside water droplets and promoted the incorporation of the gold precursor into the porous structure. After reduction with sodium citrate, monodispersed gold NPs about 7 nm were obtained.

It should be noted, the catalytic activity of the composite material could be lower than expected due to the hindrances from mass transport in MOF crystal. However, MOF rigid carcass enhances the selectivity of catalysis. Moreover, the introduction of functional groups through the linker molecules could further affect catalytic properties.

In our recent work, we used the target functionalization of defect pores in UiO-66 with palladium NPs. For this purpose, at the first step, we have obtained UiO-66 type MOFs with defect pores.<sup>4</sup> Then we have decorated these pores with NH<sub>2</sub>-groups using the post-synthetic treatment. Finally, we have introduced PdCl<sub>4</sub><sup>2-</sup> ions into the MOF matrix, where they have bonded with amino-groups. After reduction, it resulted in localization of Pd NPs inside defect pores connected to each other through vacant regular pores. Such a multistep process combines advantages of high MOF selectivity with higher availability of active NPs.

Synthesis approach when NPs are obtained inside pores of MOFs is often called “the ship inside the bottle”. The opposite approach of design composite catalytically active MOFs is the so-called “bottle around the ship”. It implements the synthesis of the MOF shell on the surface of the NP’s core.<sup>5</sup> In this way, the MOF layer protects NPs from aggregation and corrosion, while porous structure opens access to the surface of catalyst only for small enough molecules. In both mentioned methods, the MOF matrix used in combination with catalytically active NPs. However, the MOF matrix could be considered as a sacrificial precursor for synthesis catalytically active NPs. According to this approach, metal-contained NPs could be obtained from the MOF material by means of decomposition.<sup>6</sup> It provides a list of advantages, such as narrow particle size distribution, the possible introduction of active species from the pores. Moreover, linkers in oxygen-free pyrolysis form porous carbon optionally doped with heteroatoms.

In the present work, we used MOFs from the ZIF-8 family to obtain zinc oxide doped with cobalt as photocatalytic nanoparticles. At the first step, bimetallic ZIFs were obtained using an MW-assisted solvothermal technique.<sup>7</sup> It allowed us to mix zinc and cobalt ions inside one porous structure. Using pyrolysis, we have obtained monodisperse Zn<sub>1-x</sub>Co<sub>x</sub>O particles about 20-30 nm. To reduce the size of oxide NPs, we applied impregnation of ZIFs with tetraethoxysilane prior to the pyrolysis. It results in 5-7 nm nanoparticles covered with a silica shell.

To sum up, the module structure of MOFs allowed the design of suitable materials for any application. Linker molecules define the size and functionality of pores and could be considered as a source of porous carbon in the course of sacrificial pyrolysis. SBUs in the same process provide metal

ions for NPs formation. Rigid porous matrix of MOFs could be used as a nanoreactor for the synthesis of NPs, and in the same way, provides selectivity for the catalytic process. As a result, the application of MOFs in the field of catalysis is one of the most popular directions nowadays.

*This work was supported by the Russian Science Foundation grant 20-43-01015.*

## References

1. (a) Butova, V. V.; Soldatov, M. A.; Guda, A. A.; Lomachenko, K. A.; Lamberti, C., *Russ. Chem. Rev.* **2016**, 85 (3), 280-307; (b) Tranchemontagne, D. J.; Mendoza-Cortes, J. L.; O'Keeffe, M.; Yaghi, O. M., *Chem. Soc. Rev.* **2009**, 38 (5), 1257-1283.
2. Farrusseng, D.; Aguado, S.; Pinel, C., *Angew. Chem.-Int. Edit.* **2009**, 48 (41), 7502-7513.
3. Butova, V. V.; Kirichkov, M. V.; Budnyk, A. P.; Guda, A. A.; Soldatov, M. A.; Lamberti, C.; Soldatov, A. V., *Polyhedron* **2018**, 154, 357-363.
4. (a) Butova, V. V.; Budnyk, A. P.; Guda, A. A.; Lomachenko, K. A.; Bugaev, A. L.; Soldatov, A. V.; Chavan, S. M.; Oien-Odegaard, S.; Olsbye, U.; Lillerud, K. P.; Atzori, C.; Bordiga, S.; Lamberti, C., *Cryst. Growth Des.* **2017**, 17 (10), 5422-5431; (b) Butova, V. V.; Budnyk, A. P.; Charykov, K. M.; Vetlitsyna-Novikova, K. S.; Bugaev, A. L.; Guda, A. A.; Damin, A.; Chavan, S. M.; Øien-Ødegaard, S.; Lillerud, K. P.; Soldatov, A. V.; Lamberti, C., *Inorg. Chem.* **2019**, 58 (2), 1607-1620.
5. Rosler, C.; Aijaz, A.; Turner, S.; Filippousi, M.; Shahabi, A.; Xia, W.; Van Tendeloo, G.; Muhler, M.; Fischer, R. A., *Chem.-Eur. J.* **2016**, 22 (10), 3304.
6. Zhong, H. X.; Wang, J.; Zhang, Y. W.; Xu, W. L.; Xing, W.; Xu, D.; Zhang, Y. F.; Zhang, X. B., ZIF-8 *Angew. Chem.-Int. Edit.* **2014**, 53 (51), 14235-14239.
7. Butova, V. V.; Polyakov, V. A.; Budnyk, A. P.; Aboraia, A. M.; Bulanova, E. A.; Guda, A. A.; Reshetnikova, E. A.; Podkovyrina, Y. S.; Lamberti, C.; Soldatov, A. V., *Polyhedron* **2018**, 154, 457-464.

## Synthesis and catalytic properties of Ni supported on ceria-zirconia with Ti, Nb and Nb+Ti for methane dry reforming

V.E. Fedorova<sup>1</sup>, M.N. Simonov<sup>1,2</sup>, Yu.N. Bepalko<sup>1</sup>, K.R. Valeev<sup>1</sup>, E.A.Smal<sup>1</sup>, V.A.Sadykov<sup>1,2</sup>

<sup>1</sup> Boreskov Institute of Catalysis, Novosibirsk, Russia

<sup>2</sup> Novosibirsk State University, Novosibirsk, Russia

valeria@catalysis.ru

Currently, there are global problems such as limited natural resources (oil, coal, natural gas) and environmental pollution. Therefore, it is necessary to recycle carbon dioxide and methane, which called greenhouse gases. Thus, methane dry reforming is a promising way to utilize both greenhouse gases producing syngas.

Catalysts used in dry reforming of methane generally contain nickel. Ni systems are cheap, but there are disadvantages such as coke formation and Ni sintering. The use of complex oxides with high oxygen mobility as supports allows to increase stability and activity of catalysts due to the gasification of coke precursors. The oxygen mobility and reactivity can be changed by introducing additional cations with diameter which differs from those of cerium.

In this work, Ni containing ceria-zirconia systems as well as catalysts doped with Ti and Nb were synthesized, and studied in methane dry reforming process.

The mixed oxides were prepared using two methods: synthesis in supercritical medium (1<sup>st</sup> group, denoted as “sc”) and using polymer precursors (Pechini technique, 2<sup>nd</sup> group, denoted as “Pe”). Oxides were calcined in air at 700°C. It was shown that all oxide samples represented one phase – pseudocubic solid solution CeO<sub>2</sub>-ZrO<sub>2</sub>. It is worth noting that the doping cations are integrated into the fluorite structure; no separate phases of corresponding oxides were detected. According to TEM, the average crystallite size is 15 nm. Nickel was loaded by incipient wetness impregnation method followed by calcination in air at 700°C.

Then obtained catalysts were investigated in methane dry reforming reaction in following conditions: temperature range of 600–750 °C with a contact time of 7.5 and 10 ms, an initial concentration of 15% CH<sub>4</sub> and 15% CO<sub>2</sub>. Before the reaction, for all the catalysts, a pretreatment in 10 vol.% O<sub>2</sub>/N<sub>2</sub> at 600 °C for 30 minutes and reduction in 5 vol.% H<sub>2</sub>/He at 600 °C for 60 minutes were carried out.

The dependences of methane and carbon dioxide conversions, hydrogen and CO yields, and also the composition of the synthesis gas as a function of temperature and the reaction time were obtained. The CH<sub>4</sub> conversion changed in the following way: for 1<sup>st</sup> catalysts group: Ni/CeTiNbZr-sc > Ni/CeZr-sc > Ni/CeTiZr-sc > Ni/CeNbZr-sc, for 2<sup>nd</sup> catalysts group: Ni/CeZr-Pe > Ni/CeNbZr-Pe > Ni/CeTiZr-Pe > Ni/CeTiNbZr-Pe.

For catalysts synthesized in supercritical medium the catalytic activity in terms of turnover frequency (TOF) was calculated. It was accepted that the reaction order is first by methane and zero by CO<sub>2</sub>. The activity increase in the row: Ni/CeZr-sc < Ni/CeTiZr-sc < Ni/CeNbZr-sc < Ni/CeTiNbZr-sc.

The catalysts after the reaction were studied by TEM. For the 1<sup>st</sup> catalysts group, the formation of carbon nanotubes was shown, resulting in the encapsulation of Ni. For the 2<sup>nd</sup> catalysts group, the carbon nanotubes wasn't observed. In all cases, there is a homogeneous distribution of cations in the carrier. It was also found that the crystallite size after the reaction remains almost unchanged, which indicates high thermal stability.

*This work was supported by Russian Science Foundation Grant №18-73-10167.*

### References

1. Hu Y.; Ruckenstein E. *Adv.Catal.* **2004**, 48, 297.
2. Slostowski C.; Marre S.; Babot O.; Toupance T.; Aymonier C. *Langmuir*. **2012**, 28, 16658.
3. Makri M.; Vasiliades M.; K. Petallidou K.; Efstathiou A. *Catal. Today* **2015**, 259, 115.

## Ordered macroporous $\alpha$ -alumina as catalyst support for enhanced thermal stability of silver nanoparticles

P.H. Keijzer, Jeroen E. van den Reijen, Claudia J. Keijzer, Krijn P. de Jong, P.E. de Jongh

*Inorganic Chemistry and Catalysis, Debye Institute for Nanomaterials Science,  
Utrecht University, Universiteitsweg 99, 3584 CG Utrecht, The Netherlands*

p.h.keijzer@uu.nl

Supported silver catalysts are industrially used for the epoxidation of ethylene to ethylene oxide. In this process,  $\alpha$ -alumina is used as support material. Hydroxyl groups present on the surface have a negative effect on the selectivity in the epoxidation reaction [1, 2]. Therefore,  $\alpha$ -alumina, with a low specific surface area of circa  $1 \text{ m}^2 \text{ g}^{-1}$  is used in industry [3]. Even though this low surface area is beneficial for the selectivity of the reaction, it is often disadvantageous for the stability of the catalyst.

$\alpha$ -alumina, the most stable alumina crystal structure, is formed by heating aluminum hydroxide to  $1150^\circ\text{C}$ . Increasing the surface area by introducing porosity in  $\alpha$ -alumina is complicated, not only by the high temperature, but also by the many phase transformations taking place before the  $\alpha$ -phase is obtained. As a result, the pore structure collapses, when not properly stabilized. We developed a strategy to stabilize the macroporous structure up to high temperatures, and show the preparation of a range of high surface area, ordered macroporous  $\alpha$ -alumina materials with varying cage and window sizes, and show their application as support material for silver catalysts.

Ordered macroporous  $\alpha$ -alumina was obtained by using sacrificial templates consisting of polymer spheres stacked as colloidal crystals. By pyrolysis of the polymer template, we created a carbon coating which stabilized the pore structure during phase transitions even at  $1150^\circ\text{C}$  [4]. This way, ordered macroporous  $\alpha$ -alumina with a high degree of pore order and high specific surface areas ( $25\text{--}35 \text{ m}^2 \text{ g}^{-1}$ ) were synthesized. By varying the polymer sphere size in the sacrificial template, the cage and window sizes were varied. After synthesis of the support, we deposited silver on the  $\alpha$ -alumina, and demonstrated the superior stability of the silver particles compared to commercial, low surface area  $\alpha$ -alumina supports. The increased stability of the silver is not only induced by the increase in alumina surface area, but is further enhanced by the cage-like structure of the alumina, and dependent on the window size of the cage structures.

### References

1. M. O. Ozbek, I. Onal, R. A. van Santen, *J. Catal.*, **284**, 230–235 (2011)
2. J. E. van den Reijen et al, *Cat. Today*, **338**, 31–39 (2019)
3. J. K. Lee, X. E. Verykios, R. Pitchai, *Appl. Catal.*, **44**, 223–237 (1988)
4. J.E. van den Reijen & P.H. Keijzer, P.E. de Jongh, *Materialia*, **4**, 423–430 (2018)

## **Mechanochemical synthesis and investigation of catalysts based on MAI-layered double hydroxides (M - Mg, Ni, Co) for the selective hydrogenation of furfural**

E.O. Kobzar<sup>1</sup>, L.N. Stepanova<sup>1,2</sup>, O.B. Belskaya<sup>1,3</sup>, N.N. Leont'eva<sup>1</sup>, T.I. Gulyaeva<sup>1</sup>

<sup>1</sup> *Center of New Chemical Technologies BIC, Boreskov Institute of Catalysis, Omsk, Russia*

<sup>2</sup> *Dostoevsky Omsk State University, Omsk, Russia*

<sup>3</sup> *Omsk State Technical University, Omsk, Russia*

kbzlina@mail.ru

The creation of active and environmentally friendly catalysts for the process of hydrogenation of furfural is an urgent task. Systems containing nickel as an active component exhibit high activity. However, their catalytic characteristics strongly depend on the dispersion of the metal. Catalysts, based on the layered double hydroxide (LDH) can provide high dispersion. Mechanochemical method is a promising, quick and waste-free method for the synthesis of LDH. It is based on the passing of a solid-phase reaction between metal hydroxides on the surface of grinding bodies, which receive a lot of energy in a collision.

The aim of this work was the synthesis by the mechanochemical method of layered hydroxides containing simultaneously four metals (Mg, Ni, Co, Al). Influence of the composition of such catalysts on their structural properties, the process of reduction of active metals and catalytic properties in the reaction of aqueous-phase hydrogenation of furfural was studied.

The synthesis of MAI-LDH (M - Mg, Ni, Co) with a different ratio of metals in the composition of LDH by the mechanochemical method was carried out in two stages. At the first stage, metal hydroxides taken in calculated ratios were subjected to mechanochemical activation in an AGO-2C ball planetary mill. In the second stage, the samples were aged in distilled water. The metal content in the samples was determined by inductively coupled plasma atomic emission spectroscopy on a Varian 710-ES device. Investigation of structural properties of synthesized LDH was carried out by X-ray diffraction (XRD) analysis on a D8 Advance (Bruker) diffractometer. Temperature-programmed reduction of active metals was examined by H<sub>2</sub>-TPR using an AutoChem II 2920 (Micromeritics) chemisorption analyzer equipped with a thermal conductivity detector (TCD). The investigation of catalytic activity was carried out on the installation for liquid-phase hydrogenation of furfural at elevated pressure. The reaction was carried out at a temperature of 90 °C, a hydrogen pressure of 2.0 MPa and a concentration of furfural in an aqueous solution of 5 wt%. The reaction products were analyzed by gas chromatography on a Chromos GH-1000 chromatograph (Chromos) equipped with a VB-WAX capillary column and a flame-ionization detector.

During the work, the MgNiCoAl-LDH series with various Ni and Co content were synthesized at a constant M<sup>II</sup>/M<sup>III</sup> ratio of 2. The quantitative analysis of metals in the samples after their dissolution showed that the experimental ratio of metals corresponds to the calculated one, which indicated the complete course of the reaction during mechanochemical activation. Analysis of diffractograms showed that the structure of synthesized samples corresponded to the structure of LDH. It was found that the obtained catalysts showed high catalytic activity in the reaction of aqueous-phase hydrogenation of furfural. Thus, it has been established that an environmentally friendly and less laborious method of mechanochemical synthesis is a promising method for the synthesis of highly active catalysts for the selective hydrogenation of furfural based on LDH.

*This work was carried out within the state task of the Boreskov Institute of Catalysis (No. AAAA-A17-117021450095-1). The research was performed using equipment of the Shared-Use Center "National Center for the Study of Catalysts" at the Boreskov Institute of Catalysis.*

## Immobilization of gold-silver nanoparticles in porous space UiO-66

Kurmanbayeva K., Timofeev K.L., Ten S., Vodyankina O.V.

*National Research Tomsk State University, Tomsk, Russia*

rip\_richard@mail.ru

Nanoparticles of noble metals have been widely used in heterogeneous catalysis, one of the important tasks is their stabilization on the surface and/or in the porous space of the support [1]. Metal-organic frameworks (MOFs) are a new class of porous materials consisting of metal ions or metal-oxygen clusters connected by organic linker molecules. MOFs are of particular interest in heterogeneous catalysis because of their features, and allow the nanoparticles to be effectively stabilized while their catalytic properties remain unchanged.

In this work, a number of hybrid materials of the composition AgAu@UiO-66 were synthesized, and their physical and chemical characteristics were studied. The double-solvent impregnation method was employed to synthesize a series of samples with AgAu@UiO-66 structure containing 1% weight of metal with different Ag/Au ratio. Water and heptane were used as hydrophilic and hydrophobic solvents respectively.

The texture characteristics of the obtained samples were examined by low-temperature N<sub>2</sub> adsorption method. After immobilization of the metals, there was a decrease in specific surface area for all the samples. The data on the pore size distribution demonstrate that during metal immobilization the pores of the UiO-66 were partially filled and the sample with a ratio of Ag:Au = 9:1 was completely filled with a 1.1 nm width pores.

Additionally, the samples were examined by UV-Vis diffuse reflectance spectroscopy. For the monometallic samples Ag@UiO-66 and Au@UiO-66, intense absorption bands were observed at 400 nm and 542 nm respectively. Samples containing both metals had an absorption band at 535 nm, identical to the one of the Au@UiO-66 sample. Suppression of the silver plasmon resonance band for AgAu@UiO-66 samples can be attributed to the surface coating that contains silver nanoparticles with gold atoms and to the formation of bimetallic particles with a "core-shell" structure [2], along with Au<sup>0</sup> particles.

No reflexes for Ag particles were found on the diffractogram of the Ag@UiO-66 sample, which is related to the small size of the nanoparticles. Introduction of gold leads to the appearance of characteristic peak of Au particles (111) in area  $2\theta = 38.1^\circ$ . The detailed analysis of this area makes it visible that the maximum of characteristic peak for Au (111) in bimetallic samples is displaced towards the area  $2\theta = 38.2^\circ$  (peak of Ag (111)). This might be the evidence of the interaction between particles of silver and gold [3].

The catalytic activity of the obtained samples was studied in the oxidation reaction of propylene glycol to lactic acid using molecular oxygen as an oxidant and depending on temperature, oxygen pressure, solvent composition, and Ag/Au ratio.

*The work was carried out with the financial support of the Russian Science Foundation (project 19-73-30026).*

### References

1. Zhou Y.; Yu L. et al. *Industrial & Engineering Chemistry Research* **2019**, 58, 19202.
2. Leus K.; Concepcion P. et al. *RSC Advances* **2015**, 5, 22334.
3. Akbarzadeh E.; Falamarzi M.; Gholami M.R. *Materials Chemistry and Physics* **2017**, 198, 374.

## Ultra-small Pd nanoparticles on CeO<sub>2</sub> for catalytic oxidation of carbon monoxide

V.A. Polyakov, A.A. Tereshchenko, A.A. Guda

*The Smart Materials Research Institute, Southern Federal University, Rostov-on-Don, Russia*

v.polakov93@gmail.com

Noble-metal nanoparticles (NPs) on different substrates are well-known catalysts for the hydrogenation and oxidation reactions, as well as the oxidation of carbon monoxide. The catalyst efficiency depends both on the properties of the noble-metal nanoclusters (size, particle shape) [1] and on the substrate material [2]. The substrate functionalization and uniform distribution of catalytic centers on the substrate surface also play a significant role [3].

Here we are presenting the synthesis and characterization of ultra-small palladium nanoparticles on a modified cerium dioxide substrate (Pd/CeO<sub>2</sub>) obtained by impregnation and further reduction of palladium in an H<sub>2</sub>/Ar flow [4]. Cerium dioxide was treated with tetraethylenepentamine (TEPA). The resulting surface has electron-donating properties and better adsorbs positively charged noble-metal ions. Tetraaminepalladium (II) chloride was selected as the palladium precursor. This choice was made for two reasons: firstly, the complex amine salts of noble-metals are highly soluble in water and do not undergo hydrolysis, in contrast to simple chlorides; secondly, amine complexes have a high affinity for TEPA amino groups. These factors contribute to the formation of a large number of nucleation centers and reduce the size of the formed NPs. The obtained palladium nanoparticles have good dispersion, but their small size, as well as low Z-contrast, make it difficult to analyze them using traditional methods, such as X-ray powder diffraction and transmission electron microscopy. Therefore, to determine the particle size and their morphology, we used Diffuse reflectance infrared Fourier-transform (DRIFT) spectroscopy with CO probe molecules. Due to the presence of vibration frequencies characteristic for bridged sites between several Pd atoms, we proved the presence of Pd nanoparticles on the ceria surface, but not individual atoms. Using the relationship between linear and bridge sections, we were able to estimate the average size of Pd nanoparticles (1.5-2 nm). The result is consistent with measurements of chemisorption and X-ray absorption near edge structure analysis XANES.

The material showed high catalytic activity in the CO oxidation reaction: 100% CO conversion was achieved at about 50 °C, while for most of the cited literature, such a high conversion was usually observed at 100 °C or higher for Pd NPs. This fact may indirectly indicate the predominance of the surface faces of CeO<sub>2</sub> (111) [5].

*This work was supported by the Russian Science Foundation (grant No. 17-72-10245).*

### References

1. Kinoshita, K. *Journal of The Electrochemical Society* **1990**, 137, 845-848.
2. Rojluetchai, S.; Chavadej, S.; Schwank, J. W.; Meeyoo, V. *Catalysis Communications* **2007**, 8, 57-64.
3. Nie, L.; Mei, D.; Xiong, H.; Peng, B.; Ren, Z.; Hernandez, X. I. P.; DeLaRiva, A.; Wang, M.; Engelhard, M. H.; Kovarik, L.; Datye, A. K.; Wang, Y. *Science* **2017**, 358, 1419-1423.
4. Tereshchenko, A.; Polyakov, V.; Guda, A.; Lastovina, T.; Pimonova, Y.; Bulgakov, A.; Tarasov, A.; Kustov, L.; Butova, V.; Trigub, A.; Soldatov, A. *Catalysts* **2019**, 9, 385.
5. Spezzati, G.; Su, Y.; Hofmann, J. P.; Benavidez, A. D.; DeLaRiva, A. T.; McCabe, J.; Datye, A. K.; Hensen, E. J. M. *ACS Catalysis* **2017**, 7, 6887-6891.

## Synthesis of nanotubular titanium dioxide with high specific surface area

A.A. Sushnikova<sup>1,2</sup>, A.A. Valeeva<sup>1,3</sup>, I.B. Dorosheva<sup>1,2,3</sup>, A.A. Rempel<sup>1,2,3</sup>

<sup>1</sup>*Ural Federal University, Yekaterinburg, Russia*

<sup>2</sup>*Institute of Metallurgy of the Ural Branch of the Russian Academy of Sciences, Yekaterinburg, Russia*

<sup>3</sup>*Institute of Solid State Chemistry of the Ural Branch of the Russian Academy of Sciences, Yekaterinburg, Russia*

sushnikova.ann@gmail.com

In the last decade, nanostructured TiO<sub>2</sub> has attracted increasing attention of researchers around the world in connection with the promising of its use as a photocatalyst for the synthesis of organic molecules with high efficiency in accordance with the principles of green chemistry. The completeness of the synthesis reaction and the catalytic activity of the photocatalyst are affected by many factors, such as the band gap width of the photocatalyst, high specific surface, the presence of structural vacancies in crystal structure, the concentration of active centers on the surface, excited-state lifetime of electrons and holes.

Nanostructured titanium dioxide TiO<sub>2</sub> is a nontoxic, ecologically friendly, economically affordable, efficient photocatalyst with a wide range of uses [3]. In addition, titanium dioxide is a stable and environmentally resistant functional material.

The aim of this study is to find out the synthesis parameters of nanotubular titanium dioxide to improve its photocatalytic activity by increasing the specific surface area.

To achieve this goal, nanotubular titanium dioxide was synthesized by anodizing titanium foil in a potentiostatic mode for 60 minutes at a voltage of 60 V while maintaining the temperature of the electrolyte at 20 °C. A fluorine-containing solution of ethylene glycol with the addition of distilled water in the proportion of NH<sub>4</sub>F: H<sub>2</sub>O: C<sub>2</sub>H<sub>6</sub>O<sub>2</sub> = 1 : 2 : 98 by weight was used as the electrolyte.

X-ray phase analysis of the nanotubular titanium dioxide was performed using a STADI auto-diffractometer (STOE, CuK $\alpha$ <sub>1</sub> radiation, position-sensitive detector PSD, Bragg-Brentano geometry, 2 $\theta$  from 10 to 80°) with a scanning step of 0.03 ° at room temperature. An intense diffuse halo in the angles region and absence of the diffraction peaks for as-prepared film indicates that the nanotubular titanium dioxide has an amorphous structure.

The specific surface area of nanotubular titanium dioxide, after preliminary degassing at 120 °C, was low and amounted to 14.4 ± 0.1 m<sup>2</sup>/ g. A study of the morphology of nanotubular titanium dioxide, carried out using a scanning electron microscope, indicated the possibility of achieving a larger specific surface area of the samples, therefore the sample was further annealed in air at a temperature of 350 °C. After annealing, the specific surface increased several times and reached 54.2 ± 1.1 m<sup>2</sup>/g. Thus, the synthesis and additional annealing conditions used made it possible to achieve high specific surface areas, which is typical for catalysts with high catalytic activity.

This study was financially supported by the Russian Foundation for Basic Research (Project No. 20-03-00299).

### References

1. Dorosheva, I.B., Rempel, A.A., et. al., *Inorganic Materials*, **2019**, 55(2), 155-161.
2. Valeeva, A.A., Kozlova, E.A. et. al., *Scientific Reports*, **2018**, 8(1), 9607.
3. Chen, X. , Mao, S.S. , *Chem. Rev.*, **2007**, 107, 2891.



## Design of Ag-CeO<sub>2</sub>/SBA-15 catalysts for room-temperature 4-nitrophenol reduction

A.V. Taratayko, G.V. Mamontov\*

*Tomsk State University, Tomsk, Russia*

grigoriymamontov@mail.ru

Catalytic hydrogenation of nitroaromatic compounds into corresponding aminoaromatic compounds using environmentally safe materials is an attractive approach to address two challenges: efficient removal of the nitroaromatic compounds from wastewaters and enlarging the manufacturing scale of the aminoaromatic compounds employed in pharmaceutical, chemical, and agrichemical industries [1, 2]. The Ag/CeO<sub>2</sub> system is a promising catalytic composition with strong metal-support interaction resulting in charge transfer over the interface and cooperative action of the metal and oxide active sites in catalytic reactions [3]. However, Ag/CeO<sub>2</sub> systems tend to form aggregates of large size, and this substantially decreases the active surface and catalytic activity. It is required to utilize primary support, for instance, SiO<sub>2</sub>. The SBA-15 material is a mesoporous silica with hexagonally ordered cylindrical pores and high surface area (550–900 m<sup>2</sup>/g) [4] allowing its application as a catalyst support. The work aims to prepare Ag-CeO<sub>2</sub>/SBA-15 system and study the synergetic effect of the Ag-CeO<sub>2</sub> interface on catalytic activity in the 4-nitrophenol (4-NP) reduction into 4-aminophenol (4-AP) at room temperature.

The SBA-15 was prepared by the template method [5] using triblock copolymer Pluronic P123 (BAFS, Germany). Silver- and/or ceria-containing catalysts (Ag/SBA-15, CeO<sub>2</sub>/SBA-15, Ag-CeO<sub>2</sub>/SBA-15) were prepared by the incipient wetness impregnation of the Pluronic P123@SBA-15 hybrid using AgNO<sub>3</sub> and/or Ce(NO<sub>3</sub>)<sub>3</sub>·6H<sub>2</sub>O aqueous solutions with addition of citric acid. Nominal loading of silver and ceria in the catalysts was 5 and 10 wt.%, respectively. The synthesized samples were characterized by N<sub>2</sub> sorption, XRD, SAXS, UV-vis DRS, H<sub>2</sub>-TPR, and tested in 4-NP reduction into 4-AP by sodium borohydride (NaBH<sub>4</sub>) at room temperature and atmospheric pressure in water medium.

According to results of low-temperature N<sub>2</sub> sorption, the synthesized samples possess high surface area (594–754 m<sup>2</sup>/g), large pore volume (0.86–1.04 cm<sup>3</sup>/g), and a narrow pore size distribution in the range between 5.5 and 7.8 nm. The XRD and SAXS data indicate the formation of Ag and CeO<sub>2</sub> particles with sizes up to 10 and 3–4 nm, respectively, and justify hexagonally ordered porous structure of the SBA-15 material. Both the simultaneous reduction of the AgO<sub>x</sub> and surface of CeO<sub>2</sub> particles in TPR and the red shift of the surface plasmon resonance (SPR) peak of Ag nanoparticles in UV-vis spectra for Ag-CeO<sub>2</sub>/SBA-15 catalyst indicate the presence of Ag-CeO<sub>2</sub> interface in catalysts. The reduction of 4-NP reaction does not proceed without the catalyst. The support (SBA-15) and the CeO<sub>2</sub>/SBA-15 sample show rather low activity in the process, while Ag-containing samples (Ag/SBA-15 and Ag-CeO<sub>2</sub>/SBA-15) are active, with the latter showing superior activity. Rate constants were calculated within pseudo-first order reaction model and amounted to  $k_{exp} = 0.010 \text{ s}^{-1}$  and  $k_{exp} = 0.016 \text{ s}^{-1}$ , respectively.

To conclude, the obtained samples possessed the high surface area and narrow pore size distribution. The key role in stabilization of the dispersed Ag and CeO<sub>2</sub> particles (<5 nm) with the developed active surface was attributed to the confined porous structure of the SBA-15 serving as a nanoreactor, application of citric acid, and additional stabilization features of the triblock copolymer. The study of the optical properties and the reduction features indicated the developed Ag-CeO<sub>2</sub> interfacial interaction in the Ag-CeO<sub>2</sub>/SBA-15 system that enhanced the catalytic response in the 4-NP reduction.

*This work was supported by the Russian Science Foundation (grant No. 18-73-10109).*

### References

1. Song, J.; Huang, Z.-F.; Pan, L.; Li, K.; Zhang, X.; Wang, L.; Zou, J.-J. *Appl. Catal., B.* **2018**, *227*, 386–408.
2. Mali, M. *Synth. Catal.* **2017**, *2*.
3. Grabchenko, M. V.; Mamontov, G. V.; Zaikovskii, V. I.; La Parola, V.; Liotta, L. F.; Vodyankina, O. V. *Appl. Catal., B.* **2020**, *260*, 118148.
4. Meynen, V.; Cool, P.; Vansant, E. F. *Microporous mesoporous mater.* **2009**, *125*, 170–223.
5. Zhao, D.; Huo, Q.; Feng, J.; Chmelka, B. F.; Stucky, G. D. *J. Am. Chem. Soc.* **1998**, *120*, 6024–6036.

## In situ monitoring of Pd/CeO<sub>2</sub> nanoparticles growth by means of FTIR spectroscopy

A.A. Tereshchenko, A.A. Guda, V.A. Polyakov, A.V. Soldatov

*The Smart Materials Research Institute, Rostov-on-Don, Russia*

tereshch1@gmail.com

Ceria supported nanoparticles (NPs) of noble metals are well-known catalysts for diverse hydrogenation and oxidation reactions [1, 2]. Their catalytic activity depends on several factors such as the dispersion and shape of NPs [3], the material of the support [4] and the functionalization [5], etc. However, the use of high Z-support and extremely small NPs limits the diagnostics of these materials especially in laboratory conditions [6].

In this study, we demonstrate a possibility of in situ monitoring the size and surface morphology of Pd/CeO<sub>2</sub> catalysts during the growth of NPs by using FTIR spectroscopy of adsorbed CO.

Ceria NPs used as support were synthesized according to the method described in [7]. Then, CeO<sub>2</sub> was impregnated by PdCl<sub>2</sub> (procedure shown in [6]) and activated in a flow of Ar (46.5 mL/min) at 30, 150 or 300 °C (samples Pd-30, Pd-150, Pd-300) for 30 min. Then a mixture of H<sub>2</sub> (2.5 mL/min), CO (1 mL/min) and Ar (46.5 mL/min) was passed through the sample for 1 hour to reduce Pd NPs. After this samples were slowly cooled down to the room temperature in the mixture of CO (1 mL/min) and Ar (46.5 mL/min). The reduction stage was performed in the Praying Mantis Low Temperature Reaction Chamber (Harrick, USA) connected with an external gas line equipped with mass-flow controllers.

X-ray fluorescence elemental analysis confirmed the expected loading of Pd (close to 4 wt %) for all samples. X-ray powder diffraction didn't allow distinguishing Pd NPs for all samples. Particularly, the most intensive peak related to diffraction on Pd (111) planes was missing. Only a strong signal of ceria support was observed. This fact could be explained by the small size of synthesized Pd NPs which caused broadening of peaks. Tests of catalytic (procedure described in [6]) shown that CO conversion was 25–50% for all samples at 150 °C even without calcination.

The growth of NPs was monitored in situ by simultaneous CO probing molecules adsorption and measurement of infrared spectra in DRIFT geometry. Vertex 70 (Bruker, USA) spectrometer equipped with an MCT-detector was used to record spectra of the sample placed in the reaction chamber. All spectra were obtained with a 1 cm<sup>-1</sup> resolution for 64 scans and transformed into absorption spectra using the Kubelka–Munk function. Infrared spectra were collected during the entire procedure of NPs growth.

The series of spectra collected in situ demonstrated that the reduction at high temperature (Pd-300 and Pd-150) was much faster than at low temperature (Pd-30). Also, it was observed that reduction was not complete for all samples: peaks of CO adsorbed on Pd<sup>2+</sup> and Pd<sup>+</sup> ions were observed even after reduction (ca. 2160 and 2110 cm<sup>-1</sup>). The last fact is explained by ceria support that prevented complete reduction. The process of reduction was observed in details for Pd-30 sample where the decrease of CO adsorbed on Pd ions was accompanied by the increase of peaks related to bridged carbonyls – evidence of appearing and growth of the extended surfaces.

FTIR spectra allowed to determine the size of NPs which is proportional to the ratio of areas under peaks attributed to bridged (below 2000 cm<sup>-1</sup>) and linear (2000–2100 cm<sup>-1</sup>) carbonyls. Size decreased in row Pd-300>Pd-150>Pd-30. The dynamics of growth was clearly observed for Pd-30 and Pd-150 sample whereas for Pd-300 CO adsorbed only at 2- and 3-folded sites. Only carbonyls on Pd(111) faces were detected for Pd-150 and Pd-300 when both Pd(100) and Pd(111) facets were found for the Pd-30 sample.

The described method is the development of a conventional technique of catalysts probing which, as was shown in this work, could be also applied for in situ characterization. This experiment could be performed in laboratory condition and samples are not damaged by X-ray radiation (unlike SAXS and XAS). The technique allows studying the growth of NPs in powders whereas most in situ techniques (HRTEM, UV-VIS spectroscopy) are limited by liquids. Authors believe that further development of this approach will allow determining the size and morphology of NPs at any desired moment of growth.

*The study was carried out with the financial support of the Russian Foundation for Basic Research (RFBR) in the framework of the scientific project №20-32-70227. A.G. acknowledges the President's Grant of Russian Federation for young scientists MK 2730.2019.2.*

**References**

1. Zang W., Li G., Wang L., Zhang X. *Catal. Sci. Technol.*, **2015**, 5, 2532–2553.
2. Liang Q., Liu J., Wei Y., Zhao Z., MacLachlan M. *J. Chem. Comm.*, **2013**, 49, 8928–8930.
3. Kinoshita K. *J. Electrochem. Soc.*, **1990**, 137, 845–848.
4. Rojluechai S., Chavadej S., Schwank J. W., Meeyoo V. *Cat. Comm.*, **2007**, 8, 57–64.
5. Buil M. L. Esteruelas M. A., Niembro S., Oliván M., Orzechowski L., Pelayo C. *Organometallics*, **2010**, 29, 4375–4383.
6. Tereshchenko A., Polyakov V., Guda A., Lastovina T., Pimonova Y., Bulgakov A., et al. *Catalysts*, **2019**, 9, 385.
7. Benmouhoub C., Kadri A., Benbrahim N., Hadji S. *Materials Science Forum*, **2009**, 609, 189–194.

## Design of MIL-100(Fe)/diatomite composites with hierarchical porous structure

E.V. Vyshegorodtseva, P.A. Matskan, G.V. Mamontov

*National Research Tomsk State University, Tomsk, Russia*

vyshegorodtseva\_elena@mail.ru

Today, there is a great interest in designing the materials with the hierarchical porous structure. Diatomite is a low-cost natural material with the hierarchical meso-macroporous structure. Relatively low surface area of diatomite can be developed by coating its surface with a microporous MOF. Hierarchical porous structure simplifies gas and liquid transport during the adsorption process, and the novel material will be able to find practical applications in sorption, catalysis, environmental safety, etc[1]. Moreover, the most common diatomite impurities (Al and Fe) can be used for the formation of microporous MOF without additional ion sources.

In the present work, the MIL-100(Fe)/diatomite composites were prepared by the assembly of microporous MIL-100(Fe) in the meso-macroporous structure of diatomite ("Kvant" company, Russia). The diatomite mainly consisted of silica (~90%), the contents of Al and Fe were 2.53 % and 1.81 % wt., respectively. The reference sample **MIL-100(Fe)** was synthesized from Fe(III) nitrate without adding of fluoric acid according to the reported procedure [2]:  $1\text{Fe}(\text{NO}_3)_3 \cdot 0.66\text{BTC} \cdot 278\text{H}_2\text{O} \cdot 0\text{HF}$ . The mixture was stirred for 1 h at room temperature and then placed into a steel autoclave and exposed at 160 °C for 16 h. The solid product was filtered, washed with distilled water, then washed with ethanol, and dried at 120 °C. The composite **MOF/Diat** was prepared by growing MIL-100 on the diatomite using Fe impurities. The amount of diatomite corresponded to the previously mentioned ratio of Fe and trimesic acid. The pH of the mixture was ~1-2. The composite **MOF(HNO<sub>3</sub>)/Diat** was prepared by the addition of nitric acid to a mixture of trimesic acid and diatomite. Other steps of the synthesis procedure were the same as in the case of the **MIL-100(Fe)** synthesis.

The structures of the diatomite, **MIL-100(Fe)** and composites were studied by low-temperature N<sub>2</sub> adsorption. The specific surface area ( $S_{\text{BET}}$ ) was calculated by Brunauer-Emmet-Teller method from the absorption isotherm in the range of relative pressures of  $P/P_0 = 0.05 - 0.15$ . The pore volume ( $V_{\text{pore}}$ ) was calculated by the single-point adsorption method at  $P/P_0 = 0.995$ .

The **MIL-100(Fe)** has high surface area (1864 m<sup>2</sup>/g) and pore volume (1.02 cm<sup>3</sup>/g). The pore size distribution is calculated by Horvath-Kawazoe method. It is defined by maxima at 0.9 nm; 2.8 nm; 3.9 nm. It is in agreement with the literature [3] and proves obtaining of the MIL-100(Fe). The initial diatomite is characterized by surface area and pore volume of 29 m<sup>2</sup>/g and 0.08 cm<sup>3</sup>/g, respectively. The surface area of MOF/Diat composite is 39 m<sup>2</sup>/g and pore volume is 0.13 cm<sup>3</sup>/g. By adding nitric acid into the mixture, the surface area and pore volume of MOF/diatomite composites were increased to  $S_{\text{BET}} = 88 \text{ m}^2/\text{g}$  and  $V_{\text{pore}} = 0.15 \text{ cm}^3/\text{g}$  for **MOF(HNO<sub>3</sub>)/Diat**. The micropore size distributions of the composites were characterized by maxima corresponding to the MIL-100(Fe)-structure. The intensity of maxima are higher from **MOF(HNO<sub>3</sub>)/Diat** and this improves the formation of large amount of microporous MIL-100(Fe). For the composites the presence of a hysteresis loop at a relative pressure of 0.85-1.0 on the isotherms of N<sub>2</sub> adsorption-desorption indicates the retaining of meso-macroporous diatomite structure in the composites.

Thus, the diatomite was used as both the source of Fe and a primary matrix with opened wide pores to create the hierarchical material. The MOF/Diatomite composites with the developed hierarchical porous structure may be easily prepared from the diatomite by the addition of nitric acid and trimesic acid and using the hydrothermal treatment.

*This work was supported by the state assignment of the Ministry of Science and Higher Education of the Russian Federation (project No. 0721-2020-0037) and Russian Foundation for Basic Research (Project No 19-43-700008).*

### References

1. Cychosz, K. A.; Guillet-Nicolas, R.; García-Martínez, J.; Thommes, M. *Chem. Soc. Rev.* **2017**, 46, 389–414.
2. Zhang, F.; Shi, J.; Jin, Y.; Fu, Y.; Zhong, Y.; Zhu, W. *J. Chem. Eng.* **2015**, 259, 183–190.
3. Fang, Y.; Yang Z.; Li, H.; Liu, X. *Environ. Sci. Pollut. Res.* **2020**, 27, 4703–4724.

## Formation of nickel particles on the surface of Ni/La<sub>2</sub>O<sub>3</sub> catalyst

A.A. Fetisova, N.V. Dorofeeva, O.V. Vodyankina

*Tomsk State University, Tomsk, Russia*

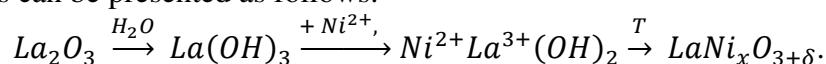
*nv-dorofeeva@yandex.ru*

Lanthana-based Ni-containing catalysts are widely studied in different processes such as dry reforming of methane (DRM) [1], CO<sub>2</sub> hydrogenation [2], oxidation of methane, methanol [3] and soot. In particular, the Ni/La<sub>2</sub>O<sub>3</sub> catalysts (Ni/La<sub>2</sub>O<sub>3</sub>/inert support) are active in high-temperature DRM process and can be competitive as compared to noble metal-based systems. A selection of lanthana as a support or modifying additive is caused by its basic properties and the ability to stabilize Ni particles that causes reduction of carbon deposits and prevents sintering of Ni<sup>0</sup> particles. The temperature of formation of active Ni<sup>0</sup> particles under reducing conditions as well as their size depend on the nature of Ni-containing precursors and their distribution.

The present work is focused on the effect of composition of lanthana-based support on the formation of Ni-containing precursor phases of active component Ni<sup>0</sup> and the processes of Ni ion reduction.

Lanthanum oxides were synthesized using citrate method at pH of 2 and 9 (LO-2, LO-9, respectively). The obtained gels were calcined at temperatures of 600, 700, and 800 °C for 4 h and then impregnated with the nickel nitrate solution. The Ni-containing systems were calcined at 700 °C. The structure and composition of the supports and Ni-containing systems were studied by low-temperature N<sub>2</sub> adsorption, XRF, XRD, and IR spectroscopy. The reducibility of Ni ions was studied by H<sub>2</sub>-TPR method.

The phase composition of the support was shown to affect the Ni distribution. Depending on the synthesis method and calcination temperature, the support compositions feature different ratios of La<sub>2</sub>O<sub>3</sub>, La(OH)<sub>3</sub> and La<sub>2</sub>O<sub>2</sub>CO<sub>3</sub>, with the latter phase decomposing upon support calcination above 600 °C. In the presence of lanthanum oxycarbonate in the composition of the LO-2 and LO-9 supports, the Ni ions are distributed as the particles of NiO and lanthanum nickelates with the composition La<sub>4</sub>Ni<sub>3</sub>O<sub>10</sub> and La<sub>2</sub>NiO<sub>4</sub>. The pH affects the texture of the supports and Ni-containing systems. The impregnation of supports calcined at 700 and 800 °C results in their peptization by the solution of Ni(NO<sub>3</sub>)<sub>2</sub> followed by the formation of Ni<sup>3+</sup> and Ni<sup>2+</sup>-containing dispersed lanthanum nickelates during the temperature treatment. A scheme of formation of lanthanum nickelates in the presence of La<sub>2</sub>O<sub>3</sub> and La(OH)<sub>3</sub> in the composition of supports can be presented as follows:



For all Ni-containing samples, the reduction of Ni ions from the structures of lanthanum nickelates occurs through two stages: the Ni<sup>3+</sup> ions are reduced to Ni<sup>2+</sup> in the temperature range of 250-450 °C, and from 450 to 635 °C the formation of nickel particles occurs via the reaction Ni<sup>2+</sup>+H<sub>2</sub>→Ni<sup>0</sup>. In the samples obtained on the basis of carbonate-containing supports in the temperature range of 250-450 °C, the Ni<sup>0</sup> particles are formed upon nickel oxide reduction. The temperature of reduction of surface lanthanum nickelates increases with the increase in the temperature of support treatment.

*This work was supported by the Russian Science Foundation (Project No. 19-73-30026).*

### References

1. Rabelo-Neto, R.C.; Sales, H. B. E.; Sales, H. B. E.; Varga, E.; Oszko, A.; Erdohelyi, A.; Noronha, F.B.; Mattos, L.V. *Appl. Cat. B: Environ.* **2018**, *221*, 349.
2. Garbarino, G.; Wang, C.; Cavattoni, T.; Finocchio, E.; Riani, P.; Flytzani-Stephanopoulos, M.; Busca, G. *Appl. Cat. B: Environ.* **2019**, *248*, 286.
3. Choisset, J.; Abadzhieva, N.; Stefanov, P.; Klissurki, D.; Bassat, J.M.; Rives, V.; Minchev, L. *J. Chem. Soc. Faraday Trans.* **1994**, *90(13)*, 1987.

## Control of Pt species formation in Pt/CeO<sub>2</sub> catalysts via pretreatment of support and catalyst

A.V. Filonenko, T.A. Bugrova, A.S. Savel'eva, T.S. Kharlamova, G.V. Mamontov

*Tomsk State University, Tomsk, Russia*

ann.filonenko@yandex.ru

Pt/CeO<sub>2</sub> catalysts are promising materials for different low-temperature oxidation and hydrogenation processes. The Pt content in such catalysts depends on the choice of support and preparation method, and plays an important role in the catalytic action of Pt/CeO<sub>2</sub> systems. Due to enhanced metal–support interaction the use of cerium oxide allows stabilizing small size platinum particles on the support surface, that, in turn, leads to higher reactivity of platinum species towards molecular oxygen or hydrogen activation. However, most methods to obtain Pt/CeO<sub>2</sub> catalysts (impregnation, co-deposition, etc.) [1,2] and control catalyst stability (CeO<sub>2</sub> morphology, different Pt precursors, etc.) [3,4] as well as high-temperature treatment lead to the formation of a solid solution of PtO<sub>x</sub>-CeO<sub>2</sub> that affects the catalytic properties. The use of pre-reduced CeO<sub>2</sub> as a support allows forming metal particles during the impregnation. It is proposed that the redox reaction between Ce<sup>3+</sup> sites and active metal precursor takes place during this step [5]. In this case, the strength of the metal–support interaction in the catalyst is high but some solid solution is formed. However, this approach is poorly discussed in the literature.

The aim of the present work is to study the role of support and catalyst pretreatment in oxidizing and/or reducing atmosphere at different temperatures on the formation of active species in the Pt/CeO<sub>2</sub> catalysts for CO oxidation and nitrobenzene hydrogenation.

In the present work ceria support was prepared by thermal decomposition of cerium nitrate at 500 °C. The series of Pt/CeO<sub>2</sub> catalysts (Pt loading of 0.5, 1.0 and 2.0 wt%) were prepared by wetness impregnation of oxidized and pre-reduced CeO<sub>2</sub> using H<sub>2</sub>PtCl<sub>6</sub> aqueous solution. Ceria was pre-reduced in H<sub>2</sub>-containing atmosphere (10 vol.%H<sub>2</sub>/Ar) up to 500 °C. All impregnated samples were dried at 120 °C. Catalysts supported on oxidized CeO<sub>2</sub> were calcined in air at 300 and 500 °C. The structure and state of Pt and the features of the formation of Pt species on the CeO<sub>2</sub> surface were studied by TPO and H<sub>2</sub>-TPR methods. The activity of the catalyst prepared was tested in CO oxidation and nitrobenzene hydrogenation into aniline. The structure and state of Pt and CeO<sub>2</sub> were studied by low-temperature N<sub>2</sub> sorption, XRD, Raman spectroscopy, and UV-vis DR spectroscopy.

According to the results obtained, various pretreatment of the catalyst and support at different preparation steps allows controlling the Pt particle size and the state of Pt species on the ceria surface. Specifically, XRD, Raman spectroscopy, UV-vis DRS, and H<sub>2</sub>-TPR results show that a direct reductive treatment of the catalysts dried at 120 °C promotes the formation of larger Pt particles (2-5 nm) that are active in the nitrobenzene hydrogenation into aniline, with the selectivity being affected by the size of Pt particles.

Thus, reductive pretreatment of support and catalysts allows controlling the size and state of Pt species and obtaining Pt/CeO<sub>2</sub> catalyst with high catalytic performance in CO oxidation and nitrobenzene hydrogenation. The use of the pre-reduced CeO<sub>2</sub> leads to the formation of metallic Pt particles and/or partial reduction of Pt<sup>4+</sup> to Pt<sup>2+</sup>. Different pretreatment of the catalyst/support plays a decisive role in the formation of Pt species in Pt/CeO<sub>2</sub> catalysts that are active in oxidation and hydrogenation reactions.

*This work was supported by Russian Science Foundation (Grant No. 18-73-10109).*

### References

1. Hong, X., and Sun, Y. *Catal. Lett.* 2016, **2001**, 146.
2. Franco, P., Martino, M., Palma, V., Scarpellini, A., and De Marco, I. *Int. J. Hydrogen Energy* **2018**, 43, 19965.
3. Abid, M., and Touroude, R. *Catal. Lett.* **2000**, 69, 139.
4. Gao, Y., Wang, W., Chang, S., and Huang, W. *ChemCatChem* **2013**, 5, 3610.
5. Grabchenko, M.V., Mamontov, G.V., Zaikovskii, V.I., La Parola, V., Liotta, L.F., and Vodyankina, O.V. *Appl. Catal., B* **2020**, 260, 118148.

## Regeneration of industrial iron-chrome catalysts for carbon monoxide conversion

I.S. Grishin, M.A. Lebedev, V.A. Goryanskaya

*Ivanovo State University of Chemistry and Technology, Ivanovo, Russia*

grish.in.03.97@gmail.com

Catalytic processes play a great role in modern chemistry. One of their major disadvantages is necessity of spent catalysts disposal. In some cases they pose a significant threat to the environment because of toxic compounds contained. Iron-chrome catalyst for carbon monoxide conversion could be considered as an example. Basically the most common method for realization of steam CO conversion in industry is two-stage process: firstly CO is converted at high temperatures (350-450°C) using Fe-Cr catalyst, and secondly at low temperatures (170-250°C) using Cu-Zn-Al-Cr oxide catalyst. However catalysts eventually lose their activity due to pore structure collapse, which indeed means decreasing of specific surface area. Iron-chrome catalyst contains toxic chromium (III) oxide, that's why its disposal is undesirable. It's due to the fact that the catalyst is usually disposed in special reinforced concrete bunkers, which could be destroyed because of aging, and the waste contained could be released into the environment polluting it. Thus regeneration of iron-chrome catalyst for its reuse is very crucial.

A method for regeneration of iron-chrome catalyst in presence of oxalic acid (Russian GOST 22180-76) and dispersing additives, namely powders of iron (Russian GOST 9849-86) and gray cast iron (Russian GOST 1412-85), by acoustic and mechanical impact is proposed in the work. Samples of regenerated Fe-Cr catalyst were analyzed using nitrogen low temperature adsorption/desorption, X-ray diffraction, synchronous thermal analysis, and scanning electron microscopy.

It was found that specific surface area of spent Fe-Cr catalyst is 13.20 m<sup>2</sup>/g. But after regeneration with oxalic acid its value had increased up to 50.69 m<sup>2</sup>/g. What's more, after adding of iron powder, specific surface area had increased even more significantly up to 168.10 m<sup>2</sup>/g. Regeneration with gray cast iron powder was a little bit less effective. In this case specific surface area of the catalyst had increased up to 159.10 m<sup>2</sup>/g. This specific surface area increase was because of iron oxalate formation and its dissolution. It should be noted that iron oxide itself and iron particles were dissolved as well under acoustic and mechanical impact, which consider particles to be rubbed against each other that improves the regeneration. Also maghemite ( $\gamma$ -Fe<sub>2</sub>O<sub>3</sub>) peaks were observed on diffraction patterns of regenerated catalyst samples. Basically that could be another explanation of specific surface area increase, because its value is quite high for maghemite. Actually  $\gamma$ -Fe<sub>2</sub>O<sub>3</sub> is an active component for ammonia synthesis, so proposed regeneration method could spread further application of the catalyst.

Still composition of regenerated catalyst doesn't correspond to that for industrial ones. That means investigations should be made to select main components, which are to be added to regenerated catalyst samples to bring the composition closer to industrial one.

*This work was carried out as part of a state assignment for research work (No. FZZW-2020-0010). Equipment of the Center of Collective Use of Ivanovo State University of Chemistry and Technology was used when carrying out the research.*

## Synthesis and characterization of the TiO<sub>2</sub> photonic crystals in the form of inverse opals

M.V. Kirichkov<sup>1</sup>, V. Likodimos<sup>2</sup>

<sup>1</sup>*The Smart Materials Research Institute, Southern Federal University, Rostov-on-Don, Russia*

<sup>2</sup>*National and Kapodistrian University of Athens, Athens, Greece*

mikhail.kirichkov@gmail.com

Photonic crystals have been established as unique periodic structures to promote photon capture and control over light-matter interactions. Their application in semiconductor, mainly TiO<sub>2</sub>, photocatalysis has emerged as a promising structural modification to boost light harvesting of photocatalytic materials by means of slow photons i.e. light propagation at reduced group velocity near the edges of the photonic band gap [1,2]. In this case, TiO<sub>2</sub> photocatalysis has been attracting huge interest as one of the most promising technologies to address global concerns over environmental pollution and meet the ever-increasing energy demands by the utilization of naturally abundant, renewable sources such as solar light.

This work reports about fabrication of TiO<sub>2</sub> inverse opals of variable photonic gap using the evaporation-induced co-assembly of polymer (PMMA) colloidal spheres of different diameters (260, 330 and 406 nm) with a hydrolyzed Ti alkoxide precursor [titanium(IV) bis(ammonium lactato)dihydroxide]. Calcination of the impregnated films, after drying and gelation, was performed in air to selectively remove the polymer matrix and crystallize amorphous titania in the inverse opal structure consisting of an fcc lattice of air spheres with an inorganic TiO<sub>2</sub> skeleton. Obtained samples are characterized by various analytical techniques, such as XRF, XRPD, XANES-spectroscopy, IR-spectroscopy and TEM/SEM. The characteristics of samples with different pore diameters are compared. Moreover, the effect of surface modification of the TiO<sub>2</sub> photonic crystals by noble metals nanoparticles on the samples photocatalytic properties are investigated.

*This work was supported by RFBR project №20-32-70227*

### References

1. Likodimos, V. Appl. Catal. B: Environ. **2018**, 230, 269–303.
2. Diamantopoulou, A.; Sakellis, E.; Romanos, G. E.; Gardelis, S.; Ioannidis, N.; Boukos N.; Falaras, P.; Likodimos, V. Appl. Catal. B: Environ. **2019**, 240, 277–290.



## Ceria-supported Pt–Ag bimetallic catalysts: Features of formation of Pt–Ag active species

M.V. Salina, T.S. Kharlamova\*, V.A. Svetlichnyi, G.V. Mamontov

*Tomsk State University, Tomsk, Russia*

kharlamova83@gmail.com

Platinum-based catalysts are among the most used metal systems in organic synthesis, petrochemical industry, mitigation of engine exhaust emissions, and abatement of volatile organic compounds [1, 2]. However, extremely high Pt activity towards oxidation and hydrogenation of organic compounds limits its wide application due to low selectivity [1,3]. Besides, its high cost and easy poisoning by carbon monoxide increase the need to develop alternative catalytic systems. The development of the Pt–Me bimetallic catalysts with reduced Pt content is a promising approach allowing both cost-cutting and inducing selectivity shifts towards desired reaction products [3]. For such catalysts, high catalytic activity and selectivity can be achieved due to the synergistic effect caused by the changes in the electronic state or geometry of the active sites due to metal interaction accompanied by the formation of solid solution, core-shell structures or interphase boundaries between the metal particles [2]. The support nature can play an important role in stabilization of the metal particles as well as in facilitating of the catalyst activity, stability and selectivity [4].

The present work is focused on designing of Pt–Ag/CeO<sub>2</sub> bimetallic catalysts. The series of Pt–Ag/CeO<sub>2</sub> catalysts (total metal loading of 2.0 wt.%) with different Pt:Ag ratio (2:0, 1.5:0.5, 1:1, 0.5:1.5, and 0:2) was prepared by consecutive wetness impregnation with water solutions of Pt and Ag precursors. The features of the formation of Pt–Ag species on the CeO<sub>2</sub> surface at different stages of the catalyst preparation were studied by a complex of methods (STA, XRD, Raman spectroscopy, UV-vis spectroscopy, TPR-H<sub>2</sub>, TPO, HR TEM, H<sub>2</sub> and CO pulse chemisorption, etc.). The catalytic properties of the samples were studied in CO oxidation and hydrogenation of nitrophenol into aminophenol. Using of H<sub>2</sub>[PtCl<sub>6</sub>] precursor and sample calcination in air at 500°C at the first stage was shown to result in a strong interaction between the adsorbed Pt precursor and ceria to form the solid solution. The subsequent use of [Ag(NH<sub>3</sub>)<sub>2</sub>]NO<sub>3</sub> precursor and sample calcination in air at 500°C provided Ag deposition in a highly dispersed state. The reduction of the Pt–Ag/CeO<sub>2</sub> bimetallic samples prepared by hydrogen allowed forming the Pt–Ag species affecting the redox properties and catalytic characteristics as compared with monometallic samples. The roles of the Pt–Ag species and the metal–support interaction are considered.

*This work was funded by RFBR, project number 20-33-70122.*

### References

1. Yu, W., Porosoff, M.D., Chen, J.G., *Chem. Rev.* **2012**, *112*, 5780–5817.
2. Bugrova, T.A., Kharlamova, T.S., Svetlichnyi, V.A., Savel'eva, A.S., Salaev, M.A., Mamontov, G.V., *Catal. Today*, Submitted.
3. Filez, M., Redekop, E.A., Dendooven, J., Ramachandran, R.K., Solano, E., Olsbye, U., Weckhuysen, B.M., Galvita, V.V., Poelman, H., Detavernier, C., Marin, G.B., *Angew. Chem. Int. Ed.* **2019**, *58*, 13220–13230.
4. Park, D., Kim, S.M., Kim, S.H., Yun, J.Y., Park, J.Y., *Appl. Catal. A.* **2014**, *480*, 25–33.

## Investigation of Pt/CeO<sub>2</sub>-MnO<sub>x</sub> catalysts in CO and methane oxidation reactions

A.A. Simanenko<sup>1,2</sup>, A.I. Stadnichenko<sup>1,2</sup>, E. M. Slavinskaya<sup>1,2</sup>, A.A. Evtushkova<sup>1,2</sup>, E. A. Fedorova<sup>2</sup>,  
O. A. Stonkus<sup>1,2</sup>, A.V. Romanenko<sup>2</sup>, A.I. Boronin<sup>1,2</sup>

<sup>1</sup>*Novosibirsk State University, Novosibirsk, Russia*

<sup>2</sup>*Boriskov Institute of Catalysis, Novosibirsk, Russia*

simanenko@catalysis.ru

For today, catalytic systems using CeO<sub>2</sub> as support are of great interest to commercial applications and fundamental researches. One of the most important applications of CeO<sub>2</sub>-based catalysts is the low-temperature CO and methane oxidation reaction using a combination with noble metals. High activity of the ceria-noble metals composition in oxidations reactions is due to the unique properties of cerium oxide – strong metal-support interaction (SMSI) with active components and high oxygen storage capacity (OSC). These properties allow accumulating absorbed oxygen, which is very important in constantly changing reaction conditions, especially in the low-temperature range or oxygen-poor gas mixtures. CO and C<sub>x</sub>H<sub>y</sub> low-temperature oxidation have wide applications in exhaust gas cleaning, energy production, gas sensors, etc. In all cases, the realization of catalytic performance at room temperatures or even below 0°C is highly demanded.

Currently, the modification of CeO<sub>2</sub> is actively applied to improve oxygen capacity and mobility due to the formation of solid solutions with dopants. Manganese is one of the promising modifiers for ceria on the base of similar redox properties of Mn and Ce using the ability of both metals in the reversible transition of oxidation states between 3+ and 4+.

In this work, a series of Ce<sub>1-x</sub>Mn<sub>x</sub>O<sub>2-δ</sub> supports were synthesized and studied. Samples were obtained by coprecipitation in an alkaline medium, with a manganese content of 10, 20 and 30% atomic. The samples calcination temperature was varied in the range of 450-600°C. According to XRD, all samples are single-phase systems and have a fluorite lattice. As the amount of manganese content increases, the lattice parameter of the fluorite phase decreases and the number of microstrains increases. According to the XPS data, the manganese on the surface of the supports is presented in two oxidation states: Mn<sup>2+</sup> and Mn<sup>3+</sup>. Also, part of Ce<sup>3+</sup> decreases when Mn is introduced into the CeO<sub>2</sub> structure.

Catalytic testing has shown that the CO conversion curves shift to a lower temperature range when the amount of manganese dopant increases. It was shown, that obtained samples have low-temperature activity: CO reaction starts at temperatures below 100°C. The low-temperature activity was correlated with the amount of mobile oxygen, available in the temperature range 0-230°C, which is not typical for pure ceria.

The studied supports were impregnated with 5% wt. platinum as the active component. According to XRD, no additional platinum-containing phases were observed. Crystalline platinum particles were also not observed using the HRTEM method. According to the XPS data, the platinum on the surface of the catalysts is stabilized in ionic forms with two oxidation states: Pt<sup>2+</sup> and Pt<sup>4+</sup>.

In the result of catalytic testing was found that the deposition of platinum on the composite supports led to the high activity of catalysts already at room temperature in the CO oxidation reaction, while in the methane oxidation reaction, the catalysts have a noticeable activity at the temperature range about 300°C. It was proposed that active sites for CO and methane oxidation can be required the different structures and surface states of Pt and Mn/Ce as well.

## Macroporous Ag/SiO<sub>2</sub> composites for monolithic flow-through catalytic reactors

O.Yu. Vodorezova, M.A. Baryshnikov, T.I. Izaak

*Tomsk State University, Tomsk, Russia*

olga.vodorezova@yandex.ru

Supported metal nanoparticles are traditionally used in the heterogeneous catalysts for different processes. The requirements for modern catalytic processes and catalysts stimulate scientists to design new materials and technologies. One of the research directions is oriented to the development of environmental responsible processes and reusable materials. According to this the monolith materials has perspective. The porous monolithic materials with controlled structure have advantages in catalysis, such as the possibility of organizing flow reactors, and ease of their separation. A hierarchically porous structure of the monolith can promote better heat and mass transfer, which is beneficial when applied to heterogeneous catalysts [1]. Here, we propose to consider the application of the physically and chemically stable porous silica monolith for the design of the flow-through catalytic systems. The hydrogenation of p-nitrophenol on silver nanoparticles supported on the porous silica monolith was chosen as a model process. This catalytic reaction is widely used as the model reaction [2]. In addition, nitrophenols are used for many medical and industrial purposes, while the presence of nitrophenols in wastewater is of great concern due to their toxicity [3].

The silica monolith was prepared by a sol-gel method according to the procedure described in [4]. Composites containing the silver nanoparticles supported on the hierarchically porous monolith with macro- and mesopores were prepared by vacuum impregnation and subsequent reduction of silver ions with formamide [5]. The prepared monoliths and composites were characterized by microscopy, diffusion reflection spectroscopy, and low-temperature nitrogen adsorption. The examination of the composites activity during the catalytic reduction of 4-nitrophenol was carried out at room temperature in the flow-through reactor.

The report presents the results of the investigation of the monoliths and composites characteristics, as well as their catalytic activity. Apart from that, the study demonstrates the reusability and potential application of the porous monoliths in continuous flow reactor.

### References

1. Galarneau, A.; Sachse, A.; Said, B.; Pelisson, C. H.; Boscaro, P.; Brun, N., ...; Fajula, F. *C. R. Chim.* **2016**, *19*(1-2), 231–247.
2. Herves, P.; Pérez-Lorenzo, M.; Liz-Marzán, L. M.; Dzubiel, J.; Lu, Y.; Ballauff, M. *Chem. Soc. Rev.* **2012**, *41*(17), 5577–5587.
3. ATSDR. Toxicological profile for nitrophenols: 2-Nitrophenol and 4-nitrophenol; Agency for Toxic Substances and Disease Registry, Public Health Service, **1992**
4. Vodorezova, O. Y.; Lapin, I. N.; Izaak, T. I. *J. Sol-Gel Sci. Technol.* **2020**, 1–9.
5. Izaak, T. I.; Martynova, D. O.; Stonkus, O. A.; Slavinskaya, E. M.; Boronin, A. I. *J. Sol-Gel Sci. Technol.* **2013**, *68*(3), 471–478.

## Hierarchical SiO<sub>2</sub> materials and Pt-Ga catalysts on basis thereof for propane dehydrogenation

A.V. Zubkov, E.V. Vyshegorodtseva, T.A. Bugrova, G.V. Mamontov

*Tomsk State University, Tomsk, Russia*

zubkov@data.tsu.ru

The catalytic non-oxidative propane dehydrogenation (PDH) is a useful performance for propylene synthesis, and its value is rapidly growing worldwide. Propylene is ranked the second after ethylene in chemical industry by production value. Many important organic compounds, namely polypropylene, polyacrylonitrile, acrolein, propylene oxide, acryl acid, glycerin, etc., are the products of reactions with propylene [1]. Alumina-chromia (CrO<sub>x</sub>/Al<sub>2</sub>O<sub>3</sub>) and platinum–tin (Pt-SnO<sub>x</sub>/Al<sub>2</sub>O<sub>3</sub>) catalysts comprise the major commercial catalysts for dehydrogenation of C<sub>3</sub>-C<sub>5</sub> alkanes. The disadvantage of CrO<sub>x</sub>/Al<sub>2</sub>O<sub>3</sub> catalysts is Cr(VI) toxicity that imposes danger during the catalyst exploitation [2]. Therefore, the topical challenge is to design the PDH catalysts in connection with the abovementioned facts.

Design of dehydrogenation catalysts based on silica support is an appropriate research area. Silica supports, namely MCM-41 and SBA-15, have the combination of high specific surface area and an ordered mesoporous (3-8 nm) structure [3]. However, the dehydrogenation processes realized at 550-600 °C are characterized by the diffusion limitations. The materials with a hierarchical porous structure are promising to address this challenge by combining a wide pore transport system (mainly above 50 nm) and mesopores providing high specific surface area of the catalyst. The aim of this study is to develop a silicate support with a hierarchical structure based on diatomite and MCM-41 and to design the Pt-Ga catalysts on the basis thereof for propane dehydrogenation to propylene. The approach features the MCM-41 synthesis on the diatomite surface without the use of additional precursors [4]. The resulting composite support MCM-41/diatomite is characterized by a biporous structure: a system of transporting pores of natural diatomite (from 20 nm to up to several μm) as well as a system of ordered mesopores of 3-4 nm related to the MCM-41 formed on the diatomite surface.

The MCM-41 was synthesized from sodium silicate in an alkaline medium (pH ≈ 12) using CTAB (cetyltrimethylammonium bromide) as a template [5]. The treated diatomite with a hydrochloric acid (LLC “Kvant”, Russia) was used as a preliminarily solution to prepare the composite MCM-41/diatomite supports. The obtained composites were used to prepare Pt-Ga catalysts. The porous structure of the supports was studied by the low-temperature nitrogen adsorption (–196 °C) and scanning electron microscopy (SEM).

The specific surface area of 1080 m<sup>2</sup>/g and a pore volume of 0.92 cm<sup>3</sup>/g are characteristics of the MCM-41 sample synthesized from sodium silicate. The MCM-41/diatomite composite samples are characterized by a regular increase in the specific surface area from 282 m<sup>2</sup>/g to 632 m<sup>2</sup>/g with an increase in the NaOH/diatomite ratio. The isotherms of composite supports show a sharp increase in the adsorption value in the relative pressure range of 0.3-0.38 indicating the presence of the MCM-41 structure in the material, and a hysteresis loop in the pressure range of 0.95-1.0 also indicates that the macroporous structure of diatomite is preserved in the material.

Thus, the present study shows the opportunity to design the supports based on diatomite and MCM-41 that are characterized by a hierarchical structure. The series of Pt-Ga catalysts was prepared on the basis of the supports, and their structure, state, distribution of Pt and Ga were studied.

*This work was supported by the Grant of Russian Fund for Basic Research (Grant № 19-43-700008 p\_a).*

### References

1. Sattler, J.J.H.B., Ruiz-Martinez, J., Santillan-Jimenez, E., Weckhuysen, B.M. *Chem. Rev* **2014**, *114*, 10613–10653.
2. Otroshchenko, T., Radnik, J., Schneider, et. al. *Chem. Comm.*, **2016**, *52*, 8164.
3. Hua, R., Zha, L., Cai, M. *Cat. Comm.* **2010**, *11*, 563-566.
4. Patent RU no. 2727393, 30.12.2019.
5. Vyshegorodtseva, E.V., Larichev, Y.V., Mamontov, G.V. (2019). *J. Sol-Gel Sci. Tech.*, **2019**, *92*, 496.



# SECTION 2

## PROMISING CATALYTIC PROCESSES



## Localized temperature in plasmonic-induced photocatalysis at the single-nanoparticle level

Andrey A. Averkiev<sup>1</sup>, Raul D. Rodriguez<sup>1</sup>, Boris N. Khlebtsov<sup>2</sup>, Ryo Kato<sup>3</sup>, Larissa Kim<sup>1</sup>, Takayuki Umakoshi<sup>3</sup>, Vladimir Kolchuzhin<sup>4</sup>, Dietrich R. T. Zahn<sup>5</sup>, Prabhat Verma<sup>3</sup>, Evgeniya Sheremet<sup>1</sup>

<sup>1</sup>*Tomsk Polytechnic University, 30 Lenin Avenue, 634050 Tomsk, Russia*

<sup>2</sup>*Institute of Biochemistry and Physiology of Plants and Microorganisms, Russian Academy of Sciences, 13 Prospekt Entuziastov, Saratov 410049, Russia*

<sup>3</sup>*NaSpec, Department of Applied Physics, Osaka University P2-333, 2-1, Yamadaoka, Suita, Osaka 565-0871, Japan*

<sup>4</sup>*Qorvo Munich GmbH, Konrad-Zuse-Platz 1, D-81829 Munich, Germany*

<sup>5</sup>*Semiconductor Physics, Chemnitz University of Technology, D-09107 Chemnitz, Germany*

raul@tpu.ru

Exact physical mechanism of plasmon photocatalysis is still under debate nowadays and being one of the most active research topics in plasmonic applications [1,2]. In particular, the role of localized temperature remains a controversial issue [3-5]. Thus, right now the community is broadly divided into two bands, those who claim that plasmonic heating is the sole and only contributor to plasmonic-driven photocatalysis, and those who claim that it is hot-electron transfer what dominates these reactions. This situation is not only for the photocatalytic reaction of 4-NBT but it is a general discussion intensively ongoing in the plasmonics and catalysis communities. In this contribution, we report novel insights at the nanoscale that show plasmon-induced photocatalytic activity and localized heating are linked together. To do this, we use 4-nitrobenzenethiol (4NBT) self-assembly monolayers formed on plasmonic nanostructures as a benchmark model of photocatalytic activity investigated by surface- and tip-enhanced Raman spectroscopy (SERS and TERS). Our SERS results show that an external temperature increase promotes the photocatalytic conversion of 4NBT to azobenzene products in agreement with Arrhenius law. However, our TERS imaging results at the single nanoparticle level show that regions with the highest catalytic conversion do not correlate with regions having the largest electromagnetic field enhancement. We attribute this mismatch between photocatalytic activity and enhancement to a competition between these two processes in terms of energy conservation.

These results imply that the hot-electron transfer is not the only contributor to these kinds of reactions but that the non-radiative plasmon decay into thermal energy does play a role. This work impacts other applications such as theranostics based on photothermal therapy and plasmonic signal enhancement, since improving one of these functions in a single plasmonic system would come at the cost of degrading the other one.

*This work was supported by the Tomsk Polytechnic University within the framework of Tomsk Polytechnic University Competitiveness Enhancement Program 5-100.*

### References

1. Wu, N., *Nanoscale* **2018**, 10 (6), 2679–2696.
2. Cortés, E., *Science* **2018**, 362 (6410), 28–29.
3. Zhou, L.; Swearer, D. F.; Zhang, C.; Robatjazi, H.; Zhao, H.; Henderson, L.; Dong, L.; Christopher, P.; Carter, E. A.; Nordlander, P., *Science* **2018**, 362 (6410), 69–72.
4. Golubev, A. A.; Khlebtsov, B. N.; Rodriguez, R. D.; Chen, Y.; Zahn, D. R., *J. Phys. Chem. C* **2018**, 122 (10), 5657–5663.
5. Keller, E. L.; Frontiera, R. R., *ACS Nano* **2018**, 12 (6), 5848–5855.



## Preparation of low-sulfur coke from tar

A.S. Chichkan<sup>1,2</sup>, V.V. Chesnokov<sup>1</sup>

<sup>1</sup>*Boriskov Institute of Catalysis, Novosibirsk, Russia*

<sup>2</sup>*Novosibirsk State Technical University, Novosibirsk, Russia*

AlexCsh@yandex.ru

The main goal of carbonization processes is to produce various types of oil cokes. Oil coke is globally used for production of anodes used in aluminum industry and graphitized electrodes for melting electric steel. The generally accepted mechanism of the oil residue carbonization is the so-called “consecutive scheme” of hydrocarbon consolidation [1]. The “carbide cycle” mechanism (carbon formation on iron group metals) [2] opens new opportunities for enhancement of the delayed coking technology [3,4].

The present study was devoted to catalytic tar carbonization in the presence of Ni/Sibunit, Cu/Sibunit and Ni-Mo/Sibunit catalysts. Particular attention was paid to the contents of sulfur compounds in the reaction products.

The tar carbonization was studied in the temperature range of 350–550 °C. Gaseous products formed during the tar carbonization at 450 °C were analyzed for the concentration of sulfur-containing compounds. H<sub>2</sub>S and COS were observed in the reaction products. An increase of the carbonization temperature from 450 to 550 °C led to the decrease of the coke yield due to deeper cracking of the tar components. The temperature increases also resulted in the decrease of the sulfur concentration in the coke from 1.28% to 1.18%.

The efficiency of the carbonization process and the properties of the obtained coke were further improved by placing three different catalysts Ni-Mo/Sibunit, Cu/Sibunit and Ni/Sibunit in different zones of the autoclave where the tar carbonization was performed.

When we used three different catalysts Ni-Mo/Sibunit, Cu/Sibunit and Ni/Sibunit in different zones of the autoclave, we got the following results:

- In zone 1 the tar was subjected to hydrocracking and desulfurization over the Ni-Mo/Sibunit catalyst.
- In zone 2 sulfur was trapped by the Cu/Sibunit catalyst in the form of copper sulfide.
- In zone 3 coke was formed over the Ni/Sibunit catalyst predominantly from gases formed by the tar cracking.

Such organization of the carbonization process increased the coke yield to 45 wt.%. The three-zone catalyst arrangement during the tar carbonization also resulted in a substantial decrease of the sulfur concentration in gaseous products, which led to lower sulfur concentration in the solid reaction products in zone 3.

*This work was supported by Russian Science Foundation, Grant № 17–73–30032.*

### References

1. Buyanov, R.A. Catalyst coking, Nauka, Novosibirsk, **1983** (in Russian).
2. Chesnokov, V.V., Buyanov, R.A. *Uspekhi Khimii*. **2000**, 69, 675–692.
3. Chesnokov, V.V.; Chichkan', A.S.; Zaikovskii, V.I.; Parmon, V.N. *Kinet. Catal.* **2013**, 54, 213–219.
4. Chesnokov, V.V.; Chichkan', A.S.; Parmon, V.N. *Catal. Ind.* **2018**, 10, 244–250.

## Syngas conversion over perovskite-like $\text{LaCu}_x\text{Ti}_{1-x}\text{O}_3/\text{KIT-6}$ catalysts

E.V. Dokuchits, T.V. Larina, E.Yu. Gerasimov, A.A. Pochtar, T.P. Minyukova

*Boreskov Institute of Catalysis, Novosibirsk, Russia*

oschtan@catalysis.ru

Synthesis of alcohols from syngas is one of the methods used to produce biofuel. The use of methanol is the most efficient in internal combustion engines. Commercial methanol production is based on CuZn-containing catalysts. The promotion of copper catalysts with alkali or rare-earth metals makes it possible to increase the methanol yield or shift the distribution of products toward higher alcohols. High activity of copper-containing catalysts may be caused by the binding of the highly dispersed copper phase to the rare-earth oxide substrate, for example, in the perovskite structure. Earlier a considerable activity and selectivity in the methanol synthesis were demonstrated for massive perovskites of the  $\text{LaCu}_x\text{Ti}_{1-x}\text{O}_3$  composition synthesized by the citrate method [1]. Here we have studied the effects of the Cu/La, Cu/Ti ratios and the increase in the specific surface area by introducing template - KIT-6 mesoporous silica on the catalytic properties of the  $\text{LaCu}_x\text{Ti}_{1-x}\text{O}_3/\text{KIT-6}$  system ( $x = 0.4\div 0.8$ ).

In the synthesized samples, with an increase in  $x$ , the perovskite phase is replaced by the  $\text{La}_2\text{CuO}_4$  phase is oxide state of the catalysts. Moreover, as evidenced by DTA in addition to separate copper reduction from the perovskite and  $\text{La}_2\text{CuO}_4$  phases, reduction of an admixture of copper oxide is observed. The mass loss exceeds the corresponding reduction of all copper in the samples, however, a comparison of the results of the differentiating dissolution (DD) of the initial samples and samples after catalytic tests indicate the preservation of the phase of the defective perovskite of the composition  $\text{La}_1\text{Cu}_{0.25}\text{Ti}_{0.1}$ . In addition, the content of copper oxide in the initial samples and after catalytic tests according to DD is similar, which indicates that copper particles formed during the reduction of copper-containing phases are incorporated into the lanthanum-containing oxide substrate. These data are well supported by UV-Vis DRS results. In this case, the red shift of the observed absorption band of  $13000\text{--}17000\text{ cm}^{-1}$  with an increase in  $x$  in  $\text{LaCu}_x\text{Ti}_{1-x}\text{O}_3$  after catalytic tests is associated not with the expected decrease in the size of copper particles [2], but with an increase in the interaction of copper particles with La-containing oxide substrate. In addition, the increase in the total background of absorption of the samples after the reaction with increasing  $x$  indicates a finely dispersed component, which is consistent with the dissolution of the samples under milder conditions of DD. According to HRTEM data, crystalline blocks of perovskite and  $\text{La}_2\text{CuO}_4$  with a common boundary on  $\text{SiO}_2$  aggregates are observed in the initial samples. After catalytic tests, amorphized particles containing all the starting cations with an average size of about 100 nm are most common.

The main liquid products of syngas conversion ( $\text{CO}+2\text{H}_2$ , 2MPa,  $240^\circ\text{C}$ ,  $500\text{--}600\text{ h}^{-1}$ ) on all synthesized samples are alcohols. In the  $\text{La}_2\text{CuO}_4/\text{KIT-6}$  and  $\text{LaCu}_x\text{Ti}_{1-x}\text{O}_3$ , with an increase in  $x$ , the methanol selectivity decreases from 88 to 77%, while the selectivity for  $\text{C}_{2+}$  alcohols (mainly ethanol and isobutanol) increases from 4.5 to 11%. Along with an increase in the selectivity for  $\text{C}_{2+}$  alcohols, the resulting water leads to an increase in the contribution of the water gas shift reaction with  $\text{CO}_2$  formation. The methanol selectivity on the industrial CuZnAl catalyst is lower than that of the worst sample in the series with  $x = 0.8$ . The observed pattern in the presented series is due to the fact that with an increase in the Cu/La ratio, the interaction of the La-containing oxide substrate and particles of metallic copper increases. The synthesized samples have comparable activity and a 5–15% higher methanol selectivity compared to the industrial CuZnAl catalyst that makes these systems promising for further study.

The studies of UV-Vis DR spectroscopy, differential dissolution method, XRD, HRTEM and DTA of all samples were performed the equipment of the Center of Collective Use "National Center of Catalyst Research". This work was supported by Ministry of Science and Higher Education of the Russian Federation (Project AAAA-A17-117041110045-9 for Boreskov Institute of Catalysis).

### References

1. Van Grieken, R.; Pena, J. L.; Lucas, A.; Galleja, G.; Rojas, M. L.; Fierro, J. L. G. *Catal. Lett.* **1991**, 8, 335–344.
2. Rojas, M. L.; Fierro, J. L. G. *J. Solid State Chem.* **1990**, 89, 299–307.

## **Bismuth silicates nanoparticles synthesized by pulsed laser ablation for photocatalytic applications**

A.G. Golubovskaya, E.D. Fakhrutdinova, V.A. Svetlichnyi

*Tomsk State University, Tomsk, Russia*

aleksandra.golubovskaya@mail.ru

Bismuth silicate (BSO) belong to new promising classes of materials for photocatalytic technologies applied in water purifying and hydrogen generation. BSO-based photocatalysts have the ability to act under the visible light irradiation, so these compounds have been actively studied in recent years [1-3]. Such materials are usually produced via hydrothermal methods, sol-gel or mechanical activation with the help of a planetary ball mill. As a result of such synthesis, particles of micron and submicron sizes are usually obtained. In this work, it is proposed to synthesize bismuth silicates by laser ablation in a liquid, which will reduce the particle size and also affect the phase composition.

The synthesis of bismuth silicates was carried out as follows. Initially, a stable colloidal silicon solution was obtained by ablation of a silicon target in water by Q-switch Nd: YAG laser with following parameters (1064 nm, 7ns, 20 Hz, 160 mJ/puls). Then, a freshly prepared solution of colloidal bismuth was mixed with a silicon solution with molar ratio 2:1, respectively. After that, the process of treatment of mixed solution was divided into 2 parts. First part was mixed and subjected to ultrasonic treatment about 30 min. Part 2 was additionally irradiated with laser beam with parameters mentioned above under stirring for 2 hours. Then the colloidal solutions were dried in open glass containers until completely dry, the obtained powder materials were annealed at 400 and 600 °C. The following conventions were adopted for materials: BSO1 (ultrasonic treatment) and BSO2 (extra irradiation treatment).

BSO1 nanopowder has specific surface 41 m<sup>2</sup>/g and consists of spherical particles with an average size of 40 nm. According to X-ray diffraction and diffuse reflection spectroscopy data the initial material contain metallic Bi and amorphous silica and absorbs in the entire range. After annealing at 400 °C the main phase of  $\alpha$ -Bi<sub>2</sub>O<sub>3</sub> with an impurity metasilicate phase Bi<sub>2</sub>SiO<sub>5</sub> are formed, and after 600 °C Bi<sub>2</sub>SiO<sub>5</sub> the main phase is metasilicate. Samples annealing at 400 and 600 °C have a wide absorption spectrum consisting of the absorption of bismuth oxide and metasilicate phases.

BSO2 nanopowder is X-ray amorphous and consists of spherical particles with an average size of 30 nm and has a specific surface area 52 m<sup>2</sup>/g. Extra irradiation treatment leads to homogenization of structure and bismuth metasilicate structure Bi<sub>2</sub>SiO<sub>5</sub> appear after annealing at 600 °C. The sample BSO2 absorb in the entire range and after annealing at 400 °C has one distinct edge at 430 nm. After annealing at 600°C the sample has absorption edge at 380 nm which can be associated with the structure of bismuth metasilicate.

The materials were tested for photocatalytic activity upon decomposition of the Rhodamine B dye under LED source ( $\lambda=378$  nm). BSO2 material shows better activity in this process, which can be associated with a homogeneous phase composition and smaller particle size.

*This work was supported by the Russian Science Foundation, project No. 19-73-30026.*

### **References**

1. Peiyang, Z.; Juncheng, H.; Li, J. *RSC Adv.* **2011**, 1, 1072–1077.
2. Gupta, S.; De Leon, L.; Subramanian, V. *Phys. Chem. Chem. Phys.* **2014**, 16, 12719–12727.
3. Karthik, K.; Devi, K.R.S.; Pinheiro, D.; Sugunan, S. *Mat. Sci. Semicon. Proc.* **2019**, 102, 104589.

## Experimental research of Fisher-Tropsh synthesis with nitrogen-rich syngas under different pressures of synthesis

A.S. Gorshkov<sup>1</sup>, I.S. Ermolaev<sup>2</sup>, K.O. Gryaznov<sup>2</sup>, L.V. Sineva<sup>2</sup>, I.G. Solomonik<sup>2</sup>, V.Z. Mordkovich<sup>1,2</sup>

<sup>1</sup>INFRA LLC

<sup>2</sup>Technological Institute for Superhard and Novel Carbon Materials

gorshkov@infra-technology.com

Fisher-Tropsh synthesis is a key stage of GTL technology, which allows converting hydrocarbon gases of different origin, such as natural gas, biogas and associated gas into high-quality synthetic oils and fuels. The main advantage of synthetic fuel is the absence of sulfur and aromatic components, so it satisfies ecological requirements [1].

The most expensive stage of GTL technology is the synthesis gas production. Fisher-Tropsh synthesis with cobalt catalysts requires the molar ratio  $H_2/CO$  equal to 2 to obtain the higher productivity of the catalyst. This molar ratio is provided by such processes as steam methane reforming (SMR) or autothermic reforming (ATR). Capital and operational costs of ATR are lower than SMR by 40–60%. However, the serious drawback of ATR technology is the necessity of the air separation plant, which increases the difficulty and hazard level of syngas production. The alternative technological way is to produce the syngas by partial oxidation with air instead of oxygen and then use nitrogen-rich syngas in Fisher-Tropsh synthesis [2].

The purpose of this work was to study how the dilution of syngas with nitrogen affects catalytic properties of Fischer-Tropsch synthesis in tubular reactors with the fixed bed cobalt catalyst layer. The long-term tests of cobalt catalyst at full-cycle GTL pilot plant were carried out to provide this study.

Diluted syngas can be obtained from different kinds of feedstocks. Some of them, such as biogas have low outlet pressure. The well studied optimal pressure of Fisher-Tropsh synthesis with cobalt catalysts, is 2MPa. Therefore, we investigated the effect of decreasing the synthesis pressure from 2MPa to 1,5MPa and 1,0MPa on the catalytic properties.

The tests were carried out using tubular reactors with inner diameter and length of reactor tubes used in commercial multi-tube reactors [3]. The investigated catalyst was produced by extrusion of pastes. Cobalt was used as an active component. The details of catalyst preparation were elucidated earlier [4].

The synthesis was carried out using the syngas diluted with large amount of nitrogen (50 % vol.). The reference synthesis was carried out using the syngas containing no more than 5% of inert components (nitrogen, methane, carbon dioxide).

The introduction of 50 % vol. of nitrogen into syngas influenced the catalytic properties such as the selectivity of the  $C_{5+}$  hydrocarbons formation, the productivity of  $C_{5+}$  and the selectivity of  $C_1$ - $C_4$  hydrocarbons. The introduction of nitrogen in syngas led to increasing the  $C_{5+}$  selectivity by 4.9%, decreasing the  $C_1$  selectivity by 7.6%. At the same time, the  $C_2$ - $C_4$  hydrocarbons selectivity and the selectivity of  $CO_2$  increased by 1.4%, and 1.5% respectively. The productivity of  $C_{5+}$  decreased in 1.8 times, while concentration of main reactants ( $CO$  and  $H_2$ ) in diluted syngas decreased in 2 times compared to the reference test. The increasing of gas-hour space velocity of diluted syngas compensated partly the productivity decreasing.

In the test with diluted syngas the impact of the pressure decreasing from 2MPa to 1,5MPa and 1.0 MPa was studied. The pressure decreasing to 1.5 MPa led to the productivity drop of 16%. The pressure decreasing to 1.0 MPa led to the further productivity drop of 22%.

To summarize, the syngas diluting by nitrogen provides considerable changes in the functional properties of Fischer-Tropsch catalyst. The results of the study can be useful for the calculations of perspective GTL plants.

### References

1. Dry, M.; Steynberg, A, Fischer-Tropsch technology (Studies in surface science and catalysis), Amsterdam: Elsevier, 2004.

2. Savost'yanov, A.P.; Jakovenko, R.; Narochnyi, G.B.; Lapidus A.L., *Solid Fuel Chem.* **2015**, 49(6), 356–359.
3. <http://www.infratechnology.ru/>
4. Mordkovich, V.Z.; Ermolaev, V.S.; Mitberg, E.B.; Sineva, L.V.; Solomonik, I.G.; Ermolaev, I.S.; Asalieva, E.Yu, *Res. Chem. Intermed.* **2015**, 41 (12), 9539–9550.

## Non-oxidative catalytic conversion of methane and C<sub>5</sub>-hydrocarbons

O.A. Kazakova, N.V. Vinichenko, A.E. Fedorov, T.I. Gulyaeva, V.A. Drozdov, A.S. Belyi

*Center of New Chemical Technologies BIC, Boreskov Institute of Catalysis, Omsk, Russia*

*o.a.kazakova@yandex.com*

Methane is one of the most abundant gases on our planet. It is the main component of natural and associated petroleum gases [1]. Methane is an inexpensive and valuable raw material for chemical industry. However, at the present time natural gas is mainly combusted for heat and electricity generation [2]. Irrational applying of gas recourses leads to negative environmental and economical consequences and primarily connected with the difficulty of activation of stable methane molecule [3]. Thus, the problem of methane activation and its conversion to high valuable products is significant target of modern heterogeneous catalysis. Direct methane dehydroaromatization (MDA) over the zeolite catalysts at high temperatures ( $\geq 973$  K) [4] is a promising area for methane processing. However, significant disadvantages of this method are the rapid deactivation of zeolite catalysts due to coke deposits formation and low yields of aromatic hydrocarbons [4].

The conversion of methane with a co-reactant allows significantly reduce the average temperature of the process. Our approach consists the methane chemisorption over the platinum-alumina catalyst with H-deficient surface hydrocarbon fragments (CH<sub>x</sub>-species) formation and hydrogen evolution. Then, pentane is feed to the chemisorbed methane at temperatures of 748–823 K and aromatic hydrocarbons (benzene and toluene) are formed [5]. However, co-conversion of methane with pent-1-ene and cyclopentane has not been studied yet and is of interest.

In this work, we established the main directions of the conversion of methane with C<sub>5</sub>-hydrocarbons of different classes over the 0.5wt.%Pt/ $\gamma$ -Al<sub>2</sub>O<sub>3</sub> catalyst. Using isotope ratio chromatography-mass spectrometry and labeled methane (<sup>13</sup>CH<sub>4</sub>) we studied the ability of CH<sub>x</sub>-species to form benzene when reacted with pentane, pent-1-ene, cyclopentane over the platinum-alumina catalyst at temperatures of 748–823 K under non-oxidizing conditions.

The platinum-alumina catalyst was characterized using the methods: atomic emission spectroscopy with ICP, infrared spectroscopy of adsorbed CO, temperature-programmed reduction and others. On the catalyst surface there are both the particles of metal platinum and the electron-deficient forms of platinum. The chemisorption of methane over platinum with the formation of surface hydrocarbon CH<sub>x</sub>-species and evolution of hydrogen into reactor starts at 748 K. The amount of chemisorbed methane increases with increasing temperature and reaches 44  $\mu$ mol/g at 823 K. To investigate the catalytic properties of the catalyst C<sub>5</sub>-hydrocarbons were fed to the chemisorbed methane (molar ratio of C<sub>5</sub>/Pt=1/1) at 748, 773, 798, 823 K. It was established that cyclic and acyclic pentenes and pentadienes are present in the mixtures of products of the co-conversion of methane with pent-1-ene and cyclopentane. The highest yield of aromatic hydrocarbons at 823 K was recorded during the co-conversion of methane and pent-1-ene (35.2 wt.%) compared with the co-conversion of methane with pentane (22.2 wt.%) and cyclopentane (16.1 wt.%). For the co-conversion of <sup>13</sup>CH<sub>4</sub> with pentane 39.8 % of benzene formed contains <sup>13</sup>C atom, and for the co-conversion of <sup>13</sup>CH<sub>4</sub> with pent-1-ene only 20.1 % of benzene is enriched.

*This work was carried out within the state task of the Boreskov Institute of Catalysis (project AAAA-A17-117021450095-1).*

### References

1. Lim, T. H.; Kim, D. H.; *Appl. Catal. A: Gen.* **2019**, 557, 10–19.
2. Wang, B.; Albarracín-Suazo, S.; Pagán-Torres, Y.; Nikolla, E. *Catal. Today.* **2017**, 185, 147–158.
3. Lou, Y.; He, P.; Zhao, L.; Chen, W.; Song, H. *Appl. Catal., B: Environ.* **2017**, 201, 278–289.
4. Ma, S.; Guo, X.; Zhao, L.; Scott, S.; Bao, X. *J. Energy Chem.* **2013**, 22, 1–20.
5. Golinskii, D. V.; Vinichenko, N. V.; Pashkov, V. V.; Udras, I. E.; Krol', O. V.; Talzi, V. P.; Belyi, A. S., *Kinet. Catal.* **2016**, 57, 504–510.

## Investigation of photocatalyst for hydrogen evolution from glucose solution

A.Y. Kurenkova<sup>1</sup>, E.A. Kozlova<sup>1,2</sup>

<sup>1</sup>*Boriskov Institute of Catalysis, Novosibirsk, Russia*

<sup>2</sup>*Novosibirsk State University, Novosibirsk, Russia*

kurenkova@catalysis.ru

Nowadays, hydrogen attracts worldwide attention as a promising energy source. But at the present time, the most commonly used method for hydrogen production is steam reforming where CO is by-product [1]. Therefore, there is a necessity to develop a new effective emission-free method for hydrogen production. One of such methods is photocatalytic hydrogen evolution from aqua solutions of electron donors. In the process, one can obtain H<sub>2</sub> using only renewable energy sources: water, solar light, and biomass component as electron donors. A Cd<sub>1-x</sub>Zn<sub>x</sub>S solid solution is an efficient photocatalyst for H<sub>2</sub> production from water solutions under visible light. To improve the photocatalytic activity of Cd<sub>1-x</sub>Zn<sub>x</sub>S solid solution, many modification approaches have been developed. Our previous work [2] has shown the hydrothermal treatment of Cd<sub>0.3</sub>Zn<sub>0.7</sub>S catalyst changes the crystal structure from cubic lattice to hexagonal one which is beneficial for photocatalytic reaction. Moreover, the deposition of Pt particles onto the photocatalyst surface is known to increase the hydrogen evolution rate.

The present work was aimed at the study of photocatalyst in the process of hydrogen evolution from aqueous solution of glucose as a model compound of biomass. A Cd<sub>0.3</sub>Zn<sub>0.7</sub>S photocatalyst was prepared by the coprecipitation method with subsequent hydrothermal treatment at 120 °C in air atmosphere. In our previous work [2] has been shown that solid sulfide solution is stratified into two phases – Cd<sub>0.6</sub>Zn<sub>0.4</sub>S and ZnS after hydrothermal treatment. Afterward, the Pt particles were deposited on the surface of prepared sample. Photocatalytic hydrogen evolution was carried out by the following method. The aqueous suspension (100 mL) with the catalyst, NaOH, and glucose (45 mM) was placed in a sealed reactor, purged with Ar and illuminated by a 450-nm LED (48 mV/cm<sup>2</sup>) under continuous stirring. Hydrogen was analyzed by gas chromatography. The concentration of NaOH was varied.

The investigation of photocatalyst stability for 15 hours has shown the rate of H<sub>2</sub> evolution in high basic condition (5 M) is increased after 1,5 hours; meantime the rate in dilute NaOH (0.1 M) reduces gradually for 15 hours. The samples of as-prepared photocatalyst and photocatalyst after hydrogen evolution reaction in both NaOH solutions were studied by XRD and XPS techniques. The XRD showed no differences between any samples. The XPS demonstrated the reduced content of S<sup>2-</sup> and increased content of O<sup>2-</sup> for both samples after photocatalytic reaction in contrast with the as-prepared sample. Therefore, we can conclude that the photocatalyst surface undergoes photocorrosion. On the other hand, platinum was found in the metallic state as well as in the oxidized state on the sulfide surface. Moreover, in high basic condition, there is an increase of Pt<sup>0</sup> content, that results in enhanced charge separation efficiency and improved photocatalytic activity. Thereby we can conclude that both samples suffer from photocorrosion to decrease activity, but there is the process to increase the activity in 5 M NaOH solution – platinum reduction.

Also, the influence of photocatalyst concentration in reaction solution and platinum concentration on the sulfide surface have been studied. The rate of H<sub>2</sub> evolution shown to increase till the concentration of catalyst 0.5 g/L and then reaches plateau. Platinum particles gradually enhances the photocatalyst activity till the concentration of 1 wt. % Pt and then the activity decreases. We can define the optimal conditions to achieve the high rate of H<sub>2</sub> evolution as following: C(1%Pt/Cd<sub>0.6</sub>Zn<sub>0.4</sub>S/ZnS) = 0.5 g/L, C<sub>0</sub>(glucose) = 45 mM, C<sub>0</sub>(NaOH) = 5 M. The AQE = 8.5%, the rate of H<sub>2</sub> evolution is 3.4 mM·g<sub>cat</sub><sup>-1</sup>·h<sup>-1</sup> in the defined conditions.

*The reported study was funded by RFBR and Novosibirsk region according to the research project № 19-43-543009*

### References

1. Christoforidis, K.C.; Fornasiero, P. *ChemCatChem* **2017**, 9, 1523-1544.  
Kurenkova, A.Y.; Kolinko P.A.; Sherepanova, S.V.; Kozlova, E.A. *Mater. Today Proc.* **2017**, 11, 11371–11374.

## Solid solutions of CdS and ZnS: comparing photocatalytic activity and photoelectrochemical properties

D.V. Markovskaya<sup>1,2</sup>, A.V. Zhuremok<sup>1</sup>, E.A. Kozlova<sup>1,2</sup>

<sup>1</sup>*Boriskov Institute of Catalysis, Novosibirsk, Russia*

<sup>2</sup>*Novosibirsk State University, Novosibirsk, Russia*

madiva@catalysis.ru

Renewable solar energy is becoming a viable source of energy to provide a clean solution to the current energetic problems. There are two main ways of solar energy utilization – photocatalytic processes and photocurrent generation. In both cases materials activated by visible light irradiation are required. The applicable material for these purposes is cadmium sulfide. However, fast recombination of photogenerated electron-hole pairs and photocorrosion are two key factors limiting both the photocatalytic activity and current generation over CdS [1]. It is known that formation of solid solution based on CdS and ZnS allows reducing these restrictions. This work is aimed at the comparative study of the photocatalytic and photoelectrochemical properties of the solid solutions  $\text{Cd}_{1-x}\text{Zn}_x\text{S}$ .

In this work the photocatalysts  $\text{Cd}_{1-x}\text{Zn}_x\text{S}$  were prepared by the deposition method [2]. Their catalytic activity was tested in the photocatalytic hydrogen evolution from aqueous 0.1 M  $\text{Na}_2\text{S}/0.1$  M  $\text{Na}_2\text{SO}_3$  solution under visible light irradiation ( $\lambda = 450$  nm). The photoelectrodes  $\text{Cd}_{1-x}\text{Zn}_x\text{S}/\text{FTO}$  were prepared by the successive ionic layer adsorption and reaction method. The electrochemical properties were studied by cyclic voltammetry and impedance spectroscopy. The photoelectrochemical cell has been fabricated by sandwiching the counter electrode and the tested photoanode using a parafilm spacer. The  $\text{Cu}_2\text{S}/\text{brass}$  was used as a counter electrode. The electrolyte consisted of 1 M  $\text{Na}_2\text{S}_n$ , 0.1 M  $\text{NaCl}$  [2].

Pure CdS and ZnS demonstrate low catalytic activity in hydrogen production. The solid solutions  $\text{Cd}_{1-x}\text{Zn}_x\text{S}$  are more active than bare samples. The dependence of the reaction rate on zinc content goes through two maxima. This behavior may be as a result of three factors. On the one hand, the increase of Zn content in the samples leads to the absorption shift in UV region and the falling of amount of electron-hole pairs [1]. On the other hand, the reduction potential of  $\text{Cd}_{1-x}\text{Zn}_x\text{S}$  enhances with the growth of the zinc content. Additionally, the defects enhancing both the electron concentration and the photocatalytic activity are formed into the solid solutions of cadmium sulfide and zinc sulfide [3]. The highest catalytic activity is demonstrated by the  $\text{Cd}_{0.3}\text{Zn}_{0.7}\text{S}$  sample.

The dependence of the short-circuit current density on zinc content goes through two maxima. The highest photocurrent is obtained by  $\text{Cd}_{0.8}\text{Zn}_{0.2}\text{S}/\text{FTO}$  ( $2.2 \text{ mA}/\text{cm}^2$ ) whereas the most active photocatalyst is  $\text{Cd}_{0.3}\text{Zn}_{0.7}\text{S}$ . In order to understand this fact, the photoelectrodes were studied by impedance spectroscopy. It has been shown that the photocurrent values grow with the increase of electron lifetime. If the electron lifetimes of the tested samples have similar values, the concentration of charge carriers plays a crucial role for the current generation over  $\text{Cd}_{1-x}\text{Zn}_x\text{S}/\text{FTO}$  photoelectrodes. Earlier, the influence of the latter factor on the efficiency of photoelectrochemical cell was only mentioned in the literature [1].

To sum up, the balance between the electron concentration and the reduction ability is crucial for the photocatalytic hydrogen production over  $\text{Cd}_{1-x}\text{Zn}_x\text{S}$ . High values of electron lifetime and concentration of charge carriers favor the effective conversion of the light energy to electricity.

*This work was supported by President of Russian Federation Scholarship SP-1029.2019.1.*

### References

1. Antoniadou, M.; Daskalaki, V. M.; Balis, N.; Kondarides, D. I.; Kordulis, C.; Lianos, P. *Appl. Catal. B. – Environ.* **2011**, *107*, 188–196.
2. Markovskaya, D. V.; Gribov, E.N.; Kozlova, E.A.; Kozlov, D.V.; Parmon, V.N. *Renew. Energ.* **2020**, doi: 10.1016/j.renene.2019.11.030.
3. Roy, A. M.; De, G. C. *J. Photoch. Photobio. A.* **2003**, *157*, 87–92.



## Combined Sorption and Catalytic Remove of Volatile Organic Compounds over Ag-CeO<sub>2</sub>/SBA-15 composites

N.N. Mikheeva<sup>1</sup>, V.I. Zaikovskii<sup>2</sup>, G.V. Mamontov<sup>1</sup>

<sup>1</sup>*Tomsk State University, Tomsk, Russia*

<sup>2</sup>*Borshchov Institute of Catalysis, Novosibirsk, Russia*

natlitv93@yandex.ru

The problem of air pollution with volatile organic compounds (VOCs) is becoming increasingly relevant and requires the search for effective ways to solve it, primarily the development of new catalysts for the deep oxidation of VOCs to CO<sub>2</sub> and H<sub>2</sub>O, as the most promising way to deal with VOCs [1]. The most active catalysts based on noble metals (Au, Pd, Pt, Ag), among which the greatest practical interest are silver-containing catalysts, which are highly stable (including in the presence of water vapor) and relatively low cost. Using approaches to create sorption-catalytic materials will make it possible to obtain a highly active catalyst for the oxidation of VOCs, which can also operate in a sorption mode at room temperature, which will significantly increase the possibility of its use.

The aim of this work is to develop sorption-catalytic materials based on SBA-15 with nanosized particles of silver and cerium oxide. The features of distribution of silver and ceria in porous structure of SBA-15, sorption and catalytic oxidation of VOCs are under discussion. The SBA-15 was synthesized by the template method with using of Pluronic P123 as template and TEOS as silica source. The Ag-CeO<sub>2</sub>/SBA-15 catalysts (the loading of Ag and CeO<sub>2</sub> of 10 and 20 wt. %, respectively) were prepared by the incipient wetness impregnation with using of aqueous solutions of cerium (III) nitrate and silver nitrate. The catalysts were characterized by low-temperature adsorption of nitrogen, XRD, SAXS, TEM, TPR H<sub>2</sub> and TPD of toluene. The catalytic properties of the catalysts were tested in the oxidation of toluene and isopropyl alcohol.

It was shown by TEM that worm-like nanoparticles with well ordered structure were obtained. It was found [2, 3] that the use of citric acid as a stabilizing agent and a special ordered structure of SBA-15 as nanoreactors allow to obtain Ag-CeO<sub>2</sub>/SBA-15 catalysts with a particle size of silver and cerium oxide predominantly less than 5 nm in size. It was shown that the synthesized samples are characterized by the presence of two types of silver particles: 0.5–3 nm in size, localized inside the SBA pores, and larger particles (4–8 nm) located on the outer surface of SBA-15. The resulting distribution of silver particles and cerium oxide leads to the presence of interaction between the particles of active components. This interaction has a positive effect on the redox and catalytic properties of synthesized catalysts.

The synthesized catalysts showed high activity in the oxidation of CO (T<sub>50%</sub> = 46 °C) and total oxidation of methanol (T<sub>50%</sub> = 98 °C). By the TPD of toluene it was shown that the presence of silver and ceria interacting particles on the SBA-15 surface leads to decreasing amount of weakly bonded toluene and appearance of second high temperature peak of toluene desorption which should be connected with the strong adsorption (probably chemisorptions) of toluene on active species of ceria and silver. In addition, the interaction of silver and ceria particles leads to an increase in the oxidative capacity of the catalyst in the reaction of deep oxidation of toluene. So for Ag/SBA-15 catalyst 50% conversion is achieved at a temperature of 255 °C, and for Ag-CeO<sub>2</sub>/SBA-15 catalyst at a temperature of 219 °C.

Thus the obtained data indicate that the synthesized catalysts are of great scientific and practical interest. The relatively high catalytic activity of Ag-CeO<sub>2</sub>/SBA-15 catalyst and its ability to chemisorb toluene allow it to be used as a system for air purification from VOC emissions by combining sorption and catalytic approaches.

*This work was supported by RFBR Grant 19-33-90189.*

### References

1. Huang, H.; Xu, Y.; Feng, Q.; Leung, D.Y. *Cat. Sci. Technol.* **2015**, 5(5), 2649–2669.
2. Mikheeva, N.N.; Zaikovskii, V.I.; Mamontov, G.V. *Microporous Mesoporous Mater.* **2019**, 277, 10–16.
3. Mikheeva, N.N.; Zaikovskii, V.I.; Mamontov, G.V. *J. Sol-Gel Sci. Technol.* **2019**, 92, 398.

## Aspen wood ethanol lignin depolymerization in supercritical ethanol in the presence of Ni-containing catalysts

A.V. Miroshnikova<sup>1</sup>, V.I. Sharypov<sup>1</sup>, S.V. Baryshnikov<sup>1</sup>, Yu.N. Malyar<sup>1</sup>, V.A. Yakovlev<sup>2</sup>,  
O.P.Taran<sup>1,2</sup>, B.N. Kuznetsov<sup>1</sup>

<sup>1</sup>*Institute of Chemistry and Chemical Technology SB RAS*

*FRC "Krasnoyarsk Scientific Center SB RAS", Russia*

<sup>2</sup>*FRC Boreskov Institute of Catalysis SB RAS, Novosibirsk, Russia*

miroshnikova.av@icct.krasn.ru

Lignin is one of the three main components of plant biomass, its content in wood reaches 30 wt%. Technical lignins produced by commercial pulping and hydrolysis processes contain sulfur and they are law reactive, which makes it difficult to process them into valuable chemical products. An effective method for the obtaining lignins without the use of mineral acids and bases is the extraction of lignocellulosic materials with low-boiling organic solvents, or their mixtures with water in the temperature range 180-200 °C [1]. The resulting organosolv lignins do not contain sulfur, possessing a low molecular weight and higher reactivity as compared to technical lignins.

The purpose of this work was to establish the effect of NiCu/SiO<sub>2</sub> and NiCuMo/SiO<sub>2</sub> catalysts (with different molybdenum contents), and on the process temperature (300 and 350 °C) on yields of liquid, gaseous, solid products and on the composition of liquid products of thermo-catalytic conversion of aspen ethanol lignin in supercritical ethanol.

Catalysts NiCu/SiO<sub>2</sub> and NiCuMo/SiO<sub>2</sub> were prepared by sol-gel method [2,3].

Under the condition used the yield of liquid products increased from 69.3 wt% to 78.8 wt% in the presence of a NiCu/SiO<sub>2</sub> catalyst as compared with the non-catalytic experiment at a temperature of 300°C.

The introduction of molybdenum into the catalyst in the amount of 8.8 and 11.7 leads to an increase in the yield of liquid products to 83.5 wt.%. The it maximum yield was 86.6 wt% for the NiCuMo/SiO<sub>2</sub> catalyst with a Mo content of 8.8 wt%

At a process temperature of 350 °C in the presence of NiCu/SiO<sub>2</sub> and NiCuMo/SiO<sub>2</sub> catalysts with a Mo content 8.8 wt% the yields of liquid and gaseous products of aspen ethanol lignin practically unchanged. The increase in the Mo content in the NiCuMo/SiO<sub>2</sub> catalyst from 8.8 to 11.7 wt% reduces in the yield of liquid products and leads to increase in the yield of gaseous products. Which main by consist of carbon oxides and methane.

According to GC-MS data, the monomer compounds of the liquid products are mainly represented syringol, guaiacol and their alkyl derivatives. The highest yields of monomer substances were obtained with the NiCuMo/SiO<sub>2</sub> catalyst at a temperature of 300 °C. Their yield higher is by 1.7 times than in the non-catalytic experiment.

The optimal conditions for the thermal conversion of aspen ethanol lignin are established. The highest yields of liquid and monomer products were obtained using a NiCuMo/SiO<sub>2</sub> catalyst at a process temperature of 300 °C. At this temperature, the changes in the Mo content in the catalyst do not lead to significant changes in the yields of liquid and monomer compounds.

*The reported study was supported by Russian Science Foundation, Grant No. 16-13-10326.*

### References

1. Zhang, K.; Pei, Z. J.; Wang, D. *Bioresour. Techno.* 2015, **199**, 21–33.
2. Ermakova, M. A.; Ermakov, D. Y. *Applied Catalysis A: General.* 2003, **245**, 277–288.
3. Alekseeva, M. V.; Rekhtina, M. A.; Lebedev, M. Y.; Zavarukhin, S. G.; Kaichev, V. V.; Venderbosch, R. H.; Yakovlev, V. A. *Chem. Select.* 2018, **3**, 5153–5164.

## Selective hydrogenation of 2-methyl-3-butyn 2-ol in microcapillary reactor.

### Effect of support on stability and kinetic parameters

L.B. Okhlopkova<sup>1</sup>, M.A. Kerzhentsev<sup>1</sup>, Z.R. Ismagilov<sup>1,2</sup>

<sup>1</sup>*Boriskov Institute of Catalysis, Novosibirsk, Russia*

<sup>2</sup>*Institute of Coal Chemistry and Material Science, Kemerovo, Russia*

corresponding-mila65@catalysis.ru

It is known that the catalytic properties of nanoparticles depend on their size and shape, which, in turn, are determined by the interaction between the supported metal and the oxide matrix. The support not only affects the distribution of metal, the structure and morphology of metal particles, surface area and pore size distribution, but also participates in the effects of internal mass transfer. The support can also change the performance of the catalyst through electronic interactions. Moreover, multicrystalline oxide coatings based on titanium dioxide ( $\text{Ti}_{1-x}\text{M}_x\text{O}_{2+y}$ ,  $\text{M} = \text{Ce}, \text{Zr}, \text{Zn}$ ) has several advantages, namely, increased mechanical strength, chemical and thermal stability. It is important to note that the properties of complex oxides based on titanium dioxide can be purposefully controlled by varying the doping cation ( $\text{M}$ ) and the molar ratio  $\text{Ti}/\text{M}$ . Thus, the possibility of controlling the dispersion and redox properties of the active metal, and, accordingly, the catalytic reaction can be realized. This work is devoted to revealing the mechanism of the influence of support composition on the catalytic behavior of PdZn nanoparticles in the hydrogenation of acetylene alcohols.

The ordered mesoporous modified  $\text{Ti}_{1-x}\text{M}_x\text{O}_{2+y}$  composites were synthesized by evaporation-induced self-assembly by varying the  $\text{Ti}/\text{M}$  molar ratio using titanium isopropoxide, zirconium oxychloride, cerium nitrate and zinc acetate as precursors and F127 triblock copolymer as template [1-3]. The structure and texture of the support and its thermal stability were systematically studied by X-ray diffraction analysis, transmission electron microscopy and low-temperature nitrogen adsorption. Catalytic coatings with 1 wt.% PdZn/ $\text{Ti}_{1-x}\text{M}_x\text{O}_{2+y}$  ( $\text{M} = \text{Ce}$ ,  $x = 0.95$ ;  $\text{Zr}$ ,  $x = 0.8$ ;  $\text{Zn}$ ,  $x = 0.2$ ) were synthesized on the inner surface of a capillary reactor with a diameter of 0.53 mm and a length of 10 m. The coatings were tested in the selective hydrogenation of 2-methyl-3-butyn-2-ol (MBY) at 333 K and 1 atm  $\text{H}_2$ . The kinetic parameters of the Langmuir - Hinshelwood model were calculated using the Matlab software.

The initial reactor productivity ( $t \leq 32$  h) increases in the series PdZn/ $\text{Ti}_{0.8}\text{Zn}_{0.2}\text{O}_{1.8}$  < PdZn/ $\text{TiO}_2$  ~ PdZn/ $\text{Ti}_{0.95}\text{Ce}_{0.05}\text{O}_2$  < PdZn/ $\text{Ti}_{0.8}\text{Zr}_{0.2}\text{O}_2$ . The selectivity at  $t = 32$  h decreases in the series PdZn/ $\text{Ti}_{0.8}\text{Zn}_{0.2}\text{O}_{1.8}$  > PdZn/ $\text{TiO}_2$  > PdZn/ $\text{Ti}_{0.8}\text{Zr}_{0.2}\text{O}_2$  > PdZn/ $\text{Ti}_{0.95}\text{Ce}_{0.05}\text{O}_2$ . The lower selectivity for 2-methyl-3-buten-2-ol (MBE) on PdZn nanoparticles embedded in the titanium-cerium oxide matrix is due to an increase in the ratio of alkene and alkyne adsorption constants. On the contrary, a decrease in the ratio of the adsorption constants of alkene and alkyne leads to an increase in the selectivity of the coating based on titanium-zinc oxides. Activity increases, and selectivity decreases with increasing reaction time for mixed coatings of titanium-zirconium and titanium-zinc oxides. Opposite patterns were obtained for titanium-cerium oxide coatings. The activity decreases slightly, and the selectivity increases with increasing reaction time as a result of the oxidation of  $\text{Ce}^{3+}$  to  $\text{Ce}^{4+}$ . The PdZn/ $\text{Ti}_{0.8}\text{Zn}_{0.2}\text{O}_{1.8}$  coating was the most active (3.8 gMBE per day) and selective for MBE (98.2%) with a long-term test of up to 168 hours.

*This work was conducted within the framework of the budget project No. AAAA-A17-117041710090-3 for Boriskov Institute of Catalysis.*

#### References

1. Okhlopkova, L.; Kerzhentsev, M.; Ismagilov, Z. *Kinet. Catal.* **2019**, 60, 474–483.
2. Okhlopkova, L.; Kerzhentsev, M.; Ismagilov, Z. *Surf. Eng.* **2015**, 31, 78–83.
3. Okhlopkova, L.; Cherepanova, S.; Prosvirin, I.; Kerzhentsev, M.; Ismagilov, Z. *Appl. Catal. A* **2018**, 549, 245–253.

## Glycerol oxidative conversion over Au NPs obtained by PLAL technique

S. Ten, K. Kurmanbaeva, E.A. Gavrilenko, V.A. Svetlichnyi, O.V. Vodyankina

*National Research Tomsk State University, Tomsk, Russian Federation*

rip\_richard@mail.ru

The use of bio-renewable feedstock is important for the modern chemical industry. Production of glycerol (Gly) as an undesired byproduct of biodiesel generation (10 % of the total volume) is rapidly growing. Aerobic oxidation of glycerol allows obtaining a wide range of valuable chemicals [1]. This makes glycerol an attractive platform molecule for the bio-based chemical industry. The main challenge in this route is a low selectivity due to parallel oxidation of primary and secondary hydroxyl groups of glycerol, C-C bond cleavage, and over-oxidation with the formation of C<sub>2</sub> products and formic acid (FA).

Supported gold nanoparticles (NPs) demonstrate high activity in glycerol conversion in alkaline media. The selectivity towards the main product strongly depends on support nature. Increasing of the support acidity leads to the reduction of glycerol conversion, selectivities towards glyceric acid (GA) and tartronic acid, while the lactic acid (LA) selectivity increases. A high concentration of the basic sites on the support strongly decreases the catalytic activity of Au NPs. One of the modern methods of laboratory synthesis of colloid NPs of various composition and structure for catalytic applications that has been intensively developed in recent years is pulsed laser ablation in liquid (PLAL). The PLAL makes it possible to obtain both "pure" nanocolloids in pure solvents without the use of stabilizers and precursors as well as the colloids using various stabilizers and functional additives.

In the present work the catalytic activity of gold dispersions prepared by PLA in water using PVA and PVP were studied in the process of glycerol oxidation into available products. Activity of Au NPs prepared by PLAL was compared with Au NPs prepared by wet chemical approach. All Au dispersions were characterized by UV-vis DRS, TEM, and  $\zeta$ -potential studies. According to the TEM data, initially spherical gold NPs fuse into extended agglomerates in secondary interaction with the laser beam during the PLA in water. The use of high molecular weight polymeric agents (PVA MW = 150000 and PVP MW = 55000) prevents particle fusion and agglomeration. The average size of individual particles is significantly reduced. In the case of PVP, the change in polymer concentration from 0.02 to 0.2 wt% does not lead to any significant changes in the morphology and dimensional characteristics of the particles, and even a slight increase in average sizes is observed.

We tested the activity of the Au NPs prepared via PLA and wet chemical technique. Au NPs prepared by PLA in water aggregated during the catalytic test and demonstrated the 50% conversion. Using PVA as a stabilizer led to suppressing of Au NPs activity due to occupying of active sites of Au NPs by PVA. Application of PVP led to enhancing of Au NPs stability and activity in Gly oxidation (up to full conversion). Increasing the reaction temperature led to growth of Gly conversion and selectivity towards LA, while the selectivities towards GA and FA decreased. The rapid increase of the Gly conversion at 100 °C can be caused by involving of Gly dehydration route in alkaline media. The Gly dehydration is an endothermic reaction, thus, this pathway can be realized at high temperatures [2]. The Au NPs prepared by chemical reduction demonstrated the same Gly conversion at 100 °C in comparison with the PLAL Au catalyst, but the selectivities towards LA and GA were slightly lower. The Au NPs obtained by the PLAL and wet chemical technique possessed different particle sizes and surface plasmon resonance (SPR) peak, but after the catalytic test, the SPR peak of Au NPs featured an identical localization. Thus, we suppose that Au NPs obtained by PLAL and wet chemical technique have the same surface organization during the catalytic experiments. The influence of NaOH concentration, the amount of Au NPs and Gly concentration, reaction time and other reaction conditions on the Au NPs activity will be discussed.

*This work was supported by Russian Science Foundation (project number 19-73-30026).*

### References

1. Walgode, P. M.; Faria, R. P.; Rodrigues, A. E. *Catal. Rev. Sci. Eng.* **2020**, 1–90.
2. Velásquez, M.; Batiot-Dupeyrat, C.; Espinal, J.F.; Sánchez, A.; Santamaría, A. *DYNA* **2019**, 86 (208), 126–135.

## Selective Hydrogenation of 1,3-butadiene over SiO<sub>2</sub>-supported Cu nanoparticles

G. Totarella, B. Donoeva, P.E. de Jongh

*Debye Institute for Nanomaterials Science, Utrecht University, Utrecht, the Netherlands*

g.totarella@uu.nl

The catalytic removal of polyunsaturated contaminants from alkene-rich streams plays a key role in the manufacture of polymer- and synthesis- grade C<sub>2</sub>-C<sub>4</sub> olefins. This purification process is usually carried out by means of Pd-based (often diluted in Ag) hydrogenation catalysts, which are required to reduce the concentration of alkadiene/alkynes in the alkene feed to less than a few tens of ppm. However, potential restructuring/segregation phenomena of the highly active Pd can compromise the catalyst stability and, more importantly, its selectivity [1,2]. It is of a great interest to investigate more forgiving and earth-abundant hydrogenation metal, such as Ni, Cu, Fe, or Co [3]. Copper, in particular, has recently drawn attention as computationally and experimentally proven to be highly effective in selective hydrogenations [2,3]. However, little is known about the parameters that determine the Cu selectivity and stability.

With this project we investigated the catalytic properties of differently sized Cu nanoparticles (2–10 nm) immobilized via incipient wetness impregnation on either silica or carbon supports. We chosen the hydrogenation of 1,3-butadiene in 100-fold excess of propene as model reaction in order to simulate the catalytic removal of dienes from industrial olefin streams.

The SiO<sub>2</sub>- and C-supported Cu catalysts showed remarkable performance, with a reactant selectivity as high as 98.7% at almost full (95%) 1,3-butadiene conversion (propene conversion <0.015%). In addition, the samples showed outstanding stability, in particular in the case of large (7 nm) particles over silica support (almost full activity is retained over 60 h of time-on-stream, T=140°C). This shows that Cu/C and Cu/SiO<sub>2</sub> are very promising in the transitioning from precious to base metal catalysts in the selective hydrogenation of polyunsaturated molecules. Further details on catalyst selectivity and particle size effect will be shown in a conference contribution.

*This work was supported by NWO-VICI grant 016.130.344 (the Netherlands).*

### References

1. Vignola, E.; Steinmann, S. N.; Vandegehuchte, B. D.; Curulla, D.; Sautet, P. *J. Phys. Chem. C* **2016**, *120*, 26320–26327.
2. Wang, Z.; Brouri, D.; Casale, S.; Delannoy, L.; Louis, C.; *J. Catal.* **2016**, *340*, 95-106.
3. Studt, F.; Abild-Pedersen, F.; Bligaard, T.; Sørensen, R. Z.; Christensen, C. H.; Nørskov, J. K. *Science* **2008**, *320*, 1320-1322
4. Masoud, N.; Delannoy, L.; Schaink, H.; Van Der Eerden, A.; De Rijk, J. W.; Silva, T. A.; Banerjee, D.; Meeldijk, J. D.; De Jong, K. P.; Louis, C.; De Jongh, P. E. *ACS Catal.*, **2017**, *7*, 5594-5603.

## Effect of platinum size of Pt/ $\gamma$ -Al<sub>2</sub>O<sub>3</sub> catalysts on propane dehydrogenation

Alexandre Van Assche, Anthony Le Valant, Catherine Especel, Florence Epron

*Institut de Chimie des Milieux & Matériaux de Poitiers (IC2MP), Université de Poitiers, 4 rue Michel Brunet, 86073 Poitiers Cedex 9, France*

alexandre.van.assche@univ-poitiers.fr

Propylene is the second most important commodity for the petrochemical industry after ethylene, explaining its growing demand. It is mainly obtained as a co-product by steam cracking of hydrocarbons at the same time as ethylene. But the wealth of natural gas following the boom in American shale gas is an opportunity to focus on its production by dehydrogenation of propane (PDH). Dehydrogenation technologies are mature and deployed worldwide on a large scale, there is still room for improvement, in particular by optimizing the catalyst design, to increase the resistance against coke deposition and metal sintering while increasing propane conversion to propene. Pt is the most active metal for dehydrogenation reactions with a low hydrogenolytic activity. As Pt/Al<sub>2</sub>O<sub>3</sub> suffers from deactivation by coke deposition, the majority of the literature works is focused on finding the best promoters to limit this deactivation, where Pt/Al<sub>2</sub>O<sub>3</sub> catalyst is only used as a reference to highlight the beneficial effect of the promoters [1]. But it seems to us necessary to better understand the role of the Pt structure in the reaction before improving the design of efficient Pt-based catalyst. In this work the performances of various Pt/Al<sub>2</sub>O<sub>3</sub> catalysts with Pt particle sizes varying between ca. 0.8 and 2.6 nm will be evaluated in PDH reaction. It will be demonstrated that, contrary to what is generally admitted, dehydrogenation is a structure-sensitive reaction, in reaction conditions used, with a strong effect of the Pt particle size on the activity but a limited influence on the selectivity to propene.

Pt/Al<sub>2</sub>O<sub>3</sub> catalysts with less than 1 wt.%Pt were prepared by impregnation via the strong electrostatic adsorption of an alumina support. In order to increase the platinum particle size, platinum was deposited on a parent 1wt.%Pt/Al<sub>2</sub>O<sub>3</sub> catalyst by the refilling method described in [2]. Catalysts were characterized by ICP-OES, H<sub>2</sub> chemisorption [3] and TEM. Propane dehydrogenation reaction was carried out in a conventional fixed-bed reactor at iso Pt content, after pretreatment of the catalyst under H<sub>2</sub> at 650 °C for 1 h. The gas mixture was composed of C<sub>3</sub>H<sub>8</sub>:N<sub>2</sub>:H<sub>2</sub> with a molar ratio of 10:9:1 under ambient pressure.

The propane conversion as well as the TOF values decreased as the Pt size increased, clearly demonstrating that, contrary to what is generally admitted [1], PDH is a structure sensitive reaction, in accordance with the results obtained for 2,3-dimethylbutane dehydrogenation [4]. On the contrary, the selectivity to propene seemed to be independent of the platinum particle size as for the same conversion values, the selectivities were similar whatever the catalyst.

For all the catalysts, a deactivation was observed during time on stream (1 h), evidenced by a decrease in conversion associated with an increase in the selectivity to propene. This deactivation phenomenon mainly occurred during the 10 first minutes of reaction and was the most important for the smallest particles, for which the TEM pictures showed a negligible increase in Pt size during the reaction. However, the amount of coke deposited on the metal and the support, as determined by TGA analysis, was similar whatever the catalyst.

### References

1. Sattler, J. J. H. B.; Ruiz-Martinez, J.; Santillan-Jimenez, E.; Weckhuysen, B. M. *Chem. Rev.* **2014**, *114*, 10613–10653.
2. Samoilă, P.; Boutzeloit, M.; Especel, C.; Epron, F.; Marécot, P. *J. Catal.*, **2010**, *276*, 237–248.
3. Le Valant, A.; Comminges, C.; Can, F.; Thomas, K.; Houalla, M.; Epron, F. *J. Phys. Chem. C* **2016**, *120*, 26374–26385.
4. Nakamura, M.; Yamada, M.; Amano, A. *J. Catal.* **1975**, *39*, 125–133.

## Ag-CeO<sub>2</sub> catalysts for toluene oxidation and 4-nitrophenol reduction

M.V. Chernykh, N.N. Mikheeva, G.V. Mamontov

*Tomsk State University, Tomsk, Russia*

msadlivskaya@mail.ru

Currently, the development of heterogeneous catalysts is important to address the challenges of environmental pollution. Toluene is an important organic solvent in the manufacturing of dyes, rubber, resins, etc. It is volatile and harmful for human health and pollute the environment. Prolonged exposure to low toluene concentrations can lead to serious diseases [1]. Thus, toluene in industrial waste gases must be effectively disposed of. The reduction of nitrocompounds to the corresponding aminocompounds is an important intermediate step in the production of medicines, plastics, agrochemicals, etc. Nitroaromatic compounds also have various negative effects on the environment and human health, therefore, its reduction is an important task in the purification of wastewater [2].

Ag-CeO<sub>2</sub> catalysts have attracted great interest since due to their unique physical-chemical characteristics they exhibit high activity in many catalytic reactions [3], including total oxidation of volatile organic compounds and reduction of nitrocompounds and aldehydes. The present work is devoted to the design of Ag-CeO<sub>2</sub> catalysts for total oxidation of toluene and room-temperature reduction of nitrophenol. The effect of the Ag content on the structure and catalytic properties of the catalysts was studied.

The CeO<sub>2</sub> support was synthesized by the thermal decomposition of Ce(NO<sub>3</sub>)<sub>3</sub>·6H<sub>2</sub>O. The series of Ag-CeO<sub>2</sub> catalysts were prepared by impregnation of CeO<sub>2</sub> with aqueous solution of AgNO<sub>3</sub>. The Ag loading was 1, 3, 5 and 10 wt.%. All samples were analyzed by a set of physical-chemical methods: low-temperature (-196 °C) adsorption of N<sub>2</sub>, TPR-H<sub>2</sub>, XRD, TPD-C<sub>7</sub>H<sub>8</sub>, TPSR. The activity of the catalysts in the reduction of nitro compounds was tested in the reaction of the reduction of 4-nitrophenol to 4-aminophenol with NaBH<sub>4</sub> in aqueous solution at room temperature and atmospheric pressure.

According to the results of low-temperature nitrogen adsorption, the decreases of the specific surface and pore volume from 76 m<sup>2</sup>/g and 0.252 cm<sup>3</sup>/g to 46 m<sup>2</sup>/g and 0.176 cm<sup>3</sup>/g occur with an increase in the silver content. All samples are characterized by the mesoporous structure with a pore size of 5-20 nm. The presence of a metallic silver phase was detected by the XRD method only for the 10Ag/CeO<sub>2</sub> sample that indicates the formation of highly dispersed silver particles in the samples with Ag loading of 1-5 wt. %. It was shown by the TPR-H<sub>2</sub> method that for all silver-containing samples the shift in low-temperature region corresponding to the reduction of surface ceria in comparison with the pure ceria support is observed. This indicates the presence of interfacial metal-support interaction in the samples.

The presence of two adsorbed forms of toluene (chemisorbed and molecular) was shown by the TPD-C<sub>7</sub>H<sub>8</sub> method. It was shown by gas-MS that strongly adsorbed toluene molecules were decomposed with CO<sub>2</sub> formation on the oxidative sites of Ag/CeO<sub>2</sub> catalysts. It was shown by the TPSR method that with an increase in the silver content in the catalysts, the amount of adsorbed toluene converted to CO<sub>2</sub> simultaneously increases. In the room-temperature reduction of 4-nitrophenol into 4-aminophenol, the pure CeO<sub>2</sub> was not active, however, with an increase in the silver content in the catalysts, an increase in the activity occurred and may be associated with an increase in the active surface of silver in catalysts.

Thus, it was shown in the work that the catalysts Ag-CeO<sub>2</sub> can have good reactivity both in the oxidation of toluene and in the reduction of 4-nitrophenol. The amount of silver in the catalyst affects the physical-chemical characteristics of the samples and the activity in the catalytic reactions.

*This work was supported by the Russian Science Foundation (Grant No.18-73-10109).*

### References

1. Bi, F.; Zhang, X.; Chen, J.; Yang, Y.; Wang, Y. *Appl. Catal. B: Environmental*. **2020**, 269, 118767.
2. Liao, G.; Gong, Y.; Zhong, L.; Fang, J.; Zhang, L.; Xu, Z.; Gao, H.; Fang, B. *Nano Res.* **2019**, 12, 2407.
3. Rao, R.; Shao, F.; Dong, X.; Dong, H.; Fang, S.; Sun, H.; Ling Q. *Appl. Surf. Sci.* **2020**, 513, 145771.

## Enhancing the photocatalytic activity of two-dimensional materials with plasmonic nanoparticles and laser processing

D. Cheshev<sup>1</sup>, R.D. Rodriguez<sup>1</sup>, A. Matkovic<sup>2</sup>, E. Sheremet<sup>1</sup>

<sup>1</sup>*Tomsk Polytechnic University, Tomsk, Russia*

<sup>2</sup>*Institute of Physics, Montanuniversität Leoben, Austria*

raul@tpu.ru

Nowadays, energy is a critical resource in many processes in modern life. Beyond generating energy by burning fossil fuels and coal, the easiest and most sustainable way is to fulfill our energy needs by harvesting sunlight. However, actual technologies do not allow us to use energy as properly as humanity would like (or need) to and to solve this problem, modern materials and new techniques are rapidly developing. In this context, we introduce a way of endowment two-dimensional graphene with photocatalytic properties and also enhancing native photocatalysts like GaSe. Our simple concept involves photoreduction and functionalization based on plasmonic Ag nanoparticles with laser processing [1]. High-powered laser patterning of GaSe induced a local reactivity increase without oxidation. We demonstrate that the resulting material has a much higher photocatalytic activity than the pristine GaSe for the reaction of 4-nitrobenzenethiol monolayers taken as a reference system. Our hybrid integration allows not only to study the interaction between atomic-layered materials and plasmonic nanoparticles but also opens the way to creating new functional and convenient methods for science and production technologies with ultrahigh spatial confinement.

*This work was funded by RFBR and FWF research project №19-52-14006. A.M. acknowledges the support by the Austrian Science Fund (FWF Der Wissenschaftsfonds) through project I4323-N36. This research is supported by the Tomsk Polytechnic University within the framework of the Tomsk Polytechnic University Competitiveness Enhancement Program, 5-100.*

### References

1. Cheshev, D.; Rodriguez, R.D.; Matković, A.; Ruban, A.; Chen, J.J.; Sheremet, E; *ACS Omega*, **2020** DOI: 10.1021/acsomega.0c0107



## Effect of pulsed laser irradiation on optical and photocatalytic properties of dark TiO<sub>2</sub>

Z.P. Fedorovich, E.D. Fakhrutdinova, V.A. Svetlichnyi

*Tomsk State University, Tomsk, Russia*

zhanna.fedorovich.99@gmail.com

The nanodispersed titanium dioxide is currently widely used in photovoltaic devices that find application in the green solar energy technologies, as well as in production of bactericidal materials and sunscreen creams [1, 2]. However, it is the heterogeneous photocatalysis that holds the most promise as a field of its application. Currently, new technologies are developed to obtain titania-based materials, which absorb light in the visible region and exhibit high photocatalytic activity. Earlier we obtained superfine dark blue titanium dioxide with intense absorption in the visible spectral range using pulsed laser ablation (PLA) method [3]. This work is devoted to the study of optical and photocatalytic properties after extra laser irradiation during the synthesis of titanium dioxide by PLA.

The synthesis of materials was carried out in two stages. At the first stage, a colloidal solution was obtained by using Nd:YAG laser (LOTIS TII, model LS2131M-20, wavelength of 1064 nm, frequency of 20 Hz, pulse duration of 7 ns). After an hour of ablation, the solution was divided into two parts, one of which was subjected to extra irradiation for an hour at the same laser radiation parameters. At the second stage, both colloidal solutions were dried at a temperature 60 °C until completely dry. After, the powders were annealed for further research. The following identifiers were assigned to the samples: TiO<sub>2</sub>\_ini for the sample without irradiation, and TiO<sub>2</sub>\_hv for the extra irradiated sample.

The powder has a dark blue color for TiO<sub>2</sub>\_ini and a gray for TiO<sub>2</sub>\_hv, which changes after heat treatment. Transmission electron microscopy (TEM) shows that the average particle size of non-irradiated material is 5-10 nm, with presents of large particles up to 80 nm in size. The specific surface area is 223 m<sup>2</sup>/g and after irradiation the specific area slightly increases to 253 m<sup>2</sup>/g, which may indicate that extra irradiation leads to a decrease in the size of large particles.

X-ray diffraction data shows that the samples have an amorphous structure, however, after heat treatment at 250 °C, the anatase crystalline phase begin to form in the structure of TiO<sub>2</sub>\_hv. After annealing at 400 °C all samples have anatase and rutile structures, however the amount of anatase is greater in TiO<sub>2</sub>\_hv.

The TiO<sub>2</sub>\_ini sample in the diffuse reflection spectra (DRS) showed intense absorption in the entire visible range, which can be attributed to the presence of different nature of defects in the structure [3]. The spectrum of the extra irradiated TiO<sub>2</sub>\_hv sample has less absorption in the long-wavelength region, but the absorption edge becomes more clear. It can be assumed that this is a consequence of the disappearance of some defects in the structure of the material. The photocatalytic activity of the samples was studied using the photodegradation of organic pollutants phenol and Rhodamine B under visible light irradiation. The results showed better efficiency for TiO<sub>2</sub>\_hv sample compared to non-irradiated sample. For phenol and Rhodamine, the percentage of decomposition increased by 2 times. Thus, extra irradiation during the synthesis of TiO<sub>2</sub> by the PLA method leads to changes in the structure and, as a result, the optical properties of materials, which also favorably affects the photocatalytic behavior of the material.

### References

1. Noman, M.; Ashraf, M.; Ali, A. *Environ. Sci. Pollut. Res.* **2019**, *26*, 3262–3291.
2. Haider, A.; Jameel, Z.; Al-Hussaini, I. *Energy Procedia.* **2019**, *157*, 17–29.
3. Fakhrutdinova, E.D.; Shabalina, A.V.; Gerasimova, M.A.; Nemoykina, A.L.; Vodyankina, O.V.; Svetlichnyi, V.A. *Materials* **2020**, *13*, 2054 (17).

## Effect of mechanical activation on the integrated extraction-catalytic processing of pine bark

V.A. Ionin<sup>1</sup>, M.Yu. Belash<sup>1</sup>, A.M. Skripnikov<sup>1</sup>, V.V. Sychev<sup>1</sup>, A.S. Kazachenko<sup>1</sup>, O.P. Taran<sup>1, 2</sup>

<sup>1</sup>*Institute of Chemistry and Chemical Technology SB RAS, Krasnoyarsk, Russia*

<sup>2</sup>*Siberian Federal University, Krasnoyarsk, Russia*

ionin.va@icct.krasn.ru

Bark wood wastes are a major problem of wood processing enterprises, where they are accumulated on large scale. A number of studies were conducted aiming to develop methods of valorization products from the bark [1, 2]. The aim of this research was to study new integrated extraction-catalytic processing of pine bark and effect of mechanical activation allowing to intensify extraction of products which have found their application as main components of drugs [3, 4].

Several samples of pine bark and wood wastes were obtained using various activating methods (activation in ball and planetary mills, “steam explosion”). Each sample was extracted using the well-known principle [5, 6] of sequential extraction with solvents with increasing polarity.

Samples of the bark were extracted with hexane in a Soxhlet apparatus with following saponifying using an alcoholic solution of sodium hydroxide while heated and extraction with diethyl ether in a separatory funnel. The analysis of obtained fractions was performed by GC/MS.

After resinous substances removal with hexane, tannins were extracted from the bark residue using ethanol, followed by sample flushing with a water module of 20 and constant stirring. Under the conditions used, tannins extraction from pine bark treated with mechanical activation resulted in higher yields of required composition of tannins confirmed by HPLC methods.

The samples residues were treated with a 1% acid solution, followed by filtration and precipitation with isopropyl alcohol. The viscosity of obtained pectins was determined using an Ostwald viscometer, the IR spectrum was recorded in the matrix KBr to determine the uronide component. Elemental composition was analyzed.

After the extraction, samples were further subjected to reduction-catalytic fractionation with presence 3% Ru/C catalyst based on oxidized at 450 °C graphite-like carbon Sibunit in ethanol/water mixture. Lignin mono- and oligomers and hemicelluloses monosaccharides and cellulose were produced in liquid phase, which was analyzed by GC/MS. The composition of the gaseous products was analyzed by GC. Content of hemicelluloses, cellulose, and lignin in initial pine bark and in the solid was determined by chemical analysis. Molecular weight distribution of obtained liquid products, weight average molecular weight (Mw), weight average molecular weight (Mn) and polydispersity of the samples were determined using gel permeation chromatography.

The obtained data allowed to carry out the experimental and mathematical optimization of the integrated processing of pine bark.

The work carried out showed the mechanical activation methods promotion of extraction-catalytic wood waste pine bark processing aimed on valorization of most valuable organic substances plant biomass-derived using «green» methods.

*This work was supported by RFBR Grant 19-43-240011.*

### References

1. Krasutsky, P., *Birch Bark Research and Development*. Natural product reports, 2007. **23**: p. 919-42.
2. Li, B., et al., *Preparation and Characterization of Bark-derived Phenol Formaldehyde Foams*. RSC Adv., 2016. **6**.
3. Tai, K., et al., *Effect of  $\beta$ -sitosterol on the curcumin-loaded liposomes: Vesicle characteristics, physicochemical stability, in vitro release and bioavailability*. Food Chemistry, 2019. **293**: p. 92-102.
4. Wusigale, L. Liang, and Y. Luo, *Casein and pectin: Structures, interactions, and applications*. Trends in Food Science & Technology, 2020.
5. Дейнеко И.П., Д.И.В., Белов Л.П., *Исследование химического состава коры сосны* Химия растительного сырья, 2007. **1**: p. 19-24.

## Enhancement of visible light activity of N-doped TiO<sub>2</sub> photocatalyst under polychromatic radiation due to a tandem effect

N.S. Kovalevskiy<sup>1,2</sup>, D.A. Svintsitskiy<sup>1,2</sup>, S.A. Selishcheva<sup>1,2</sup>, D.V. Kozlov<sup>1,2</sup>, D.S. Selishchev<sup>1,2</sup>

<sup>1</sup>*Boriskov Institute of Catalysis, Novosibirsk, Russia*

<sup>2</sup>*Novosibirsk State University, Novosibirsk, Russia*

nikita@catalysis.ru

The development of effective photocatalysts for the degradation of harmful pollutants under solar or room light is one of the main objectives of photocatalytic technologies nowadays. TiO<sub>2</sub> doped with nitrogen is a good candidate for this role because it can absorb radiation with a wavelength up to 500–550 nm and can provide the oxidative degradation of chemical and biological contaminants at a high rate. Highly active N-doped TiO<sub>2</sub> photocatalysts can be synthesized using inexpensive precursors, titanium oxysulfate and ammonium solution, via a simple precipitation method.

In addition to the features mentioned above, we have recently found a synergistic effect of polychromatic radiation on visible light activity of N-doped TiO<sub>2</sub> photocatalyst [1]. This effect consists in the fact that according to the action spectrum N-doped TiO<sub>2</sub> has no activity under radiation with wavelength higher than 600 nm but a combination of blue light (450 nm) with a low-energy radiation (e.g., red light, 630 nm) resulted in a substantial increase in the photocatalytic activity of N-doped TiO<sub>2</sub> in a wide range of radiation powers. The synergistic effect is due to the electronic structure of doped system because TiO<sub>2</sub> doping with nitrogen results in partially unoccupied impurity levels in the band gap of TiO<sub>2</sub>. As a result, an additional radiation with a low energy, which is not high enough to excite electrons to the conduction band of TiO<sub>2</sub>, can increase the rate of the photocatalytic process due to a tandem effect, when low-energy photons excite electrons from the valence band of TiO<sub>2</sub> onto the impurity levels and high-energy photons mainly excite electrons from the impurity levels into the conduction band of TiO<sub>2</sub>. Enhancement of visible light activity under polychromatic radiation was confirmed for a number of N-doped TiO<sub>2</sub> photocatalysts prepared under different conditions.

*The reported study was funded by RFBR and Novosibirsk region according to the research project 19-43-543038*

*The reported study was funded by RFBR according to the research project 18-29-17055*

### References

1. Kovalevskiy, N.; Selishchev, D.; Svintsitskiy, D.; Selishcheva, S.; Berezin, A.; Kozlov, D. *Cat. Comm.* **2020**, *134*, 105841.

## Catalytic oxidation of CO over Fe-, Sn-, and Ce-modified MnO<sub>2</sub> catalysts

E.V. Kulchakovskaya<sup>1\*</sup>, T.S. Kharlamova<sup>1</sup>, V. V. Verkhov<sup>1</sup>, V.O. Trufanov<sup>1</sup>,  
F.J. Cadete Santos Aires<sup>1,2</sup>, V.I. Sobolev<sup>1,3</sup>, O. V. Vodyankina<sup>1</sup>

<sup>1</sup>Laboratory of Catalytic Research, National Research Tomsk State University, Tomsk, Russia

<sup>2</sup>Univ. Lyon, Université Claude Bernard Lyon 1, CNRS, IRCELYON, Villeurbanne, France

<sup>3</sup>Laboratory of selective oxidation, Institute of Catalysis SB RAS, Novosibirsk, Russia

ekaterina.krv@gmail.com

Manganese oxides are promising candidates to create new catalysts possessing activity in a relatively low-temperature oxidation of formaldehyde and CO. Such materials are widely used in oxidative processes due to high oxygen mobility associated with the presence of redox pair of Mn(IV)/Mn(III), existing as oxygen vacancies  $[-\text{Mn}^{3+}-\square-\text{Mn}^{3+}-]$ . A prospective way to further improve the catalyst performances is manganese oxide modification with transition metal cations or variable valence cations [1, 2]. The CO oxidation reaction is widely used as a test process for solving fundamental problems in the field of heterogeneous catalysis [3–4], being an effective tool for studying the dependence of catalytic activity on structural features of material, e.g. the size, morphology, states of modifying cations/clusters/nanoparticles [5–6].

The aim of this work is to study the synergetic effect between transition metal modifier ( $\text{Fe}^{3+}$ ,  $\text{Sn}^{4+}$ ,  $\text{Ce}^{4+}$ ) in CO oxidation process. All catalysts were characterized by BET, TEM (HRTEM), XRD, Raman and long-tested in CO oxidation process for 100 h to obtain TOS curves. Catalyst samples were prepared using a redox reaction between required amount of  $\text{Mn}(\text{NO}_3)_2$  and  $\text{KMnO}_4$  according to procedure reported in [2].

According to XRD data,  $\alpha$ - $\text{MnO}_2$  crystalline phases were primarily formed for unmodified sample, Fe- and Sn-modified samples. For Ce-modified catalyst  $\beta$ - $\text{MnO}_2$  crystalline phases were prevailed. No reflexes of iron and cerium oxides were observed in the diffractograms of the Fe- and Ce-modified samples suggesting high dispersion of such phases. In Sn- $\text{MnO}_2$  sample a dispersed  $\text{SnO}_2$  phase was identified. The lattice-resolved HRTEM showed the regular lattice arrangement of  $\alpha$ - $\text{MnO}_2$  and  $\beta$ - $\text{MnO}_2$  for nanorod particles of unmodified sample. TEM images indicate nanorod, spindle-shaped and shapeless particles for Fe- $\text{MnO}_2$ , the nanorod particles and 3–7 nm nanoparticles agglomerated or located on the nanorod particles for Sn- $\text{MnO}_2$  and nanorod particles and agglomerates of shapeless particles for Ce- $\text{MnO}_2$ . The TEM data indicates the incorporation of Ce in the manganese oxides rather the formation of  $\text{CeO}_2$  phase for Ce-modified sample, which comes in agreement with XRD data.

Catalytic testing in CO oxidation process was carried out in quartz reactor according to procedure described in [7]. Catalysts were tested for 100 h. The temperature increased from 50 to 125 °C for Ce- $\text{MnO}_2$  and to 145 °C for other catalysts. The molar ratio of  $\text{O}_2/\text{CO}$  was 8, GHSV = 36000 h<sup>-1</sup>. It was shown that the introduction of the transition metal into the composition of  $\text{MnO}_2$  with the OMS-2 structure allowed increasing the activity of catalysts:  $\text{MnO}_2 < \text{Sn-MnO}_2 \leq \text{Fe-MnO}_2 < \text{Ce-MnO}_2$ . All catalysts were stable in CO oxidation process during 100 h. Therefore, catalysts based on manganese oxides modified with Fe, Sn or Ce possess good catalytic properties in CO oxidation and are promising candidates to create effective oxide catalysts. Further research will focus on investigation of Fe- and Ce-containing OMS-2 catalysts modified by bimetallic (Ag-Pd) nanoparticles.

*This research project is supported by Russian Science Foundation (project 19-73-30026).*

### References

1. Sultana, S.; Ye, Z. et al. *Catal. Today* **2018**, 307, 20.
2. Dotsenko, S.S.; Verkhov, V.A. et al. *Catal.Today* **2019**, in press.
3. Kropp, T.; Mavrikakis, M.; *J. Catal.* **2019**, 377, 577.
4. Royer, S.; Duprez, D. *Chem.Cat.Chem.* **2011**, 3, 24.
5. Nikolaev, S.A.; Golubina, E. et al.; *Kinet. Catal.* **2014**, 55, 311.
6. Gordon, E. B.; Karabulin, A. V. *High Energy Chem.* **2016**, 50, 305.
7. Grabchenko, M. V.; Mamontov, G. V. et al. *Appl. Catal. B: Environmental* **2020**, 260, 118148.

## Optical and photocatalytic properties of bismuth nanoparticles synthesized by pulsed laser ablation in water and air media

T.S. Nazarova, E.D. Fakhrutdinova, V.A. Svetlichnyi

*Tomsk State University, Tomsk, Russia*

tanita-naz@yandex.ru

Bismuth compounds are biocompatible and have low toxicity and also possess band gap energy in the visible region can oxidize water and produce highly reactive species for initiating oxidation reaction for degradation of dyes, gases and drugs chemistry [1]. Therefore, these materials are widely studied today. Bismuth oxide compounds have a wide polymorphic range. However, the controlled synthesis of the selected compound or modification phase is still a problem. Therefore, in this work, the synthesis of bismuth compounds from a metal during pulsed laser ablation (PLA) in water and air is proposed. One of the features of this method is the ability to obtain materials in the absence of additional precursors that could affect the phase composition and structure of the final material.

Powder materials of bismuth compounds were obtained by pulsed laser ablation in distilled water (Bi\_ini sample) and in air (Bi\_air sample) using a Q-switch Nd: YAG laser with the following parameters: wavelength 1064 nm, pulse duration 7 ns, frequency 20 Hz, and a pulse energy of 160 mJ. Metallic Bi (99.9% purity) was used as a target.

Bi\_ini material has low specific surface area – 1.3 m<sup>2</sup>/g and consist of is a large faceted lamellar particles with an average size of about 500 nm. Particles obtained by ablation in air have a predominantly spherical shape with predominance of particles with a size of 10-18 nm and the presence of large particles up to 200 nm. Specific surface area for Bi\_air is 16.4 m<sup>2</sup>/g.

According to X-ray diffraction data, Bi\_ini is a mixture of three phases of bismuth oxide  $\alpha$ -Bi<sub>2</sub>O<sub>3</sub>, bismuth oxycarbonate Bi(CO<sub>3</sub>)O<sub>2</sub> and bismuth hydroxycarbonate (BiO)<sub>4</sub>CO<sub>3</sub>(OH)<sub>2</sub>. After annealing at 200 °C, phase transitions are not observed; the sample retains its structure. However, during annealing at 400 °C, bismuth hydroxycarbonate and carbonate decompose and  $\alpha$ -Bi<sub>2</sub>O<sub>3</sub> forms as the main phase.

The Bi\_air sample is a mixture of metallic bismuth and bismuth oxide  $\beta$ -Bi<sub>2</sub>O<sub>3</sub>. After annealing at 200 °C, the amount of the metal phase reduce and no more changes in the structure are observed. However, after heat treatment at 400 °C, a phase transition occurs with the formation of the  $\alpha$ -Bi<sub>2</sub>O<sub>3</sub> structure. A study of diffuse reflection spectroscopy showed that both materials have a wide absorption spectrum in the visible region, which consists of absorption bands of the Bi(CO<sub>3</sub>)O<sub>2</sub>, (BiO)<sub>4</sub>CO<sub>3</sub>(OH)<sub>2</sub> and  $\alpha$ -Bi<sub>2</sub>O<sub>3</sub> phases for Bi\_ini and  $\beta$ -Bi<sub>2</sub>O<sub>3</sub> and Bi (metal) for Bi\_air, respectively.

All materials were tested during the photocatalytic decomposition of the Rhodamine B dye under the LED source irradiation with a wavelength of 378 nm. The highest activity was shown by materials containing Bi(CO<sub>3</sub>)O<sub>2</sub>, (BiO)<sub>4</sub>CO<sub>3</sub>(OH)<sub>2</sub> and  $\beta$ -Bi<sub>2</sub>O<sub>3</sub> phases in the structure, which is in good agreement with literature data [2, 3].

*This work was supported by the Russian Science Foundation, project No. 19-73-30026.*

### References

1. Raza, W.; Haque, M.M.; Muneer M. *J Alloy Compd.* **2015**, 648, 641–650.
2. Valencia, K.; Alejandro López, G.; Hernández-Gordillo A. *Ceram. Int.* **2018**, 44, 22329–22338.
3. Cen, W.; Xiong, T.; Tang, C. *Ind Eng Chem Res.* **2014**, 53, 15002–15011.

## Catalytic properties of nickel-aluminium-titanium NASICON-type phosphates in ethanol conversion

D.A. Osaulenko<sup>1</sup>, A.I. Pylinina<sup>1</sup>, E.A. Asabina<sup>2</sup>, I.O. Glukhova<sup>2</sup>

<sup>1</sup>*RUDN University, Moscow, Russia*

<sup>2</sup>*Lobachevsky State University of Nizhni Novgorod (UNN), Nizhni Novgorod, Russia*

dinaosa@yandex.ru

The last years new catalysts family was developed on the base of complex phosphates of NASICON type. These phosphates belong to framework materials and have general formula  $A_xB_2(ZO_4)_3$ , where A - is alkali or alkaline earth element, B - polyvalent element (Zr, Ti, Sc etc.), Z - phosphorus or silicon. Their structure is presented by edge-linked  $BO_6$  octahedra and  $ZO_4$  tetrahedra.<sup>1-3</sup>

Complex phosphates with the NASICON structure have attracted the attention of researchers due to their unique set of properties determined by their structure and composition. These properties include high ionic conductivity, low thermal expansion coefficient, high chemical, radiation, and thermal stability.

Wide variety of isomorphic ion substitutions at all crystallographic positions of NASICON structure causes the multiplicity of local characteristics (polarity, Lewis acidity etc.) of framework sites and cavities. As result, the framework phosphates may show the basic, acidic and redox properties and are applicable as the catalysts of different organic reactions. NASICONs's were drawn attention as active and stable catalysts of alcohol's dehydration, dehydrogenation, paraffin isomerization and oxidation.<sup>1-3</sup>

In this study, we have researched the catalytic activity of  $Ni_{0,5(1+x)}Al_xTi_{(2-x)}(PO_4)_3$  ( $x=0; 0,2$ ) in the model ethanol conversion reaction in flowing unit in the 260-420°C temperature range with gas chromatographic analysis of products.

The result showed that the main products on both samples were acetaldehyde, diethyl ether and ethylene. The maximum conversion of alcohol on a sample with  $x=0$  was 73% at  $T=420^\circ C$ . For a sample with  $x=0,2$ , the maximum conversion was 70% at  $T=420^\circ C$ . These phosphates are characterized by high stability, which was tested in the cooling mode and in repeated experiment. Introduction of aluminum phosphate into the structure does not lead to an increase in the total conversion of alcohol, but changes the ratio of dehydration products (ethylene and diethyl ether) starting from  $T=380^\circ C$ . The difference in the catalytic activity of the samples is due to the change of the active site caused by the addition of aluminum ions.

*The publication was prepared with support of RUDN University Program 5-100.*

### References

1. Ermilova, M.M. et al. *Catal. Today* **2012**, 193 (1), 37–41.
2. Ilin, A.B. *Catal. Today* **2016**, 268, 29–36.
3. Yaroslavtsev, A. B.; Stenina, I. A. *Russ. J. Inorg. Chem.* **2006**, 51, S97–S116.

## Decomposition of methane to hydrogen on a fiberglass catalyst

M.V. Popov<sup>1,2,3</sup>, A.G. Bannov<sup>2</sup>, A.N. Zagoruiko<sup>4</sup>

<sup>1</sup>*N.D. Zelinsky Institute of Organic Chemistry Russian Academy of Sciences, Moscow, Russia*

<sup>2</sup>*Novosibirsk State Technical University, Novosibirsk, Russia*

<sup>3</sup>*Dmitry Mendeleev University of Chemical Technology of Russia, Moscow, Russia*

<sup>4</sup>*Boriskov Institute of Catalysis, Novosibirsk, Russia*

popovmaxvik@gmail.com

One of the promising methods for processing natural gas is the catalytic decomposition process. As a result of the catalytic decomposition of the initial hydrocarbon, hydrogen and carbon nanofibers are formed.

This method is an environmentally friendly and less energy-intensive way to produce hydrogen and carbon nanofibers. The catalytic decomposition of natural gas proceeds in one stage; does not contain impurities CO and CO<sub>2</sub>; therefore, it does not require additional purification steps.

The use of catalysts allows to reduce the process temperature to 973 K [1]. In this work, we used a glass-fiber catalyst on which nickel oxide was deposited as an active component [2]. Glass-fiber was chosen as a carrier, which has an original geometric structure, high mechanical strength, and flexibility, which allows creating various forms of the catalyst with improved heat and mass transfer [3]. The high-silica glass-fiber fabric (produced by Russia), containing ~ 95 % SiO<sub>2</sub> and 4 % Al<sub>2</sub>O<sub>3</sub>, was used as the primary glass-fiber support. The glass-fiber was impregnated by the water solution of silica sol and nickel acetate. After impregnation and drying, the glass-fiber was thermally treated by heating from ambient temperature up to 773 K. Silica addition was needed to create the intermediate layer of secondary porous support in order to improve the strength of bonding between NiO and glass-fiber surface and to develop the specific surface area for better accessibility of the supported NiO by gaseous reactants

Pure methane (99.999%) was used as the starting hydrocarbon. Catalytic decomposition of methane was carried out on an Autoclave Engineers BTRS Jn unit. The composition of the gaseous reaction products was measured using a gas chromatograph. The temperature in the reactor was 823–873 K, and the pressure was 1–2 bar.

It was found that with increasing temperature of the catalytic decomposition of methane on a fiberglass catalyst, the specific rate of hydrogen formation increases. At the same time, with an increase in temperature, the service life of the catalyst decreases. With an increase in pressure from 1 to 2 bar, a significant increase in catalyst lifetime occurs. It was found that during the catalytic decomposition of methane, the rate of hydrogen production decreases. It was found that with the catalytic decomposition of methane, the specific rate of hydrogen formation increases by 25% with increasing temperature from 823 K to 873 K. With an increase in pressure up to 2 bar, the specific rate of hydrogen production practically does not change, however, the catalyst lifetime significantly increases, and accordingly, the hydrogen yield increases.

Thus, the use of a glass-fiber catalyst with a low nickel content may be promising for the catalytic decomposition of natural gas to produce hydrogen without emission of carbon oxides into the atmosphere. The accompanying carbon nanofibers that are formed as a result of the process can be used as a sorbent, a catalyst for the selective oxidation of hydrogen sulfide into sulfur, as electrode material in supercapacitors and gas sensors.

*This work was supported by the state assignment FSUN-2020-0008.*

### References

1. Popov, M.V.; Shinkarev, V.V.; Brezgin, P.I.; Solov'ev, E.A.; Kuvshinov, G.G. *Kinet. Catal.* **2013**, *54*, 481–486
2. Popov, M.V.; Zazhigalov, S.V.; Larina, T.V.; Cherepanova, S.V.; Bannov, A.G.; Lopatin, S.A.; Zagoruiko, A.N. *Catal. Sustain. Energy* **2017**, *4*, 1–6.
3. Zagoruiko, A.N.; Lopatin, S.A. *Structured Glass-Fiber Catalysts*. CRC Press, 2019, 142 p.

## Alumina-supported CuO-MoO<sub>3</sub> as catalysts for soot oxidation

E.V. Romanova, A.V. Nam, T.S. Kharlamova

*Tomsk State University, Tomsk, Russia*

evgenia.soltys@mail.ru

Soot particulate matter is the main harmful component of diesel emissions that is cleaned by the diesel particulate filter coated with catalysts. The systems based on precious metals (Pt, Pd, Rh) are used as catalysts to reduce the soot combustion temperature. The development of available and efficient catalysts is currently a topical challenge. The oxide-like catalysts such as PdO, Co<sub>3</sub>O<sub>4</sub>, Fe<sub>2</sub>O<sub>3</sub>, CuO that are reactive towards carbon as well as bulk molybdates of bismuth, chromium and copper are known [1–3]. However, supported catalysts on the basis thereof remain poorly studied despite greatest practical interest. This work is devoted to the preparation of alumina-supported copper molybdates and study of their catalytic performance in soot oxidation.

The supported copper molybdates with the different Cu:Mo molar ratios (1:1 and 3:2) were synthesized by the consecutive impregnation of the Al<sub>2</sub>O<sub>3</sub> support with (NH<sub>4</sub>)<sub>6</sub>Mo<sub>7</sub>O<sub>24</sub> and Cu(NO<sub>3</sub>)<sub>2</sub> water solutions. The order of introduction of active components was varied. The obtained samples were dried at 150°C for 12 h and then calcined at 700 °C for 4 h. The samples were investigated by a complex of methods such as XRD, H<sub>2</sub>-TPR, and UV-vis DR spectroscopy. The catalytic soot oxidation was studied using synchronous thermal analysis (STA).

According to the XRD, H<sub>2</sub>-TPR and UV-vis spectroscopy data, copper molybdate Cu<sub>3</sub>Mo<sub>2</sub>O<sub>9</sub> is formed in CuO-MoO<sub>3</sub>/Al<sub>2</sub>O<sub>3</sub> and MoO<sub>3</sub>-CuO/Al<sub>2</sub>O<sub>3</sub> samples regardless of the molar ratio and the order of introduction of active components. However, when Mo is introduced at the first stage, the interaction with the support occurs. In this case, an inactive phase of aluminum molybdate is formed and prevents the formation of the active surface of the supported catalysts. The Cu introduction at the first stage allows obtaining a predominant amount of copper molybdate. The STA data shows that all supported samples reduce the soot combustion temperature. However, their catalytic activities are significantly influenced by the order of introduction of the applied components. The catalysts prepared with the order of introduction of copper oxide and then molybdenum oxide are more active.

To study the effect of the amount of the supported active phase, a series of CuO-MoO<sub>3</sub>/Al<sub>2</sub>O<sub>3</sub> samples were additionally prepared by introduction of CuO firstly followed by the MoO<sub>3</sub> introduction. The Cu:Mo molar ratio was 3:2 for all samples, while the molybdenum content was varied (3, 6, and 10 wt%). According to the XRD, UV-vis DR spectra and TPR data, with an increase in the mass content of the supported components, the amount of copper molybdate Cu<sub>3</sub>Mo<sub>2</sub>O<sub>9</sub> increases. No other Cu and/or Mo phases are observed. The STA data show that the catalytic activity of the samples passes through a maximum with the increase of the Cu<sub>3</sub>Mo<sub>2</sub>O<sub>9</sub> amount in the samples. The most optimal is the introduction of 6 wt.% of active component calculated per MoO<sub>3</sub>.

*This work was supported by the Tomsk State University Academic D.I. Mendeleev Fund Program (Grant 8.2.03.2018).*

### References

1. Setten, B. A.; Makkee, M.; Moulijn, J. A. *Cat. Rev.* **2001**, 43(4), 489–564.
2. Deonikar, V. G.; Rathod, P. V.; Pornea, A. M.; Puguan, J. M. C.; Park, K.; Kim, H. *J. Ind. Eng. Chem.* **2020**, 86, 167–177.
3. Soltys, E. V.; Urazov, K. K.; Kharlamova, T. S.; Vodyankina, O. V. *Kinet. Catal.* **2018**, 59, 58–69.



## Stability performance of Ni/CeO<sub>2</sub> catalysts in the steam/CO<sub>2</sub> reforming of methane

A.S. Shlyakhtina<sup>1</sup>, E.V. Matus<sup>2</sup>, O.B. Sukhova<sup>2</sup>, I.Z. Ismagilov<sup>2</sup>, M.A. Kerzhentsev<sup>2</sup>, Z.R. Ismagilov<sup>2,3</sup>

<sup>1</sup>*Novosibirsk State Technical University, Novosibirsk, Russia*

<sup>2</sup>*Boriskov Institute of Catalysis, Novosibirsk, Russia*

<sup>3</sup>*Institute of Coal Chemistry and Material Science, Kemerovo, Russia*

alexandra\_issakova@mail.ru

Ni/CeO<sub>2</sub> is an effective catalytic system for fuel reforming reactions [1-3]. The high performance of this catalyst is provided by Ni metal ability to activate hydrocarbon molecules, strong metal-support interaction as well as redox chemistry of ceria support. However, the weak point of nickel catalysts remains their low resistance to carbonization. To solve this problem, the exsolution approach is used for catalyst design [3]. Here we employ the Ce<sub>1-x</sub>Ni<sub>x</sub>O<sub>y</sub> oxide as a catalyst precursor to enable the exsolution of Ni<sup>0</sup> nanoparticles under reducing atmosphere and obtain the Ni/CeO<sub>2</sub> catalyst. In this work, the effect of Ni content (2-15 wt. %) on the performance of Ni/CeO<sub>2</sub> catalysts and their stability to the deactivation in steam/CO<sub>2</sub> reforming of methane was studied. The functional properties of the catalysts are compared with their physicochemical characteristics of samples before the reaction, after activation, and the following catalytic reaction.

The Ce<sub>1-x</sub>Ni<sub>x</sub>O<sub>y</sub> catalyst precursor (x = 0.1-0.4) was prepared by the polymerizable complex method [3]. To obtain the Ni/CeO<sub>2</sub>, the Ce<sub>1-x</sub>Ni<sub>x</sub>O<sub>y</sub> oxides before the catalytic reaction were *in situ* activated by the reduction in 30% H<sub>2</sub>/Ar at 800°C for 1 hour. The Ni/CeO<sub>2</sub> catalysts were tested in 24-hour reaction of steam/CO<sub>2</sub> reforming of methane at atmospheric pressure, temperature 800°C, a flow rate of 200 mL/min and the molar ratio between reagents CH<sub>4</sub>: CO<sub>2</sub>: H<sub>2</sub>O: He = 1: 0.81: 0.38: 2.8. The samples were characterized by a group of methods (TG-DTA, BET, XRD, HRTEM-EDX, and H<sub>2</sub>-TPR).

It was found that with an increase in the nickel content from 2 to 10 wt. % conversion of reactants (X) and yield of products (Y) increase: X<sub>CH<sub>4</sub></sub> = 30 → 80%, X<sub>CO<sub>2</sub></sub> = 40 → 75%, Y<sub>H<sub>2</sub></sub> = 40 → 85%, X<sub>CO<sub>2</sub></sub> = 35 → 80%. A further increase in the nickel content to 15 wt. % does not improve reaction parameters. The catalyst performance decreases with time of stream. This effect is shown to weaken with increasing nickel content. In particular, for 2Ni/CeO<sub>2</sub> and 10Ni/CeO<sub>2</sub> samples after 24 hours of reaction, the parameters are reduced on average by 15 and 30%, respectively. The H<sub>2</sub>/CO ratio is equal to ~1.4 and weakly depends on the catalyst composition or the duration of the reaction.

It was shown that in the catalyst precursors nickel cations incorporated into the crystal lattice of cerium dioxide and the formation of the mesoporous solid solution Ce<sub>1-x</sub>Ni<sub>x</sub>O<sub>y</sub> occurred [3]. The samples have high specific surface area S<sub>BET</sub> ~ 100 m<sup>2</sup>/g and polydisperse pore system. Upon activation of the Ce<sub>1-x</sub>Ni<sub>x</sub>O<sub>y</sub> samples, nickel particles Ni<sup>0</sup> with the size of 4 ≤ (for 2Ni/CeO<sub>2</sub>) to 15 nm (for 15Ni/CeO<sub>2</sub>) are formed. The average size of CeO<sub>2</sub> crystallites increases greatly – from 6 to 25 nm, while the S<sub>BET</sub> becomes equal to 20–30 m<sup>2</sup>/g. The prolonged stay of samples under reaction medium leads to the formation of a coarsely dispersed system CeO<sub>2</sub> + Ni<sup>0</sup>, the size of coherent scattering region of which is 50 nm, regardless of the nickel content. The texture and morphology of catalysts are also changed as the result of the 24-hour reaction. The catalyst characteristics were correlated with a stability performance test and coke content, and ways to further optimize the Ni/CeO<sub>2</sub> system for the steam/CO<sub>2</sub> reforming of methane are proposed.

*The reported study was funded by RFBR and NSFC according to the research project №20-53-53018.*

### References

1. Ismagilov, Z. R.; Matus, E. V.; Ismagilov, I. Z.; Sukhova, O. B.; Yashnik, S. A.; Ushakov, V. A.; Kerzhentsev, M. A. *Catal. Today* **2019**, 323, 166–182.
2. Seo, H. O. *Catalysts*. **2018**, 8, 16–22.
3. Matus, E. V.; Shlyakhtina, A. S.; Sukhova, O. B.; Ismagilov, I. Z.; Ushakov, V. A.; Yashnik, S. A.; Nikitin, A. P.; Bharali, P.; Kerzhentsev, M. A.; Ismagilov, Z. R. *Kinet. Catal.* **2019**, 60, 221–230.

## Catalytic oxidation of formaldehyde over modified MnO<sub>2</sub> catalysts with OMS-2 structure

V.V. Verkhov<sup>1</sup>, F.J. Cadete Santos Aires<sup>1,2</sup>, V.I. Sobolev<sup>1,3</sup>, O.V. Vodyankina<sup>1,3</sup>

<sup>1</sup>Laboratory of Catalytic Research, National Research Tomsk State University, Tomsk, Russia

<sup>2</sup>Univ. Lyon, Université Claude Bernard Lyon 1, CNRS, IRCELYON, Villeurbanne, France

<sup>3</sup>Laboratory of selective oxidation, Institute of Catalysis SB RAS, Novosibirsk, Russia

valeriy\_verkhov@mail.ru

Octahedral molecular sieves (OMS-2) based on MnO<sub>2</sub> with (2x2) channels formed by octahedral units of MnO<sub>6</sub> with cryptomelane structure are promising candidates to create new catalysts possessing activity in a relatively low-temperature oxidation of formaldehyde and CO. Such materials are widely used in oxidative processes due to high oxygen mobility associated with the presence of redox pair of Mn(IV)/Mn(III), existing as oxygen vacancies  $[-\text{Mn}^{3+} - \square - \text{Mn}^{3+} -]$  [1,2].

The main idea of the present work is to study the synergetic effect between transition metal modifier (Fe<sup>3+</sup>, Sn<sup>4+</sup>, Ce<sup>4+</sup>) introduced at the stage of catalyst preparation, and MnO<sub>2</sub> with the OMS-2 structure in oxidation of CO and formaldehyde. The presence of a synergistic effect will be analyzed on the basis of the studies of state and composition of surface, phase composition, structure features, localization and states of modifying cations/clusters/nanoparticles of transition metal oxides, reaction ability in TPx modes and catalytic activity in low-temperature CO oxidation and formaldehyde abatement from the gas flow.

The elemental composition of Fe- and Sn-containing samples with different Mn/M ratio (20/1 and 10/1) corresponded theoretical composition, while for Ce-containing samples potassium and cerium amounts were lower in comparison with theoretical ones. These results were consistent well with the XRD data. According to the XRD and Raman spectroscopy data, cryptomelane phase was formed with incorporation of Sn<sup>4+</sup> and Fe<sup>3+</sup> cations inside the channel structure (mainly for Sn) with the substitution of K<sup>+</sup> and in the base crystalline structure (Fe<sup>3+</sup>). More complicated picture was observed for Ce-containing catalysts. Application of low ratio (Mn(VII)/Mn(II) = 0.72) at the stage of precipitation in the presence of Ce-containing modifier did not produce the samples with the cryptomelane structures. An increase of Mn(VII)/Mn(II) ratio to up to 2.85 allowed forming the OMS-2 phase in the composition of the samples along with the pirolusite phase. The study of internal structure of the catalysts with and without modifier allowed concluding about the formation of a well-crystalline OMS-2 phase. Additionally, the formation of small particles on the surface of anisotropic cryptomelane particles in modified samples was observed. Interestingly, these particles comprised well-crystalline structures. For Ce-containing catalysts, a number of morphologically different phases was observed. It was proposed that Ce cations restrained transformation of birnessite layers into cryptomelane at the stage of hydrothermal treatment.

The catalytic properties of the prepared materials in formaldehyde oxidation along with the possible mechanism of synergetic effect between the transition metal modifier and hosting MnO<sub>2</sub> with the cryptomelane structure will be discussed in a conference contribution.

*This work was supported by RFBR Grant project 19-73-30026*

### References

1. Hou, J.; Li, Y.; Mao, M.; Zhao, X.; Yue Y. *Royal Soc. Chem.* **2014**, 6, 15048–15058.
2. Dotsenko, S.S.; Verkhov V.A. at al. *Catal.Today* **2019**. DOI: 10.1016/j.cattod.2019.07.020.

## **Combined synthesis and hydroprocessing of hydrocarbons via Co-SiO<sub>2</sub>/Ni-ZSM-5/Al<sub>2</sub>O<sub>3</sub> catalyst**

R.E. Yakovenko, I.N. Zubkov, V.N. Soromotin, G.B. Narochniy, A.P. Savost'yanov

*M.I. Platov South-Russian State Polytechnic University (NPI), Novocherkassk, Russia*

*jakovenko39@gmail.com*

At present days, the search for alternative methods for producing motor fuels from non-oil raw materials is becoming increasingly relevant. One of such methods is GTL technology - processing of natural or associated petroleum gas into synthetic liquid fuels (SLF). One of the most important stages in the GTL technology is synthesis of hydrocarbons via Fischer-Tropsch (FT) method. The FT synthesis is complicated catalytic process which allows obtaining wide range of hydrocarbons: gaseous alkanes (C<sub>1</sub>-C<sub>4</sub>), gasoline (C<sub>5</sub>-C<sub>10</sub>) and diesel (C<sub>11</sub>-C<sub>18</sub>) fractions, paraffin's (C<sub>19</sub>-C<sub>34</sub>) and ceresin (C<sub>35</sub>+). The FT synthesis uses transition metals of VIII group (cobalt, iron, nickel and ruthenium) like catalysts. There are many different parallel and consequent reactions in the FT synthesis. It was developed the multifunctional catalyst of one-pot synthesis of fuel hydrocarbons from CO and H<sub>2</sub>. This catalyst prepared from powders of cobalt silica promoted by alumina (FT catalyst), zeolite HZSM-5 (acid component) and alumina (binder). It was found that synthetic fuel obtained on that catalyst contains many alkenes (40%), which affect negatively on the properties of motor fuels. In the present study was researched the insertion method of nickel into cobalt-zeolite catalyst for decreasing part of unsaturated hydrocarbons, its activity and selectivity of combined synthesis and hydroprocessing of hydrocarbons.

It was determined that insertion method of hydrogenating component (Ni) into multifunctional catalyst affects dramatically on composition of synthesized products. The highest hydrogenating activity has catalyst which was impregnated by nickel into silica on the stage of forming cobalt-silica catalyst. The containing of unsaturated hydrocarbons obtained via this catalyst was decreased of 1.76 times compared to catalyst without hydrogenating addition.

*This work was supported by the Ministry of Education and Science of the Russian Federation within of the state task for R&D, application number 2019-0990 using the equipment of the "Nanotechnology" Center for collective use at the M.I. Platov South-Russian State Polytechnic University.*

## Photocatalytic hydrogen production from aqueous solutions of methylene blue under UV light over Cu modified TiO<sub>2</sub>

A.V. Zhurenok<sup>1</sup>, A.Y. Kurenkova<sup>1</sup>, D.V. Markovskaya<sup>1,2</sup>, S.V. Cherepanova<sup>1,2</sup>, V.V. Kaichev<sup>1,2</sup>, E.A. Kozlova<sup>1,2</sup>

<sup>1</sup>*Boreskov Institute of Catalysis, Novosibirsk, Russia*

<sup>2</sup>*Novosibirsk State University, Novosibirsk, Russia*

angelinazhurenok@gmail.com

Dyes are known to be widespread water pollutant [1]. Industrial wastewater may contain dyes, such as methylene blue (MB), which can be removed by photocatalytic way [1, 2] and alcohol compounds, which are important sacrificial agents in photocatalysis [3]. Titanium dioxide is a widely used heterogeneous photocatalyst. The aim of the work was synthesis and study new photocatalysts based TiO<sub>2</sub> for hydrogen evolution from water-ethanol solutions of methylene blue.

TiO<sub>2</sub> Evonik P25 with deposited copper was used as a photocatalyst. Samples were prepared by annealing commercial Evonik P25 for 3 hours at 400-800 °C. Cu (1 wt. %) was deposited onto heat-treated TiO<sub>2</sub> by impregnation of Cu(NO<sub>3</sub>)<sub>2</sub>, followed by 2.5-fold reduction with an excess of NaBH<sub>4</sub>, then the catalysts were washed and dried at 50 °C for 4 hours. Photocatalysts were labeled Cu/Tx, where Tx is the calcination temperature. Photocatalytic tests for the production of hydrogen were carried out a water-ethanol solution of MB, volume fraction of ethanol was 10%. Concentrations of MB in the experiments were as follows: 2, 5, 10, and 20 mg×L<sup>-1</sup>. The reaction mixture was illuminated by UV light ( $\lambda = 386$  nm).

Titanium dioxide consists of anatase and rutile phases, their molar ratio is dependent on the calcination temperature, as confirmed by XRD analysis. Rutile phase forms at the annealing temperature of 800 °C, while at the annealing temperature of 400-600 °C the mixture of anatase and rutile is identified; 75-85% anatase is observed. In addition, rutile phase predominates in the Cu/TiO<sub>2</sub>-700 sample. It is also worth noting that the copper in the catalysts is in the form of CuO in the catalysts Cu/TiO<sub>2</sub>-400-600, while CuO and Cu<sub>2</sub>O are found in the catalysts Cu/TiO<sub>2</sub>-700 and Cu/TiO<sub>2</sub>-800, as demonstrated by XANES method.

The rate of hydrogen production from aqueous solution of methylene blue was measured over the prepared photocatalysts, no hydrogen was identified. After that ethanol was added into the reaction mixture as a sacrificial agent. In this case, non-zero values of reaction rate were obtained and discoloration of solution was fixed. The reaction rate increases with increasing concentration of dye to 10 mg L<sup>-1</sup> for all photocatalysts. Further growth of the MB concentration to 20 mg L<sup>-1</sup> leads to the fall of photocatalytic hydrogen production rate over all tested samples. In this case, strong light absorption by the dye is observed and small amount of electron-hole pairs are generated on the photocatalyst surface. The most active samples were Cu/TiO<sub>2</sub>-600 and Cu/TiO<sub>2</sub>-700. The maximum catalytic activity, 1.24 mmol g<sub>cat</sub><sup>-1</sup> h<sup>-1</sup>, was observed over the Cu/TiO<sub>2</sub>-600 photocatalyst, concentration of MB was equaled to 10 mg L<sup>-1</sup>. Additionally, the hydrogen production from aqueous solution of ethanol without dye is carried out. In these experiments the hydrogen production rate was lower than in the case of solutions with MB. Thus, presence both ethanol and methylene blue is beneficial for the photocatalytic hydrogen production.

*This work was supported by RSF Grant №19-73-20020*

### References

1. Nguyen C. H., Fu C.-C., Juang R.-S. *Journal of Cleaner Production* **2018**, 202, 413–427.
2. Davis R. J., Gainer J. L., O'Neal G., Wu I. W. *Water Environ. Res.* **1994**, 66, 50–53.
3. Patwardhan A.D. *Industrial Wastewater Treatment*, PHI Learning Pvt. Ltd., 2008.



# SECTION 3

## PHYSICAL-CHEMICAL FUNDAMENTALS OF CATALYSIS



## Effect of high-temperature treatment of Sibunit and content of Ru on the activity of Ru-Cs/Sibunit catalysts in ammonia synthesis

V.A. Borisov<sup>1,2</sup>, K.N. Iost<sup>1</sup>, V.L. Temerev<sup>1</sup>, P.A. Fedotova<sup>2</sup>, Yu.V. Surovikin<sup>1,2</sup>, D.A. Shlyapin<sup>1</sup>

<sup>1</sup>*Center of New Chemical Technologies BIC, Omsk, Russia*

<sup>2</sup>*Omsk State Technical University, Omsk, Russia*

borisovtiger86@mail.ru

The use of Sibunit ruthenium catalysts instead of iron ones deposited on the Sibunit carbon composite material in ammonia synthesis makes it possible to reduce the process temperature from 450 °C to 350 °C and the pressure from 20–30 MPa to 8 MPa. The aim of this project was to study the effect of thermal modification of Sibunit on the structural features of the support, and the activity of ruthenium catalysts of low-temperature ammonia synthesis supported on Sibunit.

The original Sibunit (Sib20) with a specific surface area of 303 m<sup>2</sup>/g was subjected to high-temperature treatment in a closed graphite crucible in a nitrogen atmosphere at the temperatures 1400, 1600, 1800, 2000 and 2200 °C. The specific surface area of Sibunit after treatment decreased by an order of magnitude: to 29 m<sup>2</sup>/g for Sib2200.

According to X-ray phase analysis (XRD), the structure of Sibunit is ordered: the interplanar distance  $d(002)$  decreases from 0.349 nm (Sib20) to 0.344 nm (Sib2200). The Raman scattering spectra show the same thing: the  $I_D/I_G$  ratio decreases from 1.59 for Sib20 to 1.18 for Sib2200, the intensity of the 2D line increases significantly. Electron paramagnetic resonance (EPR) also shows significant ordering of the Sibunit structure. In the Sib2200 EPR spectrum, the signal shifts to  $g = 2.0059$  (for graphite 2.0025), and the concentration of paramagnetic centers per unit surface of the material increases several times. It is very interesting that, according to IR spectroscopy data, in addition to the absorption bands at 1530–1580 cm<sup>-1</sup>, corresponding to the stretching vibrations of C=C bonds of conjugated aromatic structures (including graphite), the absorption band at 1640 cm<sup>-1</sup>, which can correspond to the stretching vibrations of C=O (NH) amide bonds in amide functional groups and amine bonds, is appear in the Sib2200 sample.

According to the TEM the average particle size of Ru decreases with increasing carrier treatment temperature, for example, for 4% Ru-13.6% Cs/Sib20 – 8 nm catalyst, for 4% Ru-13.6% Cs/Sib1400 catalyst – 5 nm and for 4% Ru-13.6% Cs/Sib2200 catalyst – 3 nm.

The catalytic activity in ammonia synthesis was determined by chromatography with a column filled with Haeyesep C sorbent, as well as by back titration of the H<sub>2</sub>SO<sub>4</sub> solution, through which the gas mixture flow after the reactor was passed. According to the obtained results, the achieved concentration of NH<sub>3</sub> in the gas phase is higher for all catalysts modified with cesium compared to barium-containing samples and increases with the rise in calcination temperature of the support. The specific activity (0.6 MPa) increases almost 30 times from ~0.019 to ~0.59 mol NH<sub>3</sub>/(g<sub>Ru</sub>·h) for catalysts 4% Ru-13.6% Cs/Sib20 and 0.38% Ru-1.25% Cs/Sib2200.

*This work was supported by Russian Science Foundation, Project No. 18-73-00255.*



## Alcohol effect on the catalytic properties of CuO<sub>x</sub> water-ethanol colloids obtained by laser ablation in 4-nitrophenol hydrogenation

D.A. Goncharova, T.S. Kharlamova, O.A. Reutova, V.A. Svetlichnyi

<sup>1</sup>*Tomsk State University, Tomsk, Russia*

dg\_va@list.ru

Currently, great attention is paid to the catalytic reduction of nitro compounds, in particular 4-nitrophenol (PNP), with sodium borohydride (NaBH<sub>4</sub>) representing an effective and environmentally friendly reducing agent. In this reaction the catalysts based on noble (Pt, Ag, Au, Pd) and transition (Co, Fe, Ni, Mn, Cu) metals are used. The Cu-containing catalysts are less expensive and potentially can be selective, while the catalytic characteristics are comparable to those of nanocatalysts based on noble metals [1]. A rapidly developing and promising method to prepare the catalytically active surfactant-free colloidal nanoparticles is pulsed laser ablation in a liquid (LAL) [2]. We have recently shown that CuO<sub>x</sub> NPs with various phase composition (Cu, Cu<sub>2</sub>O, Cu@Cu<sub>2</sub>O), sizes and morphology are formed by LAL of copper in water and ethanol [3]. In this work, the LAL of copper in water-ethanol solution was carried out and the catalytic activity of the obtained colloids was investigated in the PNP hydrogenation with NaBH<sub>4</sub>.

CuO<sub>x</sub> NPs dispersions (40-60 mg/l) were prepared by the LAL of copper in distilled water, ethanol and water-ethanol solution (10, 20, 30, 50, 70%wt. of ethanol) according to the technique described in Ref. [3]. The prepared samples were characterized by XRD (XRD6000, Shimadzu (Japan)), UV-vis absorption spectroscopy (Cary100, Varian (Australia)), and TEM (CM 12, Philips (Netherlands)). The catalytic properties of the obtained CuO<sub>x</sub> NPs in PNP reduction were studied using aqueous solutions of PNP and NaBH<sub>4</sub> at 19 °C. Typically, 1.7 ml of distilled water, 200 µl dispersion of CuO<sub>x</sub> NPs (15 mg/l) aged for 3 days and 300 µl of freshly prepared NaBH<sub>4</sub> aqueous solution (5×10<sup>-2</sup> mol/l) were mixed at a rate of 300 rpm during 2 min and added to 300 µl of the PNP aqueous solution (2.57×10<sup>-4</sup> mol/l). The reaction was performed inside the quartz cuvette (10 mm), and the reduction processes were monitored online by following the PNP optical absorption peak at 400 nm with 10 s intervals using CM 2203 spectrophotometer (SOLAR (Belarus)).

As a result, the composition of the used water-ethanol solution in the studied range of alcohol concentration from 10% to 70% was shown to affect the size of the resulting particles and the sedimentation stability of the obtained sols, but did not significantly affect the phase composition of the particles obtained during the LAL as well as changing of their phase composition and morphology during the sol aging.

The results of the catalytic studies of CuO<sub>x</sub> NPs in sols obtained by LAL indicated their high activity in the PNP reduction comparable to or higher than the one of CuO<sub>x</sub>-based catalysts obtained by other methods. An increase in the alcohol concentration in the reaction medium was shown to generally increase the induction period and decrease the effective reaction rate constant. It has been determined that the alcohol effect on the kinetics of PNP reduction was found to be due to the alcohol adsorption on the catalyst surface that was well described within the framework of the Langmuir-Hinshelwood kinetic model. The alcohol presented in the reaction medium showed an inhibitory effect on the process of substrate reduction due to the alcohol sorption on the same sites of the catalyst surface along with the reagents.

*This work was supported by the Tomsk State University competitiveness improvement programme.*

### References

1. Prucek, R.; Kvítek, L.; Panáček, A.; Vančurová, L.; Soukupová, J.; Jančík, D.; Zbořil, R. *J. Mater. Chem.* **2009**, *19* (44), 8463–8469.
2. Reichenberger, S.; Marzun, G.; Muhler, M.; Barcikowski, S. *ChemCatChem* **2019**, *11* (18), 4489–4518.
3. Goncharova, D.A.; Kharlamova, T.S.; Lapin, I.N.; Svetlichnyi, V.A. *J. Phys. Chem. C* **2019**, *123*, 21731–21742.

## Rh-doped CeO<sub>2</sub> catalytic systems for low-temperature NO reduction

L.S. Kibis<sup>1,2</sup>, A.I. Krotova<sup>1,2</sup>, D.A. Svintsitskiy<sup>1,2</sup>, E.A. Fedorova<sup>1</sup>, E.M. Slavinskaya<sup>1,2</sup>, O.A. Stonkus<sup>1,2</sup>, V.A. Svetlichnyi<sup>3</sup>, A.I. Boronin<sup>1,2</sup>

<sup>1</sup>*Boriskov Institute of Catalysis, Novosibirsk, Russia*

<sup>2</sup>*Novosibirsk State University, Novosibirsk, Russia*

<sup>3</sup>*Tomsk State University, Tomsk, Russia*

kibis@catalysis.ru

Rh-based systems are indispensable components of the automobile catalytic converters responsible for neutralization of the exhaust gases. Nowadays a lot of attention is focused on developing ways to improve the stability of the current catalysts and increase their low-temperature activity while keeping an expensive active component at the minimal loading. Recent works [1,2] show that variation of the size of the active components can substantially influence the activity of the Rh-based systems. Due to a high degree of metal-support interaction in Rh-CeO<sub>2</sub> catalysts the particle size and oxidation state of rhodium in these systems can be varied in a wide range. In the present work, we focused on the detailed study of the activity of Rh-CeO<sub>2</sub> catalysts in the reaction of low-temperature NO reduction depending on the nature of the active component.

The Rh-doped CeO<sub>2</sub> catalysts were prepared by coprecipitation of rhodium and cerium nitrates. Rh loading was varied in a range of 1-8 wt.%. Samples were pre-treated in the reductive and oxidative atmosphere at a temperature range 450-1000°C. Samples were studied by a complex of physical-chemical methods: X-ray diffraction, X-ray photoelectron spectroscopy, Transmission electron microscopy, Raman spectroscopy, Infrared spectroscopy, Temperature-programmed reaction with CO (TPR-CO). The catalytic activity of the samples was studied in the Temperature-programmed reaction of NO reduction with CO (TPR-CO+NO).

Initial samples calcined at 450°C show Rh<sup>3+</sup> species highly dispersed in CeO<sub>2</sub> (Rh<sup>3+</sup>-CeO<sub>2</sub>). Pretreatment of the samples in the reductive atmosphere results in a formation of small reduced Rh<sup>δ+</sup> species on a defect CeO<sub>2</sub> surface. However, these reduced species are easily oxidized to the initial Rh<sup>3+</sup> state under treatment with O<sub>2</sub> or NO, thus showing high reversibility of Rh<sup>3+</sup> ↔ Rh<sup>δ+</sup> transitions. Calcination of Rh<sup>3+</sup>-CeO<sub>2</sub> samples at temperatures higher 800°C results in the formation of individual RhO<sub>x</sub> species close to Rh<sub>2</sub>O<sub>3</sub> oxides. These species can be reduced with the formation of Rh<sup>0</sup> nanoparticles which are more resistant to further reoxidation.

Rh<sup>3+</sup> ions dispersed in CeO<sub>2</sub> show the highest low-temperature activity with NO conversion at temperature higher 50°C. The activity of pre-reduced Rh<sup>δ+</sup>-CeO<sub>2</sub> samples in the CO+NO reaction is close to the one of initial Rh<sup>3+</sup>-CeO<sub>2</sub> catalysts pointing to the close nature of the active species. The fast Rh<sup>3+</sup> ↔ Rh<sup>δ+</sup> redox transitions were proposed to be responsible for the low-temperature activity of the samples. RhO<sub>x</sub> nanoparticles on the surface of CeO<sub>2</sub> show activity only at T>150°C, however their activity might be increased by pretreatment in the reductive atmosphere.

*This work was partially supported by RFBR and the government of the Novosibirsk region Grant #18-43-543009.*

### References

1. Jeong, H.; Lee, G.; Kim, B.; Bae, J.; Han, J. W.; Lee, H. *J. Am. Chem. Soc.* **2018**, *140*, 9558–9565.
2. Ohyama, J.; Nishiyama, T.; Satsuma, A. *ChemCatChem* **2018**, *10*, 1651–1656.

## Active sites on the surface of mayenite during catalytic ethanol dehydration

E.I. Shuvarakova, A.F. Bedilo, A.S. Chichkan, E.V. Ilyina

*Boreskov Institute of Catalysis, Novosibirsk, Russia*

katerina.shuv@gmail.com

Highly dispersed oxide systems are widely used as highly effective adsorbents, functional additives for polymers, abrasive materials, and in many other areas of modern chemical technologies. At the same time, the synthesis of many complex oxide materials, including calcium aluminates with the structure of C12A7 mayenite, usually occurs only at high (above 1000 °C) temperatures. Moreover, when the part of the oxygen anions are replaced by  $O^-$  or  $O_2^-$  radical anions, such samples are of great interest due to their high activity in catalytic oxidation.

C12A7 samples were synthesized according to the procedure described previously [2]. CaO obtained by decomposing the  $CaCO_3$  at 700 °C was quickly poured under vigorous stirring into a suspension containing the calculated amount of aluminum hydroxide in water. The resulting mixed hydroxide was dried and calcined in air. This technique makes it possible to significantly reduce the synthesis temperature and to obtain highly dispersed nanocrystalline materials with mayenite crystalline structure and a specific surface area of about 80 m<sup>2</sup>/g after calcination at 500 °C.

The active sites on the surface of the synthesized materials were studied by EPR using phenothiazine, trinitrobenzene and diphenylamine as spin probes. The weakest electron-acceptor sites capable of ionizing phenothiazine and electron-donor sites capable of ionizing trinitrobenzene were present on the surface of all the studied calcium aluminate samples.

It was recently shown [3] that stable diphenyl nitroxyl radicals can be formed during the adsorption of diphenylamine on the surface of mayenite samples. In the present work, such radicals were also detected during the adsorption of diphenylamine on the surface of calcium aluminates samples calcined at temperatures of 500 and 900 °C. Their formation, apparently, indicates the existence of noticeable concentrations of OH or  $O^-$  radicals on the surface of highly dispersed mayenites.

The catalytic activity of several calcium aluminates of with different Ca/Al ratios in the reaction of ethanol dehydration in a flow reactor was investigated. It was found that the activity of all the studied calcium aluminates was approximately 2 orders of magnitude lower than that of the  $\gamma$ - $Al_2O_3$  sample used for comparison. In this case, the catalytic activity of calcium aluminates decreased with increasing Ca/Al ratio.

The disappearance of weak electron-acceptor sites during ethanol dehydration on calcium aluminates, in contrast to  $\gamma$ - $Al_2O_3$ , was shown for the first time. Phenothiazine radical cations are formed upon adsorption of this probe on samples of mayenite activated in an argon flow at 250 °C. Moreover, on the samples of mayenites after 10 minutes of reaction with ethanol, such sites completely disappear. This correlates with their significantly lower catalytic activity in the ethanol dehydration compared to  $Al_2O_3$ .

At the same time, we discovered the formation of new radicals as a result of the detachment of the hydrogen atom from the nitrogen in the phenothiazine molecule. Moreover, the sites responsible for this process, apparently associated with radical forms of oxygen, remained on the surface of calcium aluminates during the reaction with ethanol for at least 1 hour.

*This work was supported by RFBR Grant 19-03-00834.*

### References

1. Meza-Trujillo, I.; Devred, F.; Gaigneaux, E. M. *Mater. Res. Bull.* **2019**, *119*, 110542.
2. Yakovlev, I. V.; Volodin, A. M.; Papulovskiy, E. S.; Andreev, A. S.; Lapina, O. B. *J. Phys. Chem. C* **2017**, *212*, 22268.
3. Volodin, A. M.; A. F., Bedilo; Stoyanovskii, V. O.; Zaikovskii, V. I. *Nanosystems: Phys., Chem., Mathem.* **2018**, *9*, 558.

## **Structure-activity relationships of Pt/TiO<sub>2</sub> catalysts for ammonia low-temperature oxidation: comparison of pulsed laser ablation and impregnation methods of catalysts synthesis**

A.I. Stadnichenko<sup>1,2</sup>, L.S. Kibis<sup>1</sup>, E. M. Slavinskaya<sup>1</sup>, D.A. Svinitskiy<sup>1</sup>, E. A. Fedorova<sup>1</sup>, O. A. Stonkus<sup>1</sup>, A.V. Romanenko<sup>1</sup>, V.A. Svetlichnyi<sup>2</sup>, V. Marchuk<sup>3</sup>, D. Doronkin<sup>3</sup>, J.-D. Grunwaldt<sup>3</sup>, A.I. Boronin<sup>1</sup>

<sup>1</sup>*Boriskov Institute of Catalysis, Novosibirsk, Russia*

<sup>2</sup>*Tomsk State University, Tomsk, Russia*

<sup>3</sup>*Karlsruhe Institute of Technology, Karlsruhe, Germany*

stad@catalysis.ru

Exhaust gas aftertreatment systems of power plants and automobiles contains NO<sub>x</sub>. For NO<sub>x</sub> neutralization excess of NH<sub>3</sub> is dosed in the stream, resulting in its slip in the exhaust. Because of its toxicity, NH<sub>3</sub> needs to be removed from exhaust gas before it reaches the environment. From other hand, ammonia and its derivatives are considered as excellent energy storage materials alternative to elementary hydrogen and, thus, as energy carriers for mobile applications. Since NH<sub>3</sub> decomposition is an equilibrium process, NH<sub>3</sub> slip inevitably occurs during H<sub>2</sub> generation. Selective oxidation of NH<sub>3</sub> to N<sub>2</sub> over so-called ammonia slip catalysts (ASC) is currently the only way to prevent unreacted ammonia reaching the environment. Due to their high activity and stability under realistic working conditions (e.g. with H<sub>2</sub>O vapour), Pt-based catalysts are predominantly used as ASCs. In order to efficiently improve low-temperature activity of Pt catalysts and to increase their selectivity to N<sub>2</sub> it is essential to understand structure activity relationships of Pt based catalysts in selective NH<sub>3</sub> oxidation.

In order to highlight the role of platinum interaction with support three different types of 2%Pt/TiO<sub>2</sub> catalysts were used. The first series of catalysts was synthesized by coprecipitation/incipient wetness impregnation (IMP) technique based on commercial TiO<sub>2</sub> P-25 aerioxide (Evonik). The second one was synthesized by annealing mixture of TiO<sub>x</sub> and Pt NPs produced by pulsed laser ablation (PLA). The third series of catalysts was synthesized by incipient wetness impregnation technique based on TiO<sub>x</sub> produced by pulsed laser ablation (MIX). Catalytic properties were studied in an automated installation with a flow quartz reactor using the temperature-programmed reaction method (TPR-NH<sub>3</sub>+O<sub>2</sub>). Used reaction mixture was 0.1 vol% NH<sub>3</sub> and 4 vol% O<sub>2</sub> in helium, a flow rate of 500 cm<sup>3</sup>/min (GHSV 120 000 h<sup>-1</sup>). The samples were tested twice up to 400°C at the rate of 10°C/min. Concentrations of NH<sub>3</sub>, N<sub>2</sub>O, NO, NO<sub>2</sub> were recorded using IR spectroscopy. Concentrations of O<sub>2</sub> and N<sub>2</sub> were recorded using gas chromatography. Catalysts were characterized using XRD, XPS, HRTEM, XANES analysis. To understand the possible changes of platinum oxidation state and interaction with TiO<sub>2</sub> under reaction conditions operando XAS measurements were performed at PETRA III P65.

Pt/TiO<sub>2</sub> (IMP) catalyst is characterized by rutile and anatase phases mixture, the platinum is presented by NP size ≤ 1nm. According to the XPS results, platinum is present in oxidized states Pt<sup>2+</sup> and Pt<sup>4+</sup>. Pt<sup>0</sup> appears after calcination at 600-800°C. In case of (PLA) catalysts the produced samples consist of amorphous TiO<sub>x</sub> particles; and anatase phase appears after annealing at 400°C. Platinum is presented by 1-3 nm metallic particles. (MIX) samples contain ionic platinum Pt<sup>2+</sup>/Pt<sup>4+</sup> in the initial state, but under the reaction conditions platinum is reduced to Pt<sup>δ+</sup>/Pt<sup>2+</sup> mixture. All the catalysts are active in NH<sub>3</sub> oxidation starting from approx. 140°C. (PLA) catalysts with metallic platinum on the surface show excellent selectivity to N<sub>2</sub> production at low temperature range. Calcination leads to a slight increase of activity of PLA samples and activity loss of impregnated samples. In situ XAS investigations allow correlating changes in catalytic activity with transformations of Pt oxidation states.

*The work was supported by Helmholtz – Russian Science Foundation Joint Research Groups grant #18-43-06201 from 03.09.2018 (RSF) / #HRSF-0046 from 01.09.2018 (HGF).*

## Selective oxidation of ammonia over Pt-based catalysts

D.A. Svintsitskiy<sup>1</sup>, E.M. Slavinskaya<sup>1</sup>, E.A. Fedorova<sup>1</sup>, L.S. Kibis<sup>1</sup>, A.I. Stadnichenko<sup>1</sup>,  
A.V. Romanenko<sup>1</sup>, A.S. Zaguzin<sup>1</sup>, O.A. Stonkus<sup>1</sup>, D.E. Doronkin<sup>2,3</sup>, V. Marchuk<sup>2</sup>, Maria Casapu<sup>2</sup>,  
J.-D. Grunwaldt<sup>2,3</sup>, A.I. Boronin<sup>1</sup>

<sup>1</sup>*Boreskov Institute of Catalysis, Novosibirsk, Russia*

<sup>2</sup>*Institute for Chemical Technology and Polymer Chemistry, Karlsruhe, Germany*

<sup>3</sup>*Institute of Catalysis Research and Technology, Karlsruhe Institute of Technology, Karlsruhe, Germany*

sad@catalysis.ru

The catalyst for selective NH<sub>3</sub> oxidation is an essential component of NO<sub>x</sub> removal systems for diesel exhaust gas aftertreatment. In such systems excess of ammonia is usually dosed to increase NO<sub>x</sub> conversion resulting in its slip in the exhaust [1]. To remove the remaining NH<sub>3</sub> before it reaches the environment an ammonia slip catalytic system is additionally installed. Such system usually includes Pt-based catalyst for ammonia oxidation to N<sub>2</sub>, while NO<sub>x</sub> formed during unselective NH<sub>3</sub> oxidation is further removed on a Cu- or Fe- containing zeolite layer operating as a selective reduction catalyst [2]. Among different catalysts, Pt-based systems are considered to be very efficient for selective NH<sub>3</sub> oxidation at low temperatures but suffer from selectivity loss above 200 °C [3]. To rationally improve the performance of Pt catalysts in selective ammonia oxidation structure-activity relationships for Pt catalysts need to be understood which requires further systematic fundamental studies.

This contribution presents a systematic study of various Pt-based catalysts supported on Al<sub>2</sub>O<sub>3</sub>, TiO<sub>2</sub>, and CeO<sub>2</sub> under conditions of low-temperature NH<sub>3</sub> oxidation. All catalysts containing 2 wt. % Pt were prepared by incipient wetness impregnation using Pt(NO<sub>3</sub>)<sub>4</sub> or H<sub>2</sub>PtCl<sub>6</sub> solutions. The size of Pt particles and its oxidation state were varied depending on the Pt precursor and the calcination temperature and/or reducing treatment [4]. To characterize Pt-based catalysts a complex of physicochemical techniques including XPS, XRD, TEM, XANES/EXAFS was applied.

*Operando* XANES study allowed us to determine the average oxidation state of Pt during the NH<sub>3</sub>+O<sub>2</sub> reaction. It was shown that the improvement of catalytic properties at low temperatures correlates with Pt reduction. Substantial part of Pt sites remains oxidized as PtO<sub>x</sub> under NH<sub>3</sub> oxidation conditions at temperature below 200°C. During the light-off the highest degree of Pt reduction and selectivity to N<sub>2</sub> are observed. At higher temperature, reoxidation of Pt surface takes place leading to the formation of undesirable products limiting the N<sub>2</sub> selectivity. In case of TiO<sub>2</sub>-based Pt catalysts the strong-metal support interaction was observed. This effect is responsible for the stabilization of highly dispersed Pt species even after calcination at 800°C resulting in similar catalytic performance of the samples regardless of their calcination temperature in contrast to Pt/Al<sub>2</sub>O<sub>3</sub> catalysts. The nature of catalyst support as well as its structure can significantly influence on the properties of active component including the activity in NH<sub>3</sub> oxidation and selectivity to N<sub>2</sub>.

To further tune the catalytic properties of Pt-based catalysts in NH<sub>3</sub> oxidation the optimization of Pt particle size is required. The size of Pt particles should be large enough to prevent oxidation under reaction conditions with O<sub>2</sub> excess, while the upper limit of Pt particles size is defined by the requirement to efficiently use the expensive active component of the catalysts.

*This work was supported by Helmholtz – Russian Science Foundation Joint Research Groups grant #18-43-06201 from 03.09.2018 (RSF) / HRSF-0046 from 01.09.2018 (HGF). We acknowledge DESY (Hamburg, Germany), a member of the Helmholtz Association HGF, for the provided beamtime.*

### References

1. Colombo, M.; Nova, I.; Tronconi, E.; Schmeißer, V.; Bandl-Konrad, B.; Zimmermann, L. *Appl. Catal. B Environ.* **2013**, 142–143, 861–876.
2. Scheuer, A.; Hauptmann, W.; Drochner, A.; Gieshoff, J.; Vogel, H.; Votsmeier, M. *Appl. Catal. B Environ.* **2012**, 111–112, 445–455.
3. Chmielarz, L.; Jabłońska, *RSC Adv.* **2015**, 5, 43408–43431.
4. Svintsitskiy D.A.; Kibis L.S.; Stadnichenko A.I. et al. *ChemCatChem* **2020**, 12, 867–880.

## Machine learning application for XANES spectroscopy of Pd nanocatalyst

O.A. Usoltsev<sup>1</sup>, A.L. Bugaev<sup>1,2</sup>, A.A. Guda<sup>1</sup>, S.A. Guda<sup>1</sup>, A.V. Soldatov<sup>1</sup>

<sup>1</sup>*Southern Federal University, Rostov-on-Don, Russia*

<sup>2</sup>*Federal State Budgetary Institution of Science "Federal Research Centre The Southern Scientific Centre of The Russian Academy of Sciences", Rostov-on-Don, Russia*

oleg-usol@yandex.ru

The machine learning (ML) is an advanced analytical approach which is now applied in many areas of science. This method has proven for tasks with a large number of parameters and is effective for big data processing. X-ray absorption near edge structure (XANES) spectroscopy is powerful tool widely applied for defining atomic and electronic properties of working catalysts [1]. In many cases, analysis of XANES data requires construction of theoretical models with a huge number of variable parameters. Therefore, application of ML to in situ and operando XANES offers new horizons for structural characterization.

It was XANES analysis that allowed us to detect formation of carbide and hydride phases in the core and shell of Pd nanoparticles (NPs) during hydrogenation reactions [2]. Interplay between these phases is known to significantly affect the activity and selectivity of the catalysts. Thereby, the investigation of the carbide phase formation in Pd NPs in presence of hydrocarbons is of practical interest for catalytic science.

In this work, we applied the Extra Trees approach for time-resolved XANES spectra of Pd NPs. Evolution of the structural parameters were obtained and compared with the principle component analysis (PCA) and multidimensional interpolation approach [3]. We constructed a training set based on theoretical XANES spectra calculated in the FDMNES code for Pd NPs with different interatomic distances and in presence of hydrogen- and carbon-containing species. We used Latin hypercube sampling for modelling 5000 spectra corresponding to 7 independent parameters in training set. The transient curves for fixed 6 parameters depended on interatomic distances are demonstrated in Fig. 1.

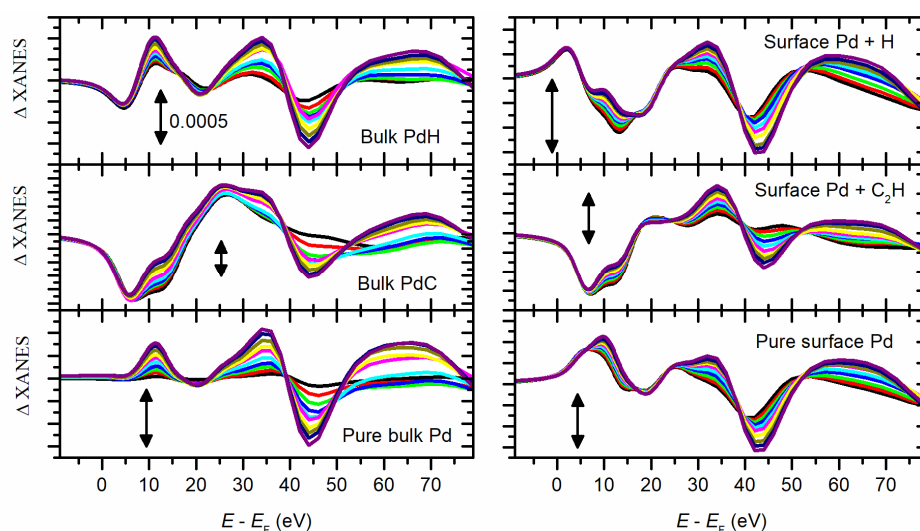


Fig. 1. Theoretical transient spectra for group of parameters depending on the interatomic distance from 3.87 Å (black) to 4.02 Å (purple).

Then, we performed ML to get structural parameters by tuning the theoretical spectrum to the experimental one. The example of such fitting for the XANES spectrum of Pd NPs in presence of acetylene is shown in Fig. 2. The parameters obtained from this fit allowed us to make a conclusion that under these conditions: (i) no hydride phase was formed; (ii) the fraction of surface atoms in the Pd NPs was close to 0.4; (iii) relative fraction of carbon atoms in the bulk (C/Pd) was  $\sim 0.13$ ; (iv) at the surface, there was 1 acetylene molecule per 4 palladium atoms. Further analysis of big dataset of operando data is now in progress.

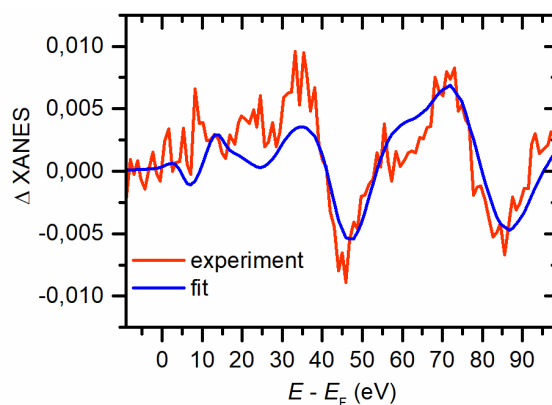


Fig. 2. The result of XANES fitting for Pd NPs in presence of acetylene.

This work was supported by the President's Grant of Russian Federation for young scientists MK 2554.2019.2. (№ 075-15-2019-1096)

#### References

1. Guda, A. A. et al. *Catal. Today* **2019**, 336, 3–21.
2. Bugaev, A. L. et al. *Faraday Discuss.*, **2018**, 208, 187–205.
3. Smolentsev, G.; Soldatov, A. V. *J. Synchrotron Radiat.*, **2006**, 13, 19–29.

## Microscopy study of the catalytic etching of platinum metals during ammonia oxidation

N.M. Chesnokova, A.N. Salanov

*Boreskov Institute of Catalysis, Novosibirsk, Russia*

kochurova@catalysis.ru

Industrial oxidation of ammonia with air on platinum alloy gauzes is widely applied for the production of nitric acid, which is used to obtain fertilizers and many other substances. The catalytic oxidation of  $\text{NH}_3$  is accompanied by intense catalytic etching of the gauze surface, which leads to a loss of platinum metals, mechanical degradation of gauzes, and reduces the period of efficient operation of the catalyst. To solve these problems, it is necessary to investigate the catalytic etching of platinum metals, which is the main component of catalytic gauzes.

In this work, to reveal the mechanism of the initial step of catalytic etching, images of the platinum surface after the catalytic oxidation of  $\text{NH}_3$  with air oxygen were obtained. The study was carried out using the polycrystalline platinum foils (Pt(poly)), (Pd(poly)), (Rh(poly)) with the size of  $10 \times 5 \times 0.04$  mm. The oxidation of  $\text{NH}_3$  with air was performed in a laboratory flow-type quartz reactor. The surface morphology and microstructure were studied using a SU-8220 (Hitachi) scanning electron microscope (SEM) at the energy of beam electrons ( $E_0$ ) 20 keV in the secondary electron (SE) mode.

High-resolution SEM was used to obtain microimages of the Pt(poly) surface after the oxidation of  $\text{NH}_3$  with air at 1133 K for 1 h. The highly exothermic oxidation of  $\text{NH}_3$  with the oxygen intercalated at defects leads to etching of the grain surface. The grain structure substantially affects the etching process. On the surface of grains with the (111) structure, the oxidation of  $\text{NH}_3$  on defects induces a local increase in temperature, which leads to segregation of Pt atoms to the surface. Pt atoms migrating on the surface create a saturated surface layer from which Pt atoms and volatile oxides like  $\text{PtO}_2$  and others are released to the gas phase. During the  $\text{NH}_3$  oxidation, the vaporized oxides and Pt atoms migrating on the surface form pyramids on dislocations, whereas upon cooling of the catalyst they form single-crystal Pt particles on the vertices of pyramids.  $\text{NH}_3$  oxidation is accompanied by the formation of regions with the width  $\sim 1$   $\mu\text{m}$  and length up to 5  $\mu\text{m}$  on the surface of (110) grains; Pt atoms are intensively released from such regions, thus producing voids with the depth up to 1  $\mu\text{m}$ . Taking into account that the voids have close orientation and order for each grain, they may be formed on the dislocation walls that occur as the ordered structures in grains and contain high concentration of defects. Upon  $\text{NH}_3$  oxidation, N and O atoms are intensively dissolved on these defects in subsurface layers. Migration of these atoms on defects and their recombination on the surface lead to the formation of  $\text{NO}_{\text{gas}}$  molecules. Owing to these processes, the etching layer is formed, which includes deep elongated voids that appear on dislocation walls of (110) grains, and pyramids that grow on individual dislocations of (111) grains. A similar etching layer is observed at the backside of the first platinum alloy gauze along the gas stream.

The deepest etching occurs on Pd, to a lesser degree was at Rh and slightly at Pt. The pyramidal crystal layer is formed on the Rh and a continuous layer of crystalline aggregates with a size of 10-20  $\mu\text{m}$  with through-pores of 1-5  $\mu\text{m}$  in diameter formed was on the Pd. Catalytic etching occurs in the reaction of  $\text{NH}_3$  molecules with the oxygen atoms in the metal oxide and the oxygen atoms which were dissolved in the surface layer of the metal by the mechanism of Redox. Thus, the surface structure of Pt(poly) grains exerts an essential effect on the catalytic etching of platinum surface initiated by  $\text{NH}_3$  oxidation. The surface of (111) grains contains individual defects represented by dislocations. During the oxidation of  $\text{NH}_3$ , the Pt atoms segregated to the surface form 0.1-1.0  $\mu\text{m}$  pyramids on dislocations. The surface of (110) grains contains elements of dislocation walls with high concentration of defects. In the region of dislocation walls, the highly exothermic oxidation of  $\text{NH}_3$  leads to a pronounced segregation of Pt atoms to the surface and formation of elongated voids with the depth up to 1  $\mu\text{m}$  and length up to 5  $\mu\text{m}$ .

*This work was supported by Ministry of Science and Higher Education of the Russian Federation (project AAAA-A17117041710079-8).*



## **Investigation of the semiconducting properties of bismuth silicate-based photocatalysts by electrochemical methods**

O.V. Dubinina, A.V. Shabalina, E. Yu. Gotovtseva, O.V. Vodyankina

*National Research Tomsk State University, Tomsk, Russia*

kamchatuska@rambler.ru

In recent years much attention has been attended to semiconductor materials due to a large number of fields of their application. The bismuth silicate-based semiconductors because of their electric, mechanical, optical properties found wide application in piezotechnician, acusto- and optoelectronics. However, there are not many ideas to use these materials as photocatalysts in the process of hydrogen production [1].

The bismuth silicate-based semiconductors possess a wide band gap, high resistivity, and low charge transfer despite their high photoconductivity. Therefore, there is an interest to synthesize the bismuth silicate-based semiconductors, which will be able to be the photocatalysts in the process of hydrogen production under solar light irradiation. Such photocatalytic systems must possess the following requirements: firstly, they must have a high quantum yield of the photocatalytic oxidation process; secondly, high photocatalytic stability; thirdly, environmental safety and a relatively inexpensive cost.

Of course, there is an interest to study electrochemical processes that will occur both at the semiconductor – electrolyte interface and the bulk properties of the semiconductors. However, the investigation of the semiconductor – electrolyte interface is a complicated task, it is not well understood. As a result, a wide variety of chemical and physical techniques are currently in use to probe this interface. One of the best technique to determine the electrical properties of semiconductors in contact with electrolytes is electrochemical impedance spectroscopy (EIS). Impedance dispersion analysis is a valuable tool and has the potential to provide information about charge transfer phenomena, double layer charging, carrier recombination-generation at the interface and in the space charge region [2, 3].

Therefore, the study of electrochemical processes at the semiconductor – electrolyte interface, as well as the study of electrical bulk properties of the semiconductor is an important component of a comprehensive assessment of the semiconductor as a material used for the process of photocatalytic hydrogen production.

In this work, the electrochemical properties of the bismuth silicate-based semiconductors of various compositions are studied. The bismuth silicate-based semiconductors are prepared by the hydrothermal method and laser ablation method. The electrochemical properties are investigated using cyclic voltammetry and electrochemical impedance spectroscopy (EIS) using the three-electrode system. The flat band potentials ( $E_{fb}$ ) and the number of charge carriers (ND) in the bismuth silicate-based semiconductors of various compositions were determined from the Mott-Schottky equation [4].

### **References**

1. Avanesyan, V.T.; Abramova, N. M. *Phys. Solid State*, **2015**, 2112–2114.
2. McCann, J. F.; Badwal, S. P. S. *J. Electrochem. Soc.*, **1982**, 551–559.
3. Brattain, W. H.; Garret, C. G. B. *Physica XX, Ams. Conf. Sem.* **1954**, 885–892.
4. Gelderman, K.; Lee, L.; Donne, S.W. *J. Chem. Ed.*, **2007**, 685–688.

## Paramagnetic complexes of 9,10-anthraquinone on a zirconium dioxide surface

Yu.A. Fionov<sup>1</sup>, A.V. Fionov<sup>2</sup>, A.I. Pylinina<sup>1</sup>, A.N. Kharlanov<sup>2</sup>

<sup>1</sup>PFUR, Faculty of Physical, Mathematical and Natural Sciences, 117198, Mikluho-Maklaya st., 6, Moscow, Russia

<sup>2</sup>Department of chemistry, Lomonosov Moscow State University, 119899, Leninskie Gory, 1, bld.3, Moscow, Russia

fionovyurii@icloud.com

9,10-Anthraquinone is able to form paramagnetic complexes with coordinatively unsaturated cations of aluminum or gallium on a dehydroxylated surface of oxide catalysts [1]. EPR spectra of such complexes have hyperfine splitting (h.f.s.) from one or two aluminum or gallium nuclei. There are also anthraquinone's paramagnetic complexes on a surface of zirconium dioxide which EPR spectra are hard to interpret due to low (11.23%) amount of <sup>91</sup>Zr isotope [2]. Two zirconium dioxides were studied in this work: common monoclinic ZrO<sub>2</sub> and ZrO<sub>2</sub> enriched with <sup>91</sup>Zr isotope (amount is 91.1±0.5 %) (from State fund of stable isotopes IAE named after M.V. Kurchatov). We studied in detail EPR spectra of paramagnetic complexes which had been formed by the interaction of 9,10-anthraquinone and octadeutero-9,10-anthraquinone with a dehydroxylated surface of common ZrO<sub>2</sub> and ZrO<sub>2</sub> enriched with <sup>91</sup>Zr isotope (fig.1). The spectra were simulated by Easyspin program [4]. It has been shown that an EPR spectrum has a superposition of single line spectrum as well as of a spectrum with h.f.s. from one zirconium cation. The latter had 6 h.f.s. components with an anisotropic hyperfine constant and anisotropic g value. Relative amount of 6-component spectrum was proportional to the content of <sup>91</sup>Zr, which proves a supposition that the paramagnetic complex forms with zirconium cation. It has been found that a paramagnetic complex with two zirconium cations did not form. Substitution of protons in the anthraquinone by deuterium decreased the line widths of both EPR spectra. This suggests that both spectra have h.f.s. from protons of 9,10-anthraquinone.

The EPR data are consistent with results of IR-spectroscopy of adsorbed carbon monoxide. It has been shown that after carbon monoxide adsorption on the surface of both zirconia samples absorption bands were observed in the range of 2186-2192 cm<sup>-1</sup>, corresponding to complexes of carbon monoxide with Lewis acid centers. These data are consistent with literature ones [3].

As a result, the important conclusion has been made, that is: the anthraquinone form paramagnetic complex with one coordinatively unsaturated zirconium cation, which is also a Lewis acid site, on the dehydroxylated zirconium dioxide surface.

*Researches were conducted with use of experimental base of CKP "Nanochemistry and materials" of MSU as part of the Development Program of Moscow State University named after M.V. Lomonosov.*

### References

1. Fionov, A.V.; *Izv. AN. Ser. Chim.* **2009**, 3, 526.
2. Spravochnik Chimika, edited by B.P.Nicol'skiy, T.I, M.-L., Chimia, 1966.
3. Morterra, C.; Aschieri, R.; Volante, M.; *Mater. Chem. Phys.* **1988**, 20, 539.
4. Stoll, S.; Schweiger, A.; *J. Magn. Reson.* **2006**, 178, 42.

## Thermodynamic analysis of the steam/CO<sub>2</sub> reforming of methane

A.Yu. Korenyuk<sup>1</sup>, E.V. Matus<sup>2</sup>, I.Z. Ismagilov<sup>2</sup>, M.A. Kerzhentsev<sup>2</sup>, Z.R. Ismagilov<sup>2,3</sup>

<sup>1</sup>*Novosibirsk State Technical University, Novosibirsk, Russia*

<sup>2</sup>*Boriskov Institute of Catalysis, Novosibirsk, Russia*

<sup>3</sup>*Institute of Coal Chemistry and Material Science, Kemerovo, Russia*

alineks.07@mail.ru

The rapidly growing amount of CO<sub>2</sub> emissions causes a huge negative impact on the environment and leads to a number of environmental problems, such as global warming, ocean acidification, and climate change [1]. To prevent changes in natural conditions on Earth, a reduction in CO<sub>2</sub> emissions is required. At present the annual industrial use of CO<sub>2</sub> is equal to ca. 120 million tons which amount to only around 0.5% of its total anthropogenic emission (~ 24 Gt of CO<sub>2</sub>) [2]. In this connection, the expansion of the areas of CO<sub>2</sub> application as initial raw material for chemical processes is an urgent task.

One of the most studied processes of CO<sub>2</sub> transformation to value-added products is the process of methane reforming by CO<sub>2</sub>. This process allows utilization of two greenhouse gases (CO<sub>2</sub>, CH<sub>4</sub>) and produces the synthesis gas (a mixture of CO and H<sub>2</sub>) that serves as initial raw material for the production of synthetic liquid fuels (product of Fischer-Tropsch synthesis) and basic chemical products (hydrogen, methanol, and ammonia) [3]. In this work, as an alternative, the steam/CO<sub>2</sub> reforming of methane is considered, which allows flexible regulation of the H<sub>2</sub>/CO ratio in the syngas by variation of the composition of the initial mixture CH<sub>4</sub>/CO<sub>2</sub>/H<sub>2</sub>O. To predict the optimal reaction conditions and find the ways for coke elimination the thermodynamic equilibrium analysis of steam/CO<sub>2</sub> reforming of methane was studied by Gibbs free minimization method.

The process of steam/CO<sub>2</sub> reforming of methane includes reactions of steam and carbon dioxide reforming, leading to the desired product – synthesis gas, a number of additional reactions that increase the yield of hydrogen, as well as side reactions of the formation of carbon deposits. The effects of CO<sub>2</sub>/H<sub>2</sub>O ratio (0.5-2), reaction temperature (500–1000°C) and pressure (1–5 atm) on equilibrium conversions, product compositions, and coke content were established. With an increase in the reaction temperature from 500 to 800°C, the conversions of the reagents increase, and with a further increase in temperature they reach a plateau. Similar temperature dependence is observed for the yield of hydrogen and CO. The amount of carbon deposits decreases with increasing temperature. The increase in pressure negatively affects the conversion of the reagents, while the yield of carbon deposits increases. Varying the molar ratio of CO<sub>2</sub>/H<sub>2</sub>O affects the process parameters, mainly in the low-temperature region. With an increase in CO<sub>2</sub>/H<sub>2</sub>O from 0.5 to 2, an increase in the conversion of methane and carbon dioxide is observed, while the conversion of water, on the contrary, decreases. There is also a decrease in the H<sub>2</sub>/CO ratio and an increase in the amount of carbon deposits. Moreover, regardless of the CO<sub>2</sub>/H<sub>2</sub>O values, the residual content of CH<sub>4</sub> + CO<sub>2</sub> is less than 2% at 850°C.

The yield of carbon deposits depends on the type of oxidizing agent. In the case of water, unlike carbon dioxide, the amount of carbon deposits is lower. However, regardless of the type of oxidizing agent, it is impossible to avoid the formation of carbon deposits in the low temperature reaction region, even in the presence of an excess of the oxidizing agent. In the high-temperature region, control over the rate of coke formation is achieved through optimization of the ratio (CO<sub>2</sub> + H<sub>2</sub>O)/CH<sub>4</sub>. For a mixture with CO<sub>2</sub>/H<sub>2</sub>O = 2, the value (CO<sub>2</sub> + H<sub>2</sub>O)/CH<sub>4</sub> = 1.2-1.4 ensures a high conversion of reagents and a yield of products, as well as the absence, according to a thermodynamic calculation, of carbon deposits.

*The reported study was funded by RFBR and NSFC according to the research project №20-53-53018.*

### References

1. Liu, D.; Guo, X.; Xiao, B. *Sci. Total. Environ.* **2019**, 661, 750–766.
2. Aresta, M.; Dibenedetto, A.; Angelini A. *Chem. Rev.* **2014**, 114, 1709–1742.
3. Ismagilov, Z.R.; Matus, E.V.; Tsikoza, L.T. *Energy Environ. Sci.* **2008**, 1, 526–541.

## Quantum-chemical analysis of the effect of water molecules on the kinetics of 2-methylimidazole formation

A.V. Kotov<sup>1</sup>, A.V. Fateev<sup>1,2</sup>, V.P. Tuguldurova<sup>1</sup>

<sup>1</sup>*Tomsk State University, Tomsk, Russia*

<sup>2</sup>*Tomsk State Pedagogical University, Tomsk, Russia*

asdfec01@yandex.ru

Imidazole and its derivatives are used in production of drugs, agricultural chemicals and powder paints [1,2]. 2-methylimidazole can be obtained by the interaction of acetaldehyde, glyoxal and ammonia in an aqueous solution [3]. The reaction does not require a catalyst, and the reagents and solvent are widely available. Currently, the mechanism of this reaction has been insufficiently studied. In the literature there are no data about the effect of water molecules on the reaction pathways. The study of the reaction mechanism of the formation of 2-methylimidazole by experimental methods is complicated, however, quantum-chemical methods can provide the required information.

A calculation scheme that adequately describes the experimental data was proposed. The structures of all initial and intermediate substances as well as reaction products were optimized. Transition states (TS) for all stages of the reaction of acetaldehyde, glyoxal and ammonia without water molecules and with the participation of one and two water molecules were found. Geometry optimization of all the structures was carried out using the Gaussian'16 program package installed at the ANNEMARIE – Cluster of the Philipps-Universität Marburg. Calculation with the B3LYP-D3/6-311G(d,p) level of theory was used. The geometries of the stable conformers for each molecular structure and transitional states were optimized in the solution by using the PCM model [4].

All stages of the interaction of acetaldehyde, glyoxal, and ammonia were divided by types: nucleophilic addition ( $\Delta G^\ddagger \sim 33.7$  kcal / mol,  $\Delta H^\ddagger \sim 22.2$  kcal / mol), dehydration of aminoalcohols ( $\Delta G^\ddagger \sim 45.2$  kcal / mol,  $\Delta H^\ddagger \sim 45.9$  kcal / mol), hydrogen transfer ( $\Delta G^\ddagger = 29.4$  kcal / mol,  $\Delta H^\ddagger = 29.4$  kcal / mol). The investigation showed that the enthalpy of activation decreased by 25–30 kcal / mol and the Gibbs activation energy decreased by 20–25 kcal / mol when one water molecule was included into the TS structure. When two water molecules were included into the TS structures, the enthalpy of activation and the Gibbs energy of activation decreased by 35–40 kcal / mol and 30–35 kcal / mol, respectively. The barriers had decreased when the number of water molecules in the structure of transition states increased. It occurred due to the formation of stable six- and eight-center cycles providing proton transfer.

The most probable reaction pathway was determined. The highest barriers ( $\Delta G^\ddagger = 23.4$  kcal / mol,  $\Delta H^\ddagger = 22.0$  kcal / mol) were observed for the cyclization stage. This was the rate-limiting stage. Cyclization proceeded according to the SN2 type. In this step, the increase of the number of water molecules from one to two led to an increase in the Gibbs activation energy and the enthalpy of activation.

### References

1. Kumari, S.; Pramod, K.S.; Nitin, K. *Der Chemica sinica* **2010**, 1(3), 36–47.
2. Olivier-Bourbigou, H.; Magna, L.; Morvan, D. *Appl. Catal. A: General*. **2010**, 373, 1–56.
3. Malkov, V. S.; Knjazev, A. S.; Kotelnikov, O. A.; Odnokopylova, M. V. RF patent No. 2486176. Claim. 17.11.2011. Publ. 27.06.2013.
4. Tuguldurova, V. P. et al. *Phys. Chem. Chem. Phys.* **2019**, 21(18), 9326–9334.

## XPS study of Rh-CeO<sub>2</sub> catalysts under CO+NO treatments

A.I. Krotova<sup>1,2</sup>, L.S. Kibis<sup>1,2</sup>, D.A. Svintsitskiy<sup>1,2</sup>, E.A. Fedorova<sup>1</sup>, E.M. Slavinskaya<sup>1,2</sup>, O.A. Stonkus<sup>1,2</sup>, A.I. Boronin<sup>1,2</sup>

<sup>1</sup>*Boriskov Institute of Catalysis, Novosibirsk, Russia*

<sup>2</sup>*Novosibirsk State University, Novosibirsk, Russia*

krotova@catalysis.ru

Reducing nitrogen oxides emissions into the atmosphere is still an urgent task. Rhodium supported on ceria is used as catalyst for many processes, including NO<sub>x</sub> reduction reactions. Despite the large number of studies on this topic, further research of the activity of catalytic systems based on Rh-CeO<sub>2</sub> in the NO reduction reaction is necessary.

Previously, it was shown that the oxidized Rh species finely dispersed in CeO<sub>2</sub> exhibit high catalytic activity in the oxidation of CO even at room temperature. Also, the reductive treatment improves catalytic activity in the low-temperature range [1]. To study further the properties of highly dispersed reduced and oxidized Rh species we performed the analysis of Rh-CeO<sub>2</sub> catalysts behavior in NO reduction reaction. The charge states of the elements on the surface of the samples after treatment in CO+NO reaction mixture were studied using X-ray photoelectron spectroscopy (XPS).

Rh-CeO<sub>2</sub> catalysts were synthesized from rhodium and cerium nitrates (Rh(NO<sub>3</sub>)<sub>3</sub>, Ce(NO<sub>3</sub>)<sub>3</sub>) by coprecipitation with a 1M aqueous KOH solution at pH = 9.0 and room temperature, followed by aging and calcination at 450°C for 4 hours. The rhodium content in these samples was 8 wt.%. The X-ray photoelectron spectra of the samples after their treatment in a CO+NO gas mixture were collected on a VG Escalab HP photoelectron spectrometer. The gas treatments were carried out with a step by step heating of a sample in the temperature range  $T = 25-450^{\circ}\text{C}$  at  $p(\text{CO}) = p(\text{NO}) = 500 \text{ Pa}$ . To obtain a reduced sample, the initial Rh-CeO<sub>2</sub> sample was heated in 500 Pa CO at 300°C for 2 hours.

An analysis of the obtained Rh3d spectra showed no changes in the charge state of rhodium after interaction of the initial Rh-CeO<sub>2</sub> sample with the CO+NO reaction mixture up to  $T = 125^{\circ}\text{C}$ . The main rhodium state was Rh<sup>3+</sup>. Treatment at higher temperatures led to the appearance of a reduced state of rhodium - Rh<sup>δ+</sup>. A further increase in temperature resulted in reoxidation of the rhodium surface with the formation of Rh<sup>3+</sup> ions. After CO+NO treatment of the sample at 450°C, the state of the elements on the surface was close to that observed in the initial sample. An analysis of the Ce3d spectra did not show significant changes during the sample treatment in the CO + NO reaction mixture.

The preliminary treatment of the initial Rh-CeO<sub>2</sub> sample with CO resulted in the formation of dispersed Rh<sup>δ+</sup> species on the reduced CeO<sub>2</sub> surface (The impact of the Ce<sup>3+</sup> species to the overall Ce3d spectra was about 20%). Interaction of such reduced system with the CO+NO reaction mixture led to a partial reoxidation of the rhodium surface at temperatures below 125 °C. However, when the sample was heated above 125°C, the appearance of the reduced species of rhodium Rh<sup>δ+</sup> was detected again. With a further increase of the temperature above 250°C a gradual reoxidation of the reduced rhodium species was observed similar to the results obtained for the initial Rh<sup>3+</sup>-CeO<sub>2</sub> sample. An analysis of the Ce3d spectra showed reoxidation of Ce<sup>3+</sup> ions already at room temperature without further changes in the charge state of cerium. The impact of the Ce<sup>3+</sup> species to the overall Ce3d spectra was about 10%.

Thus, comparing the data on the interaction of the Rh-CeO<sub>2</sub> samples with the CO+NO reaction mixture, we can conclude that regardless of the preliminary treatment of the samples their exposure to the CO+NO mixture at the temperature range 125°C-250°C leads to the formation of a reduced state of rhodium (Rh<sup>δ+</sup>). Comparison of the XPS results with the catalytic data of the systems in NO reduction reaction points to the substantial role of the reduced Rh form in the activity of the catalysts.

*This work was partially supported by RFBR and the government of the Novosibirsk region Grant #18-43-543009.*

### References

1. Kibis, L. S.; Svintsitskiy, D. A.; Derevyannikova, E. A.; Kardash, T. Yu.; Slavinskaya, E. M.; Stonkus, O. A.; Svetlichnyi, V. A.; Boronin, A. I. *Applied Surface Science*. **2019**, 493, 1055–1066.

## Prediction of the catalytic activity of metals by adsorption data in reactions with hydrogen-containing gases

D.A. Prozorov, A.V. Afineevskii, D.V. Smirnov, K.A. Nikitin, T.Yu. Osadchaya

*Federal State Educational Institution of Higher Education «Ivanovo State University of Chemistry and Technology», Ivanovo, Russian Federation*

prozorovda@mail.ru

The main goal of catalysis science is the prediction of catalytic action. Reactions with hydrogen-containing gases are of great practical importance and are the most common industrial technologies for the production of fuel, mineral fertilizers, alcohols, salomas, and products of fine organic synthesis. The current selection and development of new catalysts based on metals and their oxides is the "trial and error" method, which consists selecting the optimal compounds and activity of metals, oxides and their alloys. However, it is known that the activity of the catalyst is directly related to its adsorption ability with respect to reacting substances. The search for correlation of adsorption vs catalytic properties is a traditional approach to the fundamental study of the mechanism of the catalyst action.

In this paper, approaches are proposed for predicting the activity of catalysts based on transition metals, for a reaction with hydrogen-containing gases, in liquid-phase and gas-phase processes based on the control of adsorption properties with respect to hydrogen. The idea of the proposed approach is to control the adsorption equilibria between individual adsorption forms of hydrogen, which have different energy bonds with active groups.

The theoretical foundations of the proposed ideas and their experimental confirmation are described in [1-3]. An indicator of the possibility of determining the constant characteristic features of hydrogen adsorbed on nickel in hydrogenation reactions is demonstrated. It is assumed that the proposed approaches will make it possible to predict the activity of catalytic systems in such processes as hydrotreating light oil products, methanation, methanol synthesis, the Fischer-Tropsch process. At the same time, the catalyst will exhibit distinguishable activity. Knowing the maximum values of hydrogen adsorption, as well as its distribution in individual forms, it is possible to recommend a synthesized catalyst for use in a particular process with the participation of hydrogen, as well as to predict its activity, without performing kinetic experiments.

Measuring the degree of adsorption of hydrogen individual forms is possible by using adsorption calorimetry, as well as a complex of synchronous thermal analysis and mass spectrometry [4]. For the hydrogenation, it was shown that depending on the conditions of the hydrogen presence and adsorption equilibrium. The determination of the quantity of adsorbed hydrogen by the adsorption-calorimetric method, according to the method itself, has a measurement error equal to the adsorption on the catalyst surface of the titrant introduced to remove hydrogen from the catalyst surface, in turn, the endothermic effect of adsorption of titrant on the catalyst surface does not allow to clearly fix the end of the adsorption calorimetric experiment. In addition, the determination of the hydrogen adsorption values in water by chemical dehydration is associated with difficulties in selecting a titrant and controlling the pH of the medium, on which the adsorption capacity of the catalyst largely depends. Thus, the total quantity of hydrogen in the catalytic system, measured using the method of thermal analysis and mass spectrometry more accurately reflects the state of the system, but differs significantly from the literature.

*Theme number FZZW-2020-0010. Theoretical part of the Scientific Council of the RAS on Physical Chemistry for 2020, agreed with the work plan (No. 20-03-460-28).*

### References

1. Lukin, M. V.; Prozorov, D. A.; Ulitin, M. V.; Vdovin, Yu. A. *Kinet. Catal.* 2013, 54, 412.
2. Prozorov, D. A.; Lukin, M.V. *Vestn. Tver. Gos. Univ. Ser. Khim.* 2013, 15, 168.
3. Afineevskii, A.V.; Prozorov, D.A.; Smirnov, N.N. *Izv. Vyssh. Uchebn. Zaved. Khim. Khim. Tekhnol.*, **2015**, 58 (2), 83.
4. Prozorova, D. A.; Afineevskii, A. V.; Smirnova, N. N.; Sukhacheva, Y. P.; Chelysheva, M. D. *Rus. J. Gen. Chem.* **2019**, 89 (6), 1332–1337.

## Catalytic properties of CuO<sub>x</sub> NPs obtained by pulsed laser ablation

O.A. Reutova, D.A. Goncharova, T.S. Kharlamova, O.V. Vodyankina, V.A. Svetlichnyi

*Tomsk State University, Tomsk, Russia*

reutovaolesya@mail.ru

Over the past decade, copper and copper oxide nanoparticles (CuO<sub>x</sub> NPs) have received much attention because of fundamental importance and wide potential applications in electronics, semiconductor industry, solar energy conversion, biomedicine, gas sensors, environmental science and catalysis [1]. Copper compounds are widely used as catalysts in a number of important chemical reactions such as NO<sub>x</sub> degradation, CO oxidation, reduction of nitroaromatics, etc. [2].

The size and morphology of NPs play a significant role in developing of the chemical and physical properties and largely influence their existing applications [1, 2]. Therefore, much efforts have been dedicated to the preparation of CuO<sub>x</sub> nanostructures with different sizes and morphologies. Pulsed laser ablation (PLA) in liquid was shown to be a promising method to prepare stable dispersion of CuO<sub>x</sub> NPs with various phase composition (Cu, Cu<sub>2</sub>O, Cu@Cu<sub>2</sub>O, CuO), sizes and morphology [3].

In the present work the catalytic properties of CuO<sub>x</sub> NPs prepared by PLA of copper in different liquids were studied in reduction of aromatic nitro compounds to aromatic amino compounds in water solutions in the presence of NaBH<sub>4</sub>.

CuO<sub>x</sub> NPs dispersions (100–200 mg/l) were prepared by the PLA of copper in distilled water, ethanol, isopropanol, and aqueous solution of hydrogen peroxide (0.1 wt%) according to the technique described in Ref. [1]. The prepared samples were characterized by XRD, UV–vis absorption spectroscopy, and TEM. The catalytic properties of the CuO<sub>x</sub> NPs obtained in reduction of p-nitrophenol (PNP) were studied using aqueous solutions of PNP and NaBH<sub>4</sub> at 19 °C. Typically, 1.7 ml of distilled water, 300 µl of the PNP aqueous solution, 300 µl of freshly prepared NaBH<sub>4</sub> aqueous solution and 200 µl of freshly prepared CuO<sub>x</sub> NPs dispersion were used to prepare 2.5 ml of reaction mixture with the concentrations of  $2.57 \times 10^{-4}$  mol/l,  $5 \times 10^{-2}$  mol/l and 15 mg/l, respectively. The reaction was performed inside a quartz cuvette and the reduction processes were monitored online by following the optical absorption peak of PNP at 400 nm with 10 s intervals using CM 2203 spectrophotometer equipped with a magnetic stirrer and a cuvette thermostabilizer.

PLA of copper in distilled water was shown to yield cubic Cu<sub>2</sub>O NPs, while the primary formation of the sheet-like and flower-like CuO was observed in the aqueous solution of H<sub>2</sub>O<sub>2</sub>. Using ethanol as the liquids for PLA of copper yields rather stable suspension of Cu NPs with a sub-monolayer of Cu<sub>2</sub>O. All samples obtained showed catalytic activity towards selective PNP reduction to p-aminophenol (PAP), with some peculiarities depending on liquid used to prepare the CuO<sub>x</sub> NPs dispersions. For all samples studied the induction period was observed that is usually attributed to the diffusion time required for PNP to be adsorbed onto the catalyst surface or to the time needed for NaBH<sub>4</sub> to eliminate surface oxides. The samples obtained in water and H<sub>2</sub>O<sub>2</sub> aqueous solution are characterized by high catalytic activity and relatively short induction period, while the using of CuO<sub>x</sub> NPs dispersions obtained in ethanol leads to lower activity and longer induction period. The study of the effect of alcohol adsorption and CuO<sub>x</sub> NPs reduction by NaBH<sub>4</sub> indicated that the catalytic activity of all samples was primarily determined by the formation of Cu NPs, while the presence of alcohol in the reaction mixture affected the catalytic activity via competitive sorption with PNP on the catalyst surface.

The present research describes a facile “green” synthesis of CuO<sub>x</sub> NPs serving as catalysts for selective reduction of aromatic nitro compounds to aromatic amino compounds in aqueous solution in the presence of NaBH<sub>4</sub> that is promising for industrial application.

*This work was supported by the Tomsk State University competitiveness improvement programmer.*

### References

1. Gupta, D.; Meher, S.R.; Illyaskutty, N.; and Alex, Z.C. *J. Alloys Compd.* **2018**, 743, 737–745.
2. Che, W.; Ni, Y.; Zhang, Y.; Ma, Y; *J. Phys. Chem. Solids* **2015**, 77, 1–7.
3. Goncharova, D.A.; Kharlamova, T.S.; Lapin, I.N.; Svetlichnyi, V.A. *J. Phys. Chem. C* **2019**, 123, 21731–21742.

## Physicochemical properties of gadolinium oxysulfide ( $\text{Gd}_2\text{O}_2\text{S:Tb}$ )

A.V. Rodionova<sup>1</sup>, P.Sh. Ustabaev<sup>2</sup>, T.S. Minakova<sup>1</sup>, V.V. Bakhmetyev<sup>2</sup>

<sup>1</sup>*Tomsk State University, Tomsk, Russia*

<sup>2</sup>*Saint-Petersburg State Institute of Technology, Technical University, St. Petersburg, Russia*

ranutavd@yandex.ru

It was shown in [1] that titanium dioxide modified with  $\text{Gd}_2\text{O}_2\text{S:Tb}$  film has more pronounced photocatalytic properties in the photodegradation reaction of formaldehyde. Gadolinium oxysulfide activated with terbium ( $\text{Gd}_2\text{O}_2\text{S:Tb}$ ) is known to be one of the most effective X-ray phosphors. The efficiency of phosphors depends on the defective situation in crystals, content of impurity surface phases, concentration and ratio of electron and hole traps, degree of activator ions segregation in the volume and on the surface of phosphor particles. Depending on the synthesis technique and activator content, the surface and luminescent properties of the phosphors will change.

The objects of this study were  $\text{Gd}_2\text{O}_2\text{S:Tb}$  samples obtained at Saint-Petersburg State Institute of Technology in a reducing atmosphere. The composition of the blends included  $\text{Gd}_2\text{O}_3$ ,  $\text{Tb}_4\text{O}_7$ , S,  $\text{Na}_2\text{CO}_3$ , LiF. The activator content ranged from 0.5 to 10 wt.%. Samples were identified using an X-ray diffractometer Rigaku SmartLab 3 (Rigaku Corporation, Japan).

The obtained phosphor samples were non-porous, with very small specific surface, since they were synthesized at high temperatures (more than 1000 °C).

The surface morphology of synthesized phosphors was studied by scanning electron microscopy (SEM) using a Hitachi TM 3000 electron microscope. For samples, synthesized with a high content of terbium, the particle sizes were relatively large. The addition of sodium pyrophosphate to the blend promoted particle growth in the synthesis process.

The study of acid-base phosphors properties was carried out by pH-metry. The pH-meter / ITAN ionomer was used in order to record the pH values of the aqueous suspension of phosphor powders and their change in time [2]. Samples synthesized with low activator content (up to 2% Tb) are characterized by the presence of minimum on the pH kinetic curves during first minutes of studying (pH = 6.0-6.2), which may indicate the presence of Lewis acid sites on the surface of these samples. With further experimentation, an increase in pH value to a constant value of ~ 6.5 was observed, which confirms the presence of acidic and basic Bronsted sites on the phosphor surface. At short interaction times (360 s.) a positive correlation between the average particle size of the phosphors and pH of the suspension is observed. Probably, at the initial moment of the phosphors interaction with water, the pH of the suspension is due to the dispersion of the samples, and not to their composition.

Photoluminescent (PL) performances of the synthesized phosphors were characterized using an SM-2203 spectrofluorimeter (SOLAR, Belarus). The observed luminescent bands correspond to the energy levels of trivalent terbium [3]. The increase in activator content up to 2 wt% leads to the increase in photoluminescent intensity. Further increase in Tb content leads to the decrease in photoluminescence intensity.

Studies have shown that in order to prepare more efficient titanium oxide catalyst with a deposited  $\text{Gd}_2\text{O}_2\text{S:Tb}$  film, it is necessary to control the physicochemical properties of the deposited coating surface, which are depended on the synthesis technique and activator concentration.

### References

1. Kim, B. G. Bull. Korean Chem. Soc. **2009**, 30 (3), 675
2. Syrov, M.M.; Minakova, T.S.; Slizhov, Y.G.; Shilova, O.A. Acid-Base Properties of Solids and Control over the Properties of Materials and Composites); Khimizdat Publishers: St. Petersburg, Russia, 2016
3. Silva, A. A.; Cebim, M. A.; Davolos, M. R. *J Lumin.* **2008**, 128, 1165–8.



## Investigation of catalysts of various compositions of Pd-Bi/Al<sub>2</sub>O<sub>3</sub> in the reaction of glucose oxidation into gluconic acid

M.P. Sandu, I.A. Kurzina

*National Research Tomsk State University, Tomsk, Russia*

mpsandu94@gmail.com

Gluconic acid and its derivatives are widely used in various industries (pharmaceutical, food, chemical, pulp and paper, textile, printing) [1-4]. Currently, gluconic acid and its salts are obtained by microbiological processing of sugars in the presence of microorganisms capable of secreting the glucose oxidase enzyme [5, 6]. However, this method has several disadvantages associated with the complexity of the separation of the desired product and enzymes, the low rate of formation of the desired product, the inability to reuse enzymes, problems with waste disposal [7]. An alternative method of producing gluconic acid, which eliminates these disadvantages, is aerobic oxidation of glucose in the presence of solid-phase mono- and bimetallic catalysts supported on carriers stable in an aqueous medium.

Prepared 4 samples of catalysts with atomic ratios Bi : Pd = 0.3; 1.0; 1.2; 1.8. Using high-resolution transmission electron microscopy (HRTEM), it was found that the size of the nanoparticles of the catalyst Bi : Pd = 0.3 is 2–8 nm. A 6-fold increase in the atomic fraction of bismuth towards to palladium in Pd-Bi/Al<sub>2</sub>O<sub>3</sub> catalysts leads to the formation of large particles with a size > 50 nm. The catalysts were tested in the reaction of glucose oxidation into gluconic acid with a molar ratio of «glucose: Pd» = 10 000 : 1 for 150 minutes. Catalytic investigations showed that the highest conversion values ( $X = 37.3\%$ ) were achieved in the presence of a catalyst Bi : Pd = 0.3. Despite the high selectivity for gluconic acid (97-99% for all catalysts), there is a decrease in glucose conversion from 37.3% to 13.7% with an increase in the atomic ratio of Bi : Pd from 0.3 to 1.8.

*This work was supported by competitiveness improvement program of The National Research Tomsk State University (grant no. 8.2.10.2018).*

### References

1. Anastassiadis, S.; Morgunov, I.G. *Recent Pat. Biotechnol.* **2007**, *1*, 167–180.
2. Singh, O.V.; Kumar, R. *Appl. Microbiol. Biotechnol.* **2007**, *75*, 713–722.
3. Rogers, P.; Chen, J.S.; Zidwick, M.J. Organic acids and solvent production, Part I: Acetic, lactic, gluconic succinic and polyhydroxyalkanoic acids. In *The Prokaryotes*, 3rd ed.; Springer: New York, 2006; Volume 1, pp. 511–755.
4. Liu, J.-Z.; Weng, L.-P.; Zhang, Q.-L.; Xu, H.; Ji, L.-N. *Biochem. Eng. J.* **2003**, *14*, 137–141.
5. Saleh, D.K.; Abdollahi, H.; Noaparast, M.; Nosratabad, A.F.; Tuovinen, O.H. *Hydrometallurgy* **2019**, *186*, 235–243.
6. Zhang, H.; Liu, G.; Zhang, J.; Bao, J. *Bioresour. Technol.* **2016**, *219*, 123–131.
7. Witońska, I.; Frajtak, M.; Karski, S. *Appl. Catal. A Gen.* **2011**, *401*, 73–82.

## **The catalytic effect of the surface in the formation of hydrogen bonded systems.**

### **IR spectroscopy and DFT**

I.A. Spirin, R.V. Kapustin, I.I. Grinvald, A.N. Petukhov

*Institute of Physical Chemistry and Material Science of Nizhny Novgorod State Technical University n.a.  
R.E. Alekseev, Nizhny Novgorod, Russia*

ivan.sn.92@mail.ru

Transformations in various systems near the solid-phase surface and in the solid films are of considerable interest. Catalytic features of solid surface are determined by the existence of energy sites with increased activity associated with unsaturated valence. It applies primarily to the mechanisms of catalytic processes of polymerization, processing of natural and synthetic organic components. Different intermolecular interactions in thin layers on the surface of various materials significantly affects the mechanism of coating application. Hydrogen bonding and proton transport with the formation of water intermediates in binary systems play a key role in the mechanisms of such processes. However, the role of water in these processes is unclear and often unpredictable. The water molecule connects with partner under hydrogen bond, participates wherein or as an agent, having electron pair on the oxygen atom either the proton donor.

In this work various methods of synthesis of hydrogen bonded water complexes with inorganic and organic compounds in the solid phase using the results of IR spectral measurements have been identified. We have studied the water complexes formation of organic amino boranes, triazoles and inorganic salts of alkali metals by IR spectroscopy in the solid films on the optical window (ZnSe) at ambient conditions. The studied samples were solved in acetone. Then, water was added to these solutions in certain ratio to organic components. The liquid layer of the solution was deposited on the ZnSe optical window and after drying on air the solid films were obtained. The full evaporation of acetone from the films was controlled by disappearance of acetone IR band in the region  $1800\text{--}1700\text{ cm}^{-1}$ . After this procedure the sample was situated in an IR device for spectral measurements.

In addition, the method of sample preparation for intermolecular hydrogen atom transfer investigation in benzene and ionic liquids in KBr matrix was used. Briefly, KBr powder, saturated by water vapour in a closed reactor, is mixed in a different ratio with a liquid sample. The ratio of components is chosen in such a way that the obtained sample has minimal background and noise of the absorption in IR spectra. After this procedure the KBr powder was pressed and the obtained pallet was situated in FTIR spectrometer.

The catalytic effect of the surface and material of crystalline substances on proton transfer reactions was established. In the framework of spectral experiments and quantum chemical calculations it was found that complexation with water has several competing mechanisms involving one or more water molecules and is accompanied by the transfer of a hydrogen atom to a substrate molecule. It was shown that for most salts, the hydrogen atom is transferred between water molecules in the complex. The formation of a hydronium cation thus stabilizes the formation of intermediates. It was shown that in binary systems including benzene, furan, and thiophene, water intermediates are formed due to the intermolecular  $\sigma$ - and  $\pi$ -hydrogen bonds in which the hydrogen atom of water is transferred to an organic substrate. It was found that in binary systems of 1,2,4-triazole water intermediates are formed due to the hydrogen bond with the participation of mobile hydrogen of triazole. Such complexes can also be considered as charge transfer systems. In the case of aminoboranes the formation of complexes with water arise not only due to the hydrogen but also dihydrogen bonds between water molecules and aminoborane's NH functional group.

Quantum chemical calculations were carried out in terms of DFT theory in 6-311++G(2d,2p) basis set and B3LYP functionalization by GAUSSIAN 09 program package.

## **Transfer hydrogenation of levulinic acid and its esters to $\gamma$ -valerolactone over Zr-SBA-15 catalyst**

V.V. Sychev, A.O. Eremina, O.P. Taran

*Institute of Chemistry and Chemical Technology SB RAS, FRC KSC SB RAS, Krasnoyarsk, Russia*

sychovmail@gmail.com

Currently, the chemical and energy industries rely heavily on the use of fossil resources, which results in fossil resources diminishing and severe greenhouse emission. Biomass is appearing to be one of the most promising feedstock for production of valuable chemicals. GVL attracts more and more attention as a building block for polymers, fuel additive, intermediate in fine chemicals and fuels production and as a green solvent due to its renewable and non-hazardous nature and high-boiling-point [1].

GVL usually obtained through direct hydrogenation (the use of molecular  $H_2$ ) or catalytic transfer hydrogenation (CTH) (when solvent acts as a hydrogen source) of levulinic acid (LA) and levulinic acid esters (LAE) [2].

Direct hydrogenation of LA and LAE comes with serious drawbacks, such as high hydrogen pressure required and the use of precious metals based catalysts. Cheaper alternatives such as Cu and Ni based catalyst usually undergo leaching and sintering in the course of reaction [2].

Catalytic transfer hydrogenation contrastingly requires neither a high hydrogen pressure, nor the necessarily use of precious metal based catalysts, which has a positive impact on the process economy [2].

Both cellulose and hemicelluloses can be used as a feedstock in GVL production, which makes the economics more attractive and promises a wider application.

This work aims at solid catalysts development for the processes of LA and LAE to GVL catalytic transfer hydrogenation based on mesoporous silica SBA-15 bearing Zr nanoparticles.

Series of Zr-SBA-15 catalyst prepared using zirconium (IV) propoxide solution as a precursor by two methods (layerwise deposition, co-precipitation [3,4]). Zr-SBA-15 catalysts were characterized by  $N_2$  adsorption, XRF, XRD, TEM, FTIR, DRIFT UV-vis,  $pH_{pzc}$ .

It was confirmed by XRD, that mesoporous structure SBA-15 is remained after Zr deposition.

It was found by XRF, that higher amounts of Zr are deposited on the SBA-15 surface using layerwise deposition method in comparison to co-precipitation method with highest Zr loading being 4.6 and 1.2 wt. % correspondingly. Main pore volume is attributed to 4-6 nm range, which allows transfer of reactants from the solution to catalytic active sites and product backwards.

Catalytic transfer hydrogenation of LA and LAE was carried out in autoclave, at autogenic pressure in temperature range (130-190°C), with different substrate and catalyst loadings, for 3-6 hours using isopropanol as a hydrogen source.

The products of reaction were analyzed using HPLC, equipped with polymer DIASPHERE-250 dp 5 $\mu$ m, 2.5\*75 mm column and  $H_2O$ +(85% 0.075M  $LiClO_4$ , 15% ACN) eluent.

Catalytic tests show that catalyst prepared by layerwise deposition method exhibit the highest catalytic activity, stability and can provide GVL yields as high as 80% after 90 min at 190°C using isopropanol as a hydrogen source.

*This work was supported by RFBR Grant 20-03-00636.*

### **References**

1. Alonso, D.M., Wettstein S.G., Dumesic, J.A. Green Chem. 15 (2013) 584.
2. Osatiashtiani, A., Lee A.F., Wilson, K. J Chemical Technology & Biotechnol. 92 (2017) 1125.
3. Iglesias J., Melero J. A., Morales G., Paniagua M., Hernández B., Osatiashtiani A., Lee A. F. Wilson K. Catalysis Sci Tech. 17 (2018) 4485.
4. Cecilia J. A., García-Sancho C., Mérida-Robles J. M., Santamaría-González J., Moreno-Tost R. Maireles-Torres P. Catalysis Today. 254 (2015) 43.

## SECTION 4

### INDUSTRIAL IMPLEMENTATION OF CATALYTIC PROCESSES



## Integrated catalytic purification of waste gases in nitric acid plants from nitrogen oxides ( $\text{NO}_x$ and $\text{N}_2\text{O}$ )

A.G. Sheboltasov<sup>1,2</sup>, N.V. Vernikovskaya<sup>1,2</sup>, V.A. Chumachenko<sup>1</sup>

<sup>1</sup>*Boriskov Institute of Catalysis, Novosibirsk, Russia*

<sup>2</sup>*Novosibirsk State Technical University, Novosibirsk, Russia*

vachum@catalysis.ru

Nitric acid plants are among the main sources of nitrogen oxides ( $\text{NO}_x$  and  $\text{N}_2\text{O}$ ) emission into the atmosphere.

Nitrogen oxides  $\text{NO}_x$  are highly toxic chemicals. Also,  $\text{NO}_x$  cause photochemical smog, acid rainfalls, form tropospheric ozone layer, and reduce the amount of stratospheric ozone. The content of  $\text{NO}_x$  in the industrial effluents is strictly regulated.

The atmospheric  $\text{N}_2\text{O}$  content is not limited, however the 1997 Kyoto Protocol qualifies hemioxide (nitrous oxide) as a dangerous greenhouse gas with a  $\text{CO}_2$  equivalent of 310, which causes the destruction of the ozone layer.

In the Russian Federation, all industrial nitric acid plants which operate at a single pressure 0.716 MPa are equipped with low-temperature catalytic purification of waste gases from  $\text{NO}_x$  using the selective catalytic reduction (SCR) of nitrogen oxides by  $\text{NH}_3$  over vanadium catalyst. Due to the high content of nitrous oxide in the tail gases, it is necessary to provide purification from  $\text{N}_2\text{O}$  as well. To solve this problem, a comprehensive approach was proposed in [1]. It assumes two-stage catalytic purification of  $\text{NO}$  and  $\text{NO}_2$  by SCR with ammonia, followed by  $\text{N}_2\text{O}$  decomposition. The dimensions and design of the existing reactor for catalytic purification of waste gases make it possible to displace a catalyst bed for SCR of  $\text{NO}_x$ , and a catalyst bed for  $\text{N}_2\text{O}$  decomposition; both catalysts operate in a close temperature range. An industrial vanadia-alumina catalyst for SCR process is used in the 1<sup>st</sup> catalyst bed at temperature range of 220–240 °C. Then the gas enters the 2<sup>nd</sup> bed, where the Ni-Co catalyst for the decomposition of nitrous oxide is located [1].

This work is devoted to mathematical modeling of the integrated catalytic purification of tail gases in two consecutive adiabatic catalyst beds; the reactor sizes, flow rate and composition of the tail gas were close to the industrial conditions. The two-phase mathematical model of the processes in each catalyst bed takes into account the convective heat- and mass transfer in the gas phase, axial dispersion and thermal conductivity in the gas phase, heat and mass exchange between the gas and solid phases, axial heat transfer by thermal conductivity in the solid phase, catalytic reactions of SCR of nitrogen oxides by  $\text{NH}_3$  on V/Al catalyst and decomposition of nitrous oxide on a Co-containing catalyst, heat generation as a result of an exothermic reaction in the solid phase.

The observed rate of SCR of  $\text{NO}_x$  on V/Al catalyst is of the first order for  $\text{NO}_x$ . Kinetic parameters were taken from [2]. The rate of decomposition of nitrous oxide on a Co-containing catalyst is of the first order for  $\text{N}_2\text{O}$ . Kinetic constants for 0.25–0.50 mm particles were taken from [1]. To obtain the observed rate of  $\text{N}_2\text{O}$  decomposition, the effectiveness factor for industrial catalyst grains was calculated.

The mathematical modeling was carried out by varying the volumetric flow rate, temperature and composition of the tail gases entering the reactor, the size and shape of the catalyst. The required degree of purification was no less than 98% for nitrous oxide, and no less than 97% for nitrogen oxides. The catalysts' loadings sufficient to achieve the preset degrees of the tail gases purification were calculated.

*This work was conducted within the framework of the budget project (AAAA-A17-117041710076-7) for Boriskov Institute of Catalysis.*

### References

1. Chumachenko, V.A.; Isupova, L.A.; Ivanova, Yu.A. et al. *Chem. Sustain. Develop.* **2019**, *4*, 2–7.
2. Ovchinnikova, E.V.; Chumachenko, V.A.; Piriyutko, L.V. et al., *Catal. Industry*, **2009**, *1*, 76–84.

## Table of contents

### Plenary lectures

<b>Environmental (scanning &amp; transmission) electron microscopy contribution to the study of silver-based catalysts during ethylene epoxidation</b>	7
T. Cavoué, A. Caravaca, L. Burel, M. Aouine, M. Rieu, J.P. Viricelle, P. Vernoux, F.J. Cadete Santos Aires	
<b>Selective liquid phase oxidation of alcohols: effect of supports and active metals</b>	8
V. Cortés Corberán	
<b>Methane conversion to syngas</b>	9
Valeria La Parola	
<b>Ni/CeO<sub>2</sub>-based catalysts for CO<sub>2</sub> methanation reaction: Insights into promotion effects</b>	10
L.F. Liotta	
<b>NO<sub>x</sub> SCR by ammonia in naval sector. An Italian industrial research project</b>	11
G. Pantaleo	

### Keynote lectures

<b>Pt/CeO<sub>2</sub> catalysts: active sites and reaction mechanisms in CO oxidation</b>	15
A.I. Boronin	
<b>Particles size determination in supported catalysts: new technique of light scattering</b>	16
Yu.V. Larichev	
<b>Microscopy study of the catalytic etching of platinum alloy catalyst gauzes during ammonia oxidation</b>	17
A.N. Salanov, N.M. Chesnokova	
<b>Diesel oxidation catalyst PtPd/MnO<sub>x</sub>-Al<sub>2</sub>O<sub>3</sub>: prospects for diesel soot emission control</b>	18
S.A. Yashnik	

### Section 1. Catalyst preparation

<b>Effect of preparation conditions on photocatalytic performance of Bi-based composites</b>	21
Yu.A. Belik, E.D. Fakhrutdinova, V.A. Svetlichyi, O.V. Vodyankina	
<b>The effect of linker composition on the Pd NPs distribution in UiO-66-type matrix</b>	22
Burachevskaya O.A., Butova V.V., Surzhikova Y.I., Soldatov A.V.	
<b>Metalorganic frameworks for catalytic applications</b>	24
V.V. Butova, A.L. Bugaev, E.A. Erofeeva, V.A. Polyakov, O.A. Burachevskaya, A.V. Soldatov	
<b>Synthesis and catalytic properties of Ni supported on ceria-zirconia with Ti, Nb and Nb+Ti for methane dry reforming</b>	26
V.E. Fedorova, M.N. Simonov, Yu.N. Bespalko, K.R. Valeev, E.A. Smal, V.A. Sadykov	

<b>Ordered macroporous <math>\alpha</math>-alumina as catalyst support for enhanced thermal stability of silver nanoparticles</b>	27
P.H. Keijzer, Jeroen E. van den Reijen, Claudia J. Keijzer, Krijn P. de Jong, P.E. de Jongh	
<b>Mechanochemical synthesis and investigation of catalysts based on MAI-layered double hydroxides (M - Mg, Ni, Co) for the selective hydrogenation of furfural</b>	28
E.O. Kobzar, L.N. Stepanova, O.B. Belskaya, N.N. Leont'eva, T.I. Gulyaeva	
<b>Immobilization of gold-silver nanoparticles in porous space UiO-66</b>	29
Kurmanbayeva K., Timofeev K.L., Ten S., Vodyankina O.V.	
<b>Ultra-small Pd nanoparticles on CeO<sub>2</sub> for catalytic oxidation of carbon monoxide</b>	30
V.A. Polyakov, A.A. Tereshchenko, A.A. Guda	
<b>Synthesis of nanotubular titanium dioxide with high specific surface area</b>	31
A.A. Sushnikova, A.A. Valeeva, I.B. Dorosheva, A.A. Rempel	
<b>Design of Ag-CeO<sub>2</sub>/SBA-15 catalysts for room-temperature 4-nitrophenol reduction</b>	32
A.V. Taratayko, G.V. Mamontov	
<b>In situ monitoring of Pd/CeO<sub>2</sub> nanoparticles growth by means of FTIR spectroscopy</b>	33
A.A. Tereshchenko, A.A. Guda, V.A. Polyakov, A.V. Soldatov	
<b>Design of MIL-100(Fe)/diatomite composites with hierarchical porous structure</b>	35
E.V. Vyshegorodtseva, P.A. Matskan, G.V. Mamontov	
<b>Formation of nickel particles on the surface of Ni/La<sub>2</sub>O<sub>3</sub> catalyst</b>	36
A.A. Fetisova, N.V. Dorofeeva, O.V. Vodyankina	
<b>Control of Pt species formation in Pt/CeO<sub>2</sub> catalysts via pretreatment of support and catalyst</b>	37
A.V. Filonenko, T.A. Bugrova, A.S. Savel'eva, T.S. Kharlamova, G.V. Mamontov	
<b>Regeneration of industrial iron-chrome catalysts for carbon monoxide conversion</b>	38
I.S. Grishin, M.A. Lebedev, V.A. Goryanskaya	
<b>Synthesis and characterization of the TiO<sub>2</sub> photonic crystals in the form of inverse opals</b>	39
M.V. Kirichkov, V. Likodimos	
<b>Ceria-supported Pt-Ag bimetallic catalysts: Features of formation of Pt-Ag active species</b>	40
M.V. Salina, T.S. Kharlamova, V.A. Svetlichnyi, G.V. Mamontov	
<b>Investigation of Pt/CeO<sub>2</sub>-MnO<sub>x</sub> catalysts in CO and methane oxidation reactions</b>	41
A.A. Simanenko, A.I. Stadnichenko, E. M. Slavinskaya, A.A. Evtushkova, E. A. Fedorova, O. A. Stonkus, A.V. Romanenko, A.I. Boronin	
<b>Macroporous Ag/SiO<sub>2</sub> composites for monolithic flow-through catalytic reactors</b>	42
O.Yu. Vodorezova, M.A. Baryshnikov, T.I. Izaak	
<b>Hierarchical SiO<sub>2</sub> materials and Pt-Ga catalysts on basis thereof for propane dehydrogenation</b>	43
A.V. Zubkov, E.V. Vyshegorodtseva, T.A. Bugrova, G.V. Mamontov	



## Section 2. Promising catalytic processes

<b>Localized temperature in plasmonic-induced photocatalysis at the singlenanoparticle level</b>	47
A.A. Averkiev, R.D. Rodriguez, B.N. Khlebtsov, R. Kato, L. Kim, T. Umakoshi, V. Kolchuzhin, D.R.T. Zahn, P. Verma, E. Sheremet	
<b>Preparation of low-sulfur coke from tar</b>	48
A.S. Chichkan, V.V. Chesnokov	
<b>Syngas conversion over perovskite-like <math>\text{LaCu}_x\text{Ti}_{1-x}\text{O}_3/\text{KIT-6}</math> catalysts</b>	49
E.V. Dokuchits, T.V. Larina, E.Yu. Gerasimov, A.A. Pochtar, T.P. Minyukova	
<b>Bismuth silicates nanoparticles synthesized by pulsed laser ablation for photocatalytic applications</b>	50
A.G. Golubovskaya, E.D. Fakhrutdinova, V.A. Svetlichnyi	
<b>Experimental research of Fisher-Tropsh synthesis with nitrogen-rich syngas under different pressures of synthesis</b>	51
A.S. Gorshkov, I.S. Ermolaev, K.O. Gryaznov, L.V. Sineva, I.G. Solomonik, V.Z. Mordkovich	
<b>Non-oxidative catalytic conversion of methane and <math>\text{C}_5</math>-hydrocarbons</b>	53
O.A. Kazakova, N.V. Vinichenko, A.E. Fedorov, T.I. Gulyaeva, V.A. Drozdov, A.S. Belyi	
<b>Investigation of photocatalyst for hydrogen evolution from glucose solution</b>	54
A.Y. Kurenkova, E.A. Kozlova	
<b>Solid solutions of CdS and ZnS: comparing photocatalytic activity and photoelectrochemical properties</b>	55
D.V. Markovskaya, A.V. Zhuremok, E.A. Kozlova	
<b>Combined Sorption and Catalytic Remove of Volatile Organic Compounds over <math>\text{Ag-CeO}_2/\text{SBA-15}</math> composites</b>	56
N.N. Mikhieva, V.I. Zaikovskii, G.V. Mamontov	
<b>Aspen wood ethanol lignin depolymerization in supercritical ethanol in the presence of Ni-containing catalysts</b>	57
A.V. Miroshnikova, V.I. Sharypov, S.V. Baryshnikov, Yu.N. Malyar, V.A. Yakovlev, O.P. Taran, B.N. Kuznetsov	
<b>Selective hydrogenation of 2-methyl-3-butyn 2-ol in microcapillary reactor. Effect of support on stability and kinetic parameters</b>	58
L.B. Okhlopko, M.A. Kerzhentsev, Z.R. Ismagilov	
<b>Glycerol oxidative conversion over Au NPs obtained by PLAL technique</b>	59
S. Ten, K. Kurmanbaeva, E.A. Gavrilenko, V.A. Svetlichnyi, O.V. Vodyankina	
<b>Selective Hydrogenation of 1,3-butadiene over <math>\text{SiO}_2</math>-supported Cu nanoparticles</b>	60
G. Totarella, B. Donoeva, P.E. de Jongh	
<b>Effect of platinum size of <math>\text{Pt}/\gamma\text{-Al}_2\text{O}_3</math> catalysts on propane dehydrogenation</b>	61
A. Van Assche, A. Le Valant, C. Especel, F. Epron	

<b>Ag-CeO<sub>2</sub> catalysts for toluene oxidation and 4-nitrophenol reduction</b> M.V. Chernykh, N.N. Mikheeva, G.V. Mamontov	62
<b>Enhancing the photocatalytic activity of two-dimensional materials with plasmonic nanoparticles and laser processing</b> D. Cheshev, R.D. Rodriguez, A. Matkovic, E. Sheremet	63
<b>Effect of pulsed laser irradiation on optical and photocatalytic properties of dark TiO<sub>2</sub></b> Z.P. Fedorovich, E.D. Fakhrutdinova, V.A. Svetlichnyi	64
<b>Effect of mechanical activation on the integrated extraction-catalytic processing of pine bark</b> V.A. Ionin, M.Yu. Belash, A.M. Skripnikov, V.V. Sychev, A.S. Kazachenko, O.P. Taran	65
<b>Enhancement of visible light activity of N-doped TiO<sub>2</sub> photocatalyst under polychromatic radiation due to a tandem effect</b> N.S. Kovalevskiy, D.A. Svintsitskiy, S.A. Selishcheva, D.V. Kozlov, D.S. Selishchev	66
<b>Catalytic oxidation of CO over Fe-, Sn-, and Ce-modified MnO<sub>2</sub> catalysts</b> E.V. Kulchakovskaya, T.S. Kharlamova, V.V. Verkhov, V.O. Trufanov, F.J. Cadete Santos Aires, V.I. Sobolev, O.V. Vodyankina	67
<b>Optical and photocatalytic properties of bismuth nanoparticles synthesized by pulsed laser ablation in water and air media</b> T.S. Nazarova, E.D. Fakhrutdinova, V.A. Svetlichnyi	68
<b>Catalytic properties of nickel-aluminium-titanium NASICON-type phosphates in ethanol conversion</b> D.A. Osaulenko, A.I. Pylinina, E.A. Asabina, I.O. Glukhova	69
<b>Decomposition of methane to hydrogen on a fiberglass catalyst</b> M.V. Popov, A.G. Bannov, A.N. Zagoruiko	70
<b>Alumina-supported CuO-MoO<sub>3</sub> as catalysts for soot oxidation</b> E.V. Romanova, A.V. Nam, T.S. Kharlamova	71
<b>Stability performance of Ni/CeO<sub>2</sub> catalysts in the steam/CO<sub>2</sub> reforming of methane</b> A.S. Shlyakhtina, E.V. Matus, O.B. Sukhova, I.Z. Ismagilov, M.A. Kerzhentsev, Z.R. Ismagilov	72
<b>Catalytic oxidation of formaldehyde over modified MnO<sub>2</sub> catalysts with OMS-2 structure</b> V.V. Verkhov, F.J. Cadete Santos Aires, V.I. Sobolev, O.V. Vodyankina	73
<b>Combined synthesis and hydroprocessing of hydrocarbons via Co-SiO<sub>2</sub>/Ni-ZSM-5/Al<sub>2</sub>O<sub>3</sub> catalyst</b> R.E. Yakovenko, I.N. Zubkov, V.N. Soromotin, G.B. Narochniy, A.P. Savost'yanov	74
<b>Photocatalytic hydrogen production from aqueous solutions of methylene blue under UV light over Cu modified TiO<sub>2</sub></b> A.V. Zhurenok, A.Y. Kurenkova, D.V. Markovskaya, S.V. Cherepanova, V.V. Kaichev, E.A. Kozlova	75

### Section 3. Physical-chemical fundamentals of catalysis

<b>Effect of high-temperature treatment of Sibunit and content of Ru on the activity of Ru-Cs/Sibunit catalysts in ammonia synthesis</b>	79
V.A. Borisov, K.N. Iost, V.L. Temerev, P.A. Fedotova, Yu.V. Surovikin, D.A. Shlyapin	
<b>Alcohol effect on the catalytic properties of CuO<sub>x</sub> water-ethanol colloids obtained by laser ablation in 4-nitrophenol hydrogenation</b>	80
D.A. Goncharova, T.S. Kharlamova, O.A. Reutova, V.A. Svetlichnyi	
<b>Rh-doped CeO<sub>2</sub> catalytic systems for low-temperature NO reduction</b>	81
L.S. Kibis, A.I. Krotova, D.A. Svintsitskiy, E.A. Fedorova, E.M. Slavinskaya, O.A. Stonkus, V.A. Svetlichnyi, A.I. Boronin	
<b>Active sites on the surface of mayenite during catalytic ethanol dehydration</b>	82
E.I. Shuvarakova, A.F. Bedilo, A.S. Chichkan, E.V. Ilyina	
<b>Structure-activity relationships of Pt/TiO<sub>2</sub> catalysts for ammonia low-temperature oxidation: comparison of pulsed laser ablation and impregnation methods of catalysts synthesis</b>	83
A.I. Stadnichenko, L.S. Kibis, E.M. Slavinskaya, D.A. Svinstitskiy, E.A. Fedorova, O.A. Stonkus, A.V. Romanenko, V.A. Svetlichnyi, V. Marchuk, D. Doronkin, J.-D. Grunwaldt, A.I. Boronin	
<b>Selective oxidation of ammonia over Pt-based catalysts</b>	84
D.A. Svintsitskiy, E.M. Slavinskaya, E.A. Fedorova, L.S. Kibis, A.I. Stadnichenko, A.V. Romanenko, A.S. Zaguzin, O.A. Stonkus, D.E. Doronkin, V. Marchuk, M. Casapu, J.-D. Grunwaldt, A.I. Boronin	
<b>Machine learning application for XANES spectroscopy of Pd nanocatalyst</b>	85
O.A. Usoltsev, A.L. Bugaev, A.A. Guda, S.A. Guda, A.V. Soldatov	
<b>Microscopy study of the catalytic etching of platinum metals during ammonia oxidation</b>	87
N.M. Chesnokova, A.N. Salanov	
<b>Investigation of the semiconducting properties of bismuth silicate-based photocatalysts by electrochemical methods</b>	88
O.V. Dubinina, A.V. Shabalina, E. Yu. Gotovtseva, O.V. Vodyankina	
<b>Paramagnetic complexes of 9,10-anthraquinone on a zirconium dioxide surface</b>	89
Yu.A. Fionov, A.V. Fionov, A.I. Pylinina, A.N. Kharlanov	
<b>Thermodynamic analysis of the steam/CO<sub>2</sub> reforming of methane</b>	90
A.Yu. Korenyuk, E.V. Matus, I.Z. Ismagilov, M.A. Kerzhentsev, Z.R. Ismagilov	
<b>Quantum-chemical analysis of the effect of water molecules on the kinetics of 2-methylimidazole formation</b>	91
A.V. Kotov, A.V. Fateev, V.P. Tuguldurova	
<b>XPS study of Rh-CeO<sub>2</sub> catalysts under CO+NO treatments</b>	92
A.I. Krotova, L.S. Kibis, D.A. Svintsitskiy, E.A. Fedorova, E.M. Slavinskaya, O.A. Stonkus, A.I. Boronin	

<b>Prediction of the catalytic activity of metals by adsorption data in reactions with hydrogen-containing gases</b>	93
D.A. Prozorov, A.V. Afineevskii, D.V. Smirnov, K.A. Nikitin, T.Yu. Osadchaya	
<b>Catalytic properties of CuO<sub>x</sub> NPs obtained by pulsed laser ablation</b>	94
O.A. Reutova, D.A. Goncharova, T.S. Kharlamova, O.V. Vodyankina, V.A. Svetlichnyi	
<b>Physicochemical properties of gadolinium oxysulfide (Gd<sub>2</sub>O<sub>2</sub>S:Tb)</b>	95
A.V. Rodionova, P.Sh. Ustabaev, T.S. Minakova, V.V. Bakhmetyev	
<b>Investigation of catalysts of various compositions of Pd-Bi/Al<sub>2</sub>O<sub>3</sub> in the reaction of glucose oxidation into gluconic acid</b>	96
M.P. Sandu, I.A. Kurzina	
<b>The catalytic effect of the surface in the formation of hydrogen bonded systems. IR spectroscopy and DFT</b>	97
I.A. Spirin, R.V. Kapustin, I.I. Grinvald, A.N. Petukhov	
<b>Transfer hydrogenation of levulinic acid and its esters to <math>\gamma</math>-valerolactone over Zr-SBA-15 catalyst</b>	98
V.V. Sychev, A.O. Eremina, O.P. Taran	
<b>Section 4. Industrial implementation of catalytic processes</b>	
<b>Integrated catalytic purification of waste gases in nitric acid plants from nitrogen oxides (NO<sub>x</sub> and N<sub>2</sub>O)</b>	101
A.G. Sheboltasov, N.V. Vernikovskaya, V.A. Chumachenko	

Scientific edition

# CATALYSIS: FROM SCIENCE TO INDUSTRY

*Proceedings of  
VI International scientific school-conference for young scientists*

2020, October 6 – 10

All proceedings are published as is; maintenance responsibility remains to authors

Original layout by *V.S. Malkov*  
Cover designed by *O.V. Kireeva*

**It's published at "Ivan Fedorov" publishing as provided by original layout**

Signed to print 05.10.2020. Format 60×84<sub>1/8</sub>. Offset paper №1.  
Offset print. Sheets 13,5. Relative sheets 12,56. Publisher's signature 12,17.  
Order №20252. Number of copies 20 issues.

---

---